Focal Adhesion Kinase, Maintenance of Sphingosine 1 Phosphate Receptor 1 Expression and Barrier Function

By
PASCAL YAZBECK
BS. Biomedical Sciences, Haigazian University, Beirut, 2006
MS. Molecular Biology, Lebanese American University, Byblos, 2008

THESIS

Submitted as partial fulfillment of the requirements
for the degree of Doctor of Philosophy in Cell and Molecular Pharmacology
in the Graduate College of the
University of Illinois at Chicago, 2017

Chicago, Illinois

Defense Committee:

Dolly Mehta, Chair and Advisor
Jalees Rehman
Jeffrey Jacobson (Medicine)
Andrei Karginov
Jae-Won Shin

This thesis is dedicated from the bottom of my heart to my precious parents, Nasri, Silva and Allen.

ACKNOWLEDGMENTS

First, I would like to expresses my appreciation to my advisor and mentor, Dr. Dolly Mehta, for allowing me to work in her laboratory to pursue my doctoral training. Her support and push helped me become a successful scientist. Her motivation and dedication inspired me and shaped who I am now. Thank you for the learning environment and the challenges you put me through to learn how to become a critical thinker.

I would like to thank my thesis committee members, Dr. Jalees Rehman, Dr. Jeffrey Jacobson, Dr. Andrei Karginov and Dr. Jae-Won Shin for their stanch support, constructive critique and dedication to my success throughout my graduate years.

Mehta lab, your guidance and support in training me is highly appreciated. Dr. Monica Smith and Dr. Charu Rajput, you taught me the basics since my interview day, your friendship to me is something I will cherish always. Thank you for your time and constant support. Thanks to Dr. Mohammad Tauseef for your expertise in animal work and Dr. Zahid Akhter for the help in epigenetic experiments. It has been my pleasure to work with you all. Dr. Tracy Tennes-Schmidt, thank you for generating *EC-FAK*$^{-/-}$ and providing a platform to elevate this project to another level.

Thank you faculty, staff, students and pharmacology department for making this journey an unforgettable experience.

Last, but not least, I am grateful to my family and friends. Without their support and encouragement this journey would have been tough. Thank you to my parents for their love, support and advice throughout the years.

PY

TABLE OF CONTENTS

TABLE OF CONTENTS (continued)

TABLE OF CONTENTS (continued)

LIST OF FIGURES

LIST OF FIGURES (continued)

FIGURE PAGE

LIST OF ABBREVIATIONS

AJ	Adherens junction
ALI	Acute lung injury
BSA	Bovine serum albumin
Ca^{2+}	Calcium ion
CAD	CRAC activated domain
Ccb9	Coil-coil domain b9
CRAC	Calcium release activated channel
CTID	C-terminal inhibitory domain
DMSO	Dimethyl sulfoxide
dn	Dominant negative
EBA	Evan's blue albumin
EBAE	Evan's blue albumin extravasation
EC	Endothelial cell
ECIS	Electric cell-substrate impedance sensing
ECM	Extracellular matrix
EDG	Endothelial differentiation gene
ER	Endoplasmic reticulum
ERK	Extracellular related kinase
F	Phenylalanine
FA	Focal adhesion
FAK	Focal adhesion kinase

LIST OF ABBREVIATIONS (continued)

FAT	Focal adhesion targeting
FERM	4.1 ezrin, radixin, moesin
FRNK	FAK related non-kinas
GFP	Green fluorescent protein
GJ	Gap junction
GPCR	G-protein coupled receptor
HEK	Human embryonic kidney
HPAE	Human pulmonary artery endothelial
i	Inducible
IEJs	Interendothelial junctions
i.p.	Intraperitoneal
LECs	Lung endothelial cells
MAPK	Mitogen activated protein kinase
MLC	Myosin light chain
MLCK	Myosin light chain kinase
PAR1	Protease activating receptor 1
PBS	Phosphate buffered saline
PCR	Polymerase chain reaction
PLC	Phospholipase C
PM	Plasma membrane

LIST OF ABBREVIATIONS (continued)

PR	Proline rich
PTK	Protein tyrosine kinase
PTP	Protein tyrosine phosphatase
Pyk2	Protein tyrosine kinase 2
ROCK	Rho-associated protein kinase
ROS	Reactive oxygen species
S	Serine
SAM	Sterile alpha motif
S1P	Sphingosine-1-phosphate
S1PR	Sphingosine-1-phosphate receptor
SCL	Stem cell leukemia
SDS	Sodium dodecyl sulfate
SFK	Src family kinase
SH2	Src-homology-2
SH3	Src-homology-3
SOAP	Stim1-Orai1 associated pocket
SOCE	Store operated Ca^{2+} entry
SPHK	Sphingosine kinase
STIM1	Stromal interaction molecule 1
TER	Transendothelial electrical resistance
Thap	Thapsigargin
Thr	Threonine
Thr	Thrombin

LIST OF ABBREVIATIONS (continued)

TJ	Tight junction
TLR	Toll-like receptor
TRIP	Threonine-argenine-isoleucine-proline
VE	Vascular endothelial
VEGF	Vascular endothelial growth factor
WASP	Wiskott aldrich syndrome protein
W/d	Wet/dry
WT	Wild type
Y	Tyrosine
YFP	Yellow fluorescent protein

SUMMARY

Vascular endothelium forms the innermost layer of blood vessels. It regulates many physiological and pathological processes including maintaining host defense, vasomotor tone, angiogenesis and tissue-fluid homeostasis. The single layer of endothelial cells allow the transfer of gases, low molecular weight solutes and gases across the vessel wall while restricting the passage of large macromolecules due its tightly regulated cellular barrier. It is well established that the crosstalk between interendothelial junctions (IEJs), such as adherens junctions (AJs), as well as focal adhesions (FAs) at the site of EC-ECM attachment, maintains endothelial barrier integrity. Persistent increase in vascular permeability results in leakage of fluid and large molecules into the interstitial and alveolar compartments and if left unresolved it leads to devastating and life threatening diseases such as acute lung injury (ALI). Schmidt et al., have shown that loss of FAK in endothelial cells led to increase lung vascular permeability, edema, fluid accumulation and leukocyte infiltration causing damage to the lungs. The purpose of this study was to identify a signaling node which combines both AJs and FAs to prevent endothelial damage in the lungs, thus preventing ALI.

In this regard, I propose that sphingosine-1-phosphate (S1P), a well established endothelial barrier enhancing bioactive lipid, which ligates with high affinity to S1PR1 in endothelial cells, could restore EC-FAK leaky phonotype in mouse lungs. FAK is a non-receptor tyrosine kinase that contains multiple protein-protein interacting domains that allow its interaction with proteins that governs actin dynamics, monolayer permeability and inflammation. FAK is regarded as an important protein during embryogenesis hence, the deletion of FAK in endothelial cells led to embryonic lethality due to vascular impairment and edema generation. Thus, studies in this thesis were focused on restoring EC-FAK phenotype and its impact on lung vascular permeability.

In the first chapter, I introduced S1P into EC-FAK mouse lungs as well as FAK depleted ECs to restore lung edema as well as EC barrier function. Interestingly, we found that S1P did not suppress lung edema in EC-FAK null lung. Similarly, FAK knock down cells did not respond to S1P and this failed to enhance AJ assembly. Surprisingly, we found that the mRNA and protein levels of S1PR1 were significantly low in EC-FAK null lungs and FAK depleted ECs. We show that FAK regulates S1PR1 transcriptionally by epigenetically suppressing KLF2, a key transcription factor that induces S1PR1 expression.

In the second chapter, we propose a mechanism where FAK regulates DNA methylation. We show that loss of FAK in ECs induces SOCE, and that loss of FAK induces Pyk2 phosphorylation, a member of FAK family non-receptor tyrosine kinase, which phosphorylates STIM1 at Y361 residue to recruit Orai1 to STIM1-Orai1 puncta to induce SOCE. We hypothesize that Ca^{2+} induces the activation of DNA methylation machinery through Rho pathway. Thus suppressing RhoA in FAK depleted cells will be a strategy to sustain KLF2 and S1PR1 expressions.

In summary, our studies identify FAK as a regulator of S1PR1 by suppressing DNA methylation and regulating STIM1 mediated Ca^{2+} entry. These findings have therapeutic potential against ALI. Mechanisms that preserve FAK expression or inhibiting Rho pathway could be a possible approach to prevent KLF2 and S1PR1 loss and initiation of ALI.

I. LITERATURE REVIEW

A. Lung Injury

1. Introduction

The vasculature which lines the innermost layer of all blood vessels regulates multiple key tasks including angiogenesis, vasomotor tone, blood clotting and inflammation (Mehta and Malik 2006, Matthay and Zemans 2011, Ausprunk and Folkman 1977, Folkman and Haudenschild 1980, Johnson et al. 1964). The endothelium, in a size restrictive manner, allows the passage of fluids, ions, large molecules and leukocytes across the vessel wall by either dynamically opening intercellular junctions or through paracelluler vesicles such as caveolae (Smith and Staples 1980, Abdullaev et al. 2008). Transendothelial migration of leukocytes is required for normal host defense. However, opening of intercellular junctions leads to the accumulation of protein-rich edema in the interstitial tissue which can lead to debilitating illness such as acute respiratory distress syndrome (ARDS) or acute lung injury (ALI)(Sukriti et al. 2014) **(Figure 1).**

2. Vascular Endothelial Barrier

Endothelial cells adhere to each other via intercellular connections which are called junctions. They also attach to extracellular matrix to enforce their restrictive properties **(Figure 2)**. Of the different intercellular connections, adherens junctions (AJs) predominantly form the adhesive interaction needed to maintain endothelial cell-

cell contact to control endothelial permeability. Endothelial AJs are composed of vascular endothelial (VE)-cadherin as the major structural component that orchestrates adhesion between adjacent EC membranes forming a tight zipper-like structure to prevent paracellular permeability (Mehta and Malik 2006) **(Figure 2)**.

Endothelial cells attach to the underlying ECM through cell surface integrins at sites called focal adhesions (FAs) (Mehta and Malik 2006). Integrins are composed of a transmembrane glycoproteins expressed as α/β henterodimers. Endothelial cell expresses multiple integrins with different combinations. The extracellular domain of integrin binds to ECM components, whereas the cytoplasmic domain links to actin cytoskeleton directly or via linker proteins such as focal adhesion kinase (FAK), paxillin, talin, vinculin and α-actinin. FAK recruits and phosphorylates multiple FA-associated proteins to initiate intracellular signaling events crucial for endothelial barrier (Petit and Thiery 2000).

1. Role of FAK in maintaining endothelial barrier.

a. FAK structure and function

Protein tyrosine kinase 2 (*PTK2*) gene or FAK is positioned on chromosome 8, encodes a 125 kDa non-receptor tyrosine kinase. FAK was initially identified at the focal adhesions and phosphorylated upon integrin mediated adhesion in the presence of v-src, an oncogenic tyrosine kinase (Guan, Trevithick, and Hynes 1991, Guan and Shalloway 1992, Kornberg et al. 1991). Pyk2, a member of FAK non-receptor tyrosine

kinase family shares significant sequence homology to FAK however, its expression is more constrained (Mitra, Hanson, and Schlaepfer 2005).

FAK is ubiquitously expressed and evolutionally conserved among species such as human (Whitney et al. 1993), mouse (Hanks et al. 1992), frog (Hens and DeSimone 1995) and chicken with more than 90% sequence identity suggesting FAK plays and major role in various cellular functions. FAK has been shown to be a major contributor in strengthening of endothelial monolayer (Holinstat et al. 2006, Quadri and Bhattacharya 2007), allied with endothelial monolayer function and disease (Mehta and Malik 2006, Yuan et al. 2012, Quadri et al. 2003, Zebda, Dubrovskyi, and Birukov 2012, Lu and Rounds 2012). Moreover, FAK also plays a crucial role in regulating cell survival and death (Lu and Rounds 2012). Although initially identified in the early 1990s, understanding the functional importance of FAK signaling *in vivo* using genetic approaches has been difficult since the global deletion of FAK in mice develop prominent mesodermal defects in FAK null embryos resulting in embryonic lethality at E8.5 (Ilic et al. 1995).

Since global FAK deletion causes embryonic lethality, two investigators utilized the Cre recombinase- *LoxP* approach to explicitly delete FAK in ECs (Shen et al. 2005, Braren et al. 2006). However, endothelial specific deletion of FAK causes embryonic lethality between E13.5 and E14.5 due to hemorrhage, edema and defective vasculature, suggesting FAK is essential for the formation of the endothelial barrier (Shen et al. 2005, Braren et al. 2006).

FAK protein is composed of 1052 amino acid sequence. At its N-terminus domain (FERM) composed of N-terminal 4.1 ezrin, radixin, moesin homology domain, a kinase domain at the center between two proline-rich domains and a C-terminal focal adhesion targeting domain (FAT)(Parsons 2003) **(Figure 3).**

FERM domain is approximately 300 aa and facilitates intermolecular connections with β subunit of integrins at focal adhesion complexes as well as growth factor receptors to mediate outside-in signaling cascades (Parsons 2003). FAK FERM domain interacts with various cytosolic binding partners making the N-terminus a site for interactions with other binding partners to mediate downstream signaling cascade.

The C-terminus domain of FAK is about 140aa which makes up the FAT domain that is important to localize FAK to the focal adhesion signaling complexes. This domain provides anchoring sites to the focal adhesion-associated protein complexes such as talin, paxillin, growth factor receptor-bound protein (Grb2), directing FAK to the FAs (Chen et al. 1995, Ezratty, Partridge, and Gundersen 2005, Hildebrand, Schaller, and Parsons 1993, Lulo, Yuzawa, and Schlessinger 2009, Prutzman et al. 2004, Scheswohl et al. 2008).

FAK also has a kinase domain that shares sequence identity with other receptor and non-receptor tyrosine kinases. This domain harbors a catalytic loop which contains Y576 and Y577 that is required for FAK catalytic function (Parsons 2003). These sites tightly regulate FAK catalytic activity as well as provide a binding

sites for Src-homology (SH2)-containing proteins including PLC-γ, PI_3K and Grb7 to regulate downstream signaling. Y397 lies between FERM domain and catalytic domain, is regulated by Src kinase which unfolds FAK from its native closed conformation. (Parsons 2003).

Besides FAT and kinase domain, FAK contains three proline-rich (PR) domains two of which resides between the kinase and FAT domain, whereas the third is situated between the FERM and kinase domain (Parsons 2003). PR domains are considered as protein-protein interacting domains because they contain SH3 domain interacting sequences (Parsons 2003).

The C-terminal domain of FAK contains four serine residues, S722, S843, S846 and S910, which are potential phosphorylation sites; however, they may play a role in stabilizing protein-protein interactions (Parsons 2003).

b. Role of FAK in EC barrier

Several studies elucidated the role of FAK in modulating endothelial barrier function with barrier enhancing effects being described in several models (Mehta 2012, Schmidt et al. 2013, Rajput et al. 2013). Endothelial cells isolated from FAK knockout embryos showed increased permeability compared to wild type EC. Studies in cultured rat lung microvascular ECs showed kinase-deficient FAK mutant suppressed hyperperosmolarity-induced increase in barrier function and associated peripheral VE-cadherin enhancement.

Transfection of dominant-negative FAK mutant in endothelial cells failed to anneal

AJ and barrier recovery after stimulation of H_2O_2. In human pulmonary artery ECs (HPAECs), loss of FAK expression results in prolonged disruption of barrier integrity after thrombin challenge. Holinstat et al. have shown that FAK facilitates barrier enhancement by suppressing RhoA activity through p190RhoGAP after thrombin stimulation (Holinstat et al. 2006). Furthermore, thrombin activates FAK by mechanism including the activation of PAR1 receptor, a G-protein coupled receptor, and Gβγ dissociation and Fyn tyrosine kinase to strengthen EC barrier (Knezevic et al. 2009). Schmidt et al. generated tamoxifen-inducable EC specific FAK knockout mice. They demonstrated that loss of FAK in endothelial cells induced diffuse lung hemorrhage, edema, increased transvascular albumin influx and neutrophil accumulation in the lung due to disruption of EC barrier. Mimicking ALI by intraperitoneal LPS administration or cecal ligation and puncture in wild-type mice significantly decreased FAK expression in the lungs suggesting that loss of FAK expression is perhaps responsible for the hyperpermeability and edema formation seen during ALI (Schmidt et al. 2013).

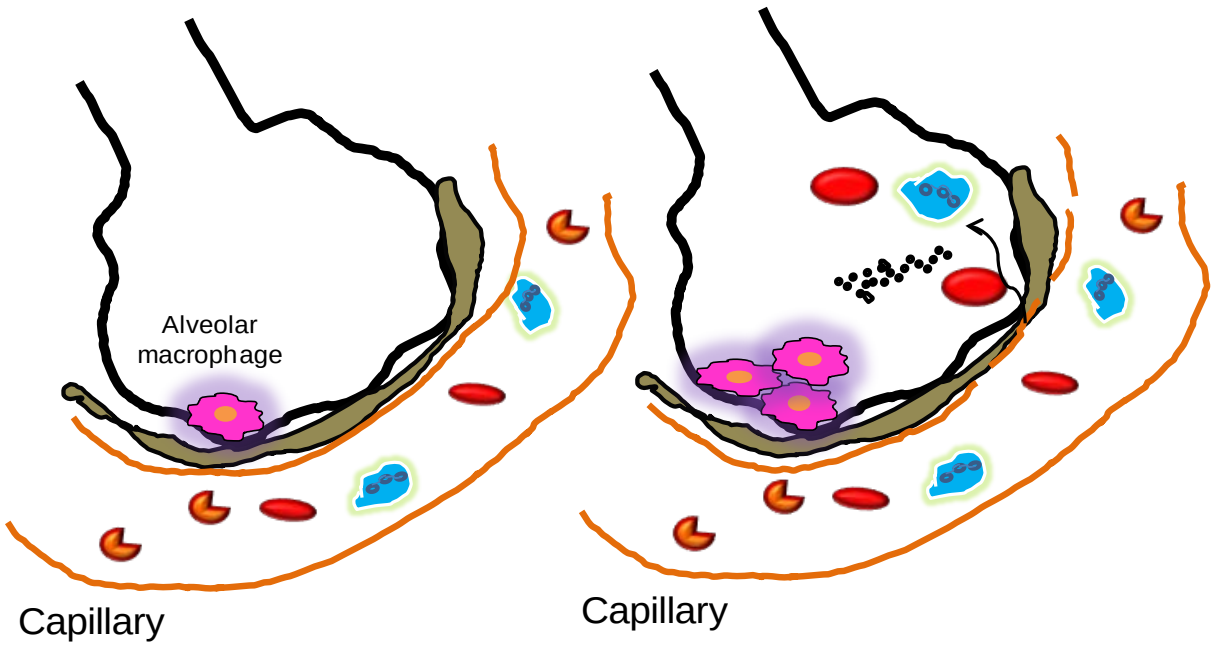

Figure 1. Normal and injured lung. The lung is highly vascularized organ. Capillaries, which are the smallest blood vessels surrounds alveoli for gas exchange. In normal lung, the fluid and macromolecules circulating in the blood capillary of endothelium forms a semi-restrictive barrier (Left). However, during endothelial dysfunction and loss of endothelial barrier integrity, blood fluid, macromolecules and leukocytes leaks into the alveolar space (Right). In addition to the protein rich fluid, there is an increase in leukocyte transmigration and red blood cell accumulation in the alveoli as well as in the interstitial space, leading to increased pro-inflammatory cytokine and reactive oxygen species generation and tissue damage.

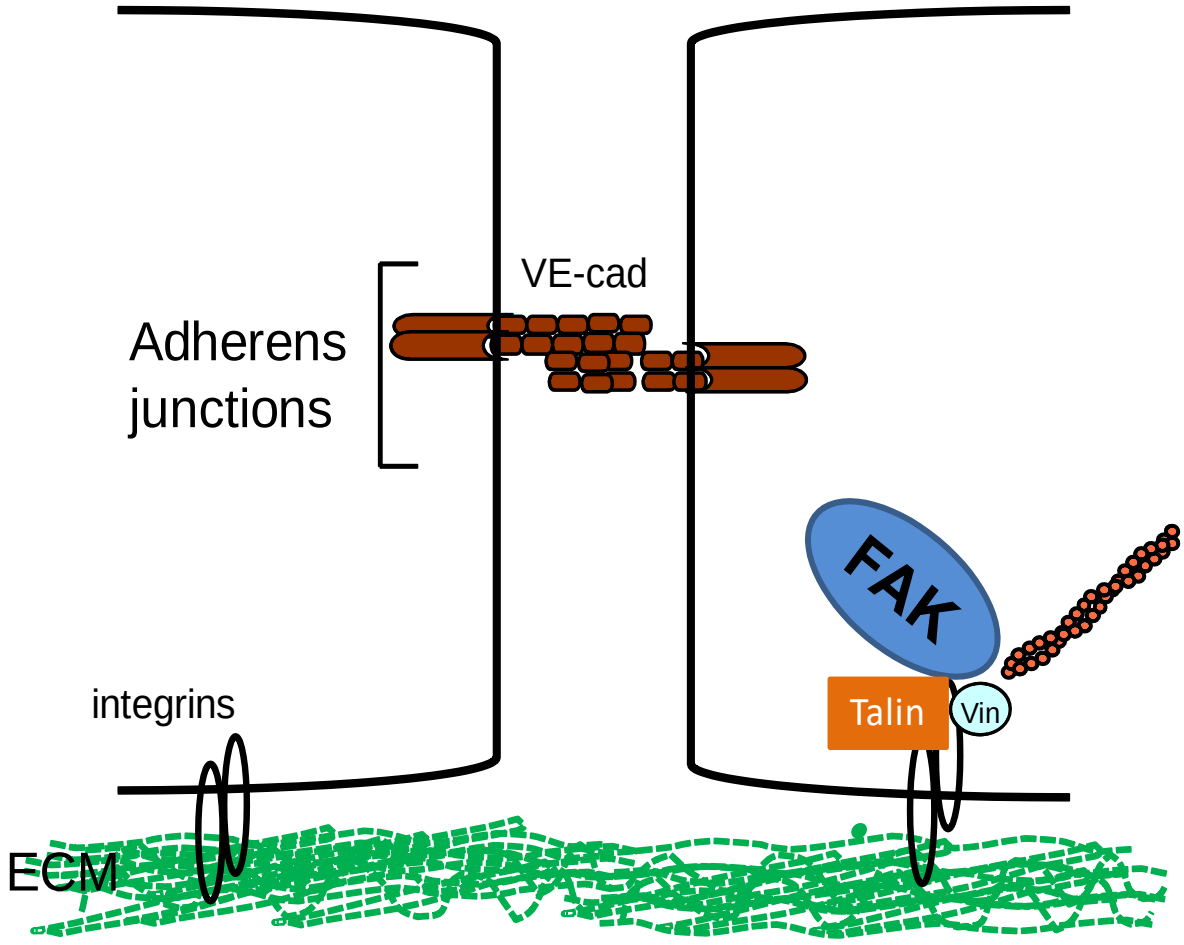

Figure 2. Endothelial cell adherens junctions and focal adhesions. Endothelial cells maintain its integrity by interacting with adjacent endothleial cells through interendothelial cell-cell junctions known as adherens junctions. They also attach to ECM via integrins to maintain their restrictive characteristics. Endothelial cells interconnect with each other via three types of intercellular junctions (IEJs); adherens junctions (AJs), tight junctions (TJs), and gap junctions (GJs). At sites where endothelial cells adhere to ECM is called focal adhesions (FAs). Endothelial cell surface integrin receptors bind to ECM proteins. The cytoplasmic domain of integrins serves as a critical site for various FA-associated proteins, such as focal adhesion kinase (FAK), vinculin, paxillin, and talin to transmit forces or signals to the actin cytoskeleton.

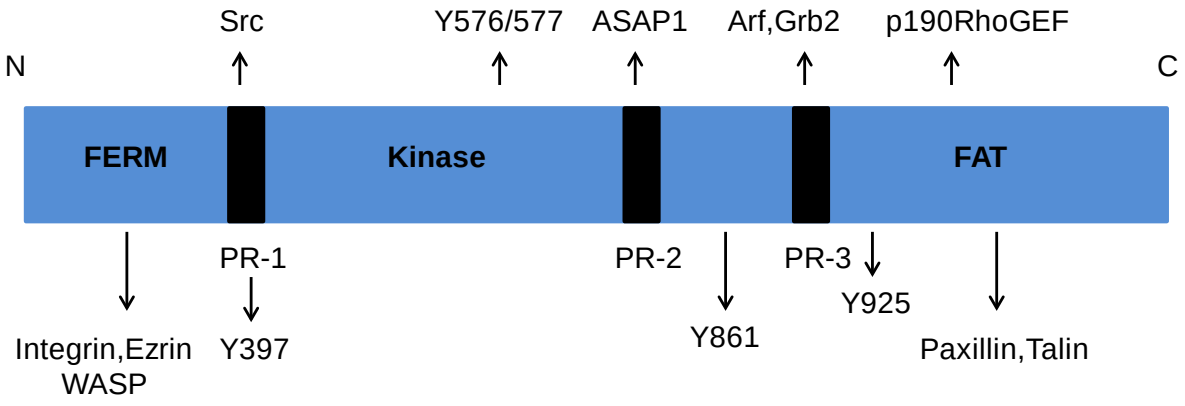

Figure 3. Structure of FAK. FAK contains an N-terminal 4.1 ezrin, radixin, moesin-homology also known as (FERM) domain, three proline rich (PR) domains (PR1-3), a central kinase domain containing tyrosine residues Y576/Y577, and a focal adhesion targeting (FAT) domain. The FERM domain interacts with multiple proteins such as integrins, ezrin, and WASP, whereas the C-terminal interacts with GAPs to regulate GTPase activity, and the FAT domain binds FA proteins such as paxillin and talin.

2. Role of S1PR1 in maintaining endothelial barrier

a. Sphingosine-1-phosphate

Sphingolipids have emerged to play a crucial role in signaling events such as cell viability, cellular homeostasis, differentiation and motility (Anliker and Chun 2004, Spiegel and Milstien 2003, Takabe et al. 2008, Young and Van Brocklyn 2006). These lipids are now considered as important mediators of inflammation and other cardiovascular related functions. Previously, Speigel lab have shown that sphingosine was capable of acting as second messenger for calcium mobilization and thus modulate gene transcription in a concentration dependent manner. More importantly, they have shown that sphingosine phosphorylation by sphingosine specific kinases (SPHKs) to be a key requirement for cell growth and survival. Further studies elucidated that the bioactive lipid, sphingosine-1-phosphate (S1P) is synthesized intracellularly by SPHK1 and SPHK2 via phosphorylation of sphingosines' primary hydroxyl group (Fu et al. 2016). Sphingosine is converted to S1P by SPHKs. On the other hand, S1P is degraded back to sphingosine by S1P phosphatases, or degraded by S1P lyase into hexadecenal and ethanolamine phosphate suggesting tight regulation of S1P signaling in organisms (Sanllehi et al. 2016).

S1P is mainly produced by platelets and endothelial cells(Igarashi and Yatomi 1998). However, epithelial cells, thrombocytes, mast cells, macrophages, cerebeller granule cells (Bassi et al. 2006) and dendritic cells can also produce S1P (Goetzl and Tigyi 2004). Circulating erythrocytes do not generate S1P but they have the ability to

store it and release it, thus preventing S1P from degradation. In the plasma, levels of S1P can reach up to 0.9 μM where it is found to be bound to high density lipoproteins (HDLs). Levels of S1P in lymph nodes are lower than in plasma. In tissues, levels of S1P range from 0.5 to 0.75 pmol/mg (Edsall and Spiegel 1999). Half life of S1P is estimated to be less than 15 min (Venkataraman et al. 2008). Once produced in the cell after SPHK1 activation, S1P is transported to the extracellular space by ATP-binding cassette (ABC) transporters such as ABCA1, ABCC1 and ABCG2 (Takabe et al. 2010). Once in the extracellular space, S1P ligates S1PRs on the membrane which in turn triggers multiple intracellular signaling cascades leading to activation of Ras/MAPK, PKC, the small GTPase Rho pathways, stimulation of PLC/Ca^{2+} mobilization and inhibition of adenylate cyclase (Moolenaar 1995, Meyer zu Heringdorf et al. 1998).

Failure in vascular integrity leads to serious outcomes such as hemorrhage, edema and inflammation. Vascular integrity is tightly regulated by multiple factors that promise proper functions of multiple components of the blood vessel wall. S1P has been identified as a strong barrier enhancing factor that serves a novel and specific therapy for endothelial cell (EC) barrier dysfunction. S1P at 1 μM exerts a rapid and drastic enhancement of polymerized F-actin and myosin light chain phosphorylation at the cell periphery (Garcia et al. 2001).

Rho family small GTPases regulate the effect of S1P on actin-dependent processes in the cell. The Rho family of GTPases (Rho, Rac and Cdc42) is a group of regulatory proteins that link surface receptors to downstream effectors regulating

multiple signaling pathways and cytoskeletal structure (Spiering and Hodgson 2011). RhoA, Rac1 and Cdc42 act as a trigger to promote actin stress fibers, lamillipodia, and filopodia. The primary S1P receptors in endothelial cells are S1PR1, S1PR2 and S1PR3 which couple to different Rho family GTPases (Ancellin et al. 2002)**(Figure 4).** S1PR1 induces Rac activation through $G\alpha_i$-dependent activation of PI3-Kinase. On the other hand, S1PR2 activates RhoA through $G\alpha_{12/13}$ and RGS family of Rho-specific guanine nucleotide exchange factors (GEFs). S1PR3 can activate Rac1 through $G\alpha_{i,}$ but could couple to $G\alpha_{q/11}$ and activate RhoA through the Trio family of Rho-GEFs (Hla 2003, Blaho and Hla 2011).

b. S1PR1

S1PR1 gene is located on chromosome 1p21 and was the primary receptor cloned from human ECs and thus named as endothelial differentiation gene-1 (EDG1)(Hla and Maciag 1990). S1P/S1PR1 signaling activates PI3K, Rac1, and ERK1/2 (Young and Van Brocklyn 2006). S1PR1 is essential for blood vessel formation and maturation. Mice deficient in S1PR1 die between E12.5 and E14.5 due to vascular hemorrhage and failure of smooth muscle cells to migrate and enclose the blood vessel. Endothelial specific S1PR1 deletion exhibits a similar phenotype, indicating the important role of S1PR1 in vascular development. S1PR1 expressed on ECs play an important role in development of mature vascular beds by regulating excessive sprouting. Uncontrolled sprouting is seen in embryos where S1PR1 has been deleted only in ECs or in inducible systems either in all tissues or specifically in ECs shortly after birth. Surprisingly, S1PR1 expression seems to be abundant in areas

of vasculature with fluid flow, indicating the possibility of S1PR1 acting as a sensor to shear flow, providing a new insight of S1PR1 in regulating vascular function.

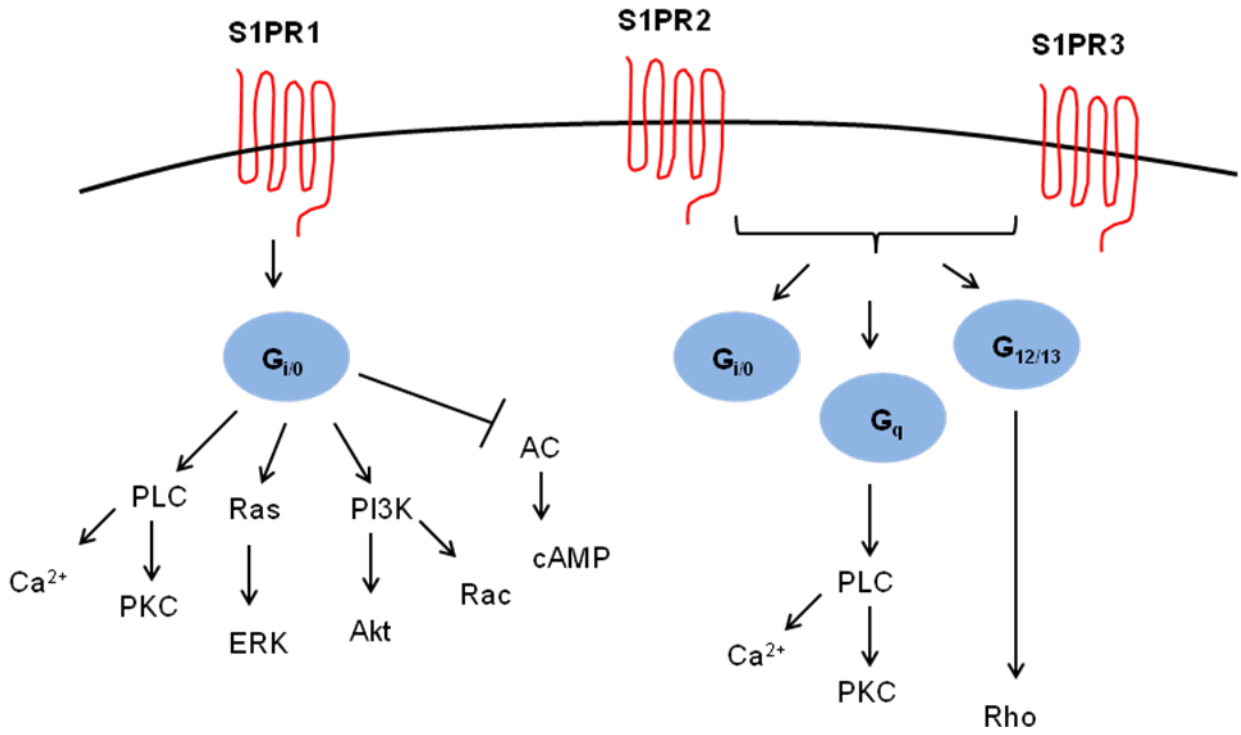

Figure 4. S1P receptor signaling. Major endothelial S1P receptors couple to various G proteins. S1PR1 couples to G_i to induce proliferation, migration and angiogenesis. S1PR2/3 couple to G_i, G_q and $G_{12/13}$ mainly inhibiting S1PR1 mediated effect on endothleial cell.

3. Role of Ca^{2+} signaling in endothelial cell biology

Ca^{2+} ions control almost every facet of cellular life. Changes in intracellular Ca^{2+} regulate a series of functions such as secretion and enzyme activity (Parekh and Putney 2005). Long term responses to Ca^{2+} oscillations include changes in gene transcription, cell cycle control, mitochondrial ATP production and apoptosis. The importance of Ca^{2+} signaling is demonstrated by variety of human disorders caused by defects in Ca^{2+} homeostasis, which include, acute pancreatitis, severe combined immunodeficiency (SCID), allergy, inflammatory bowel disease, thrombosis, breast cancer and Alzheimer's disease (Sukriti et al. 2014, Parekh and Putney 2005).

Two discrete mechanisms have been developed by eukaryotic cells to increase their cytoplasmic Ca^{2+} concentration: Ca^{2+} release from intracellular stores or Ca^{2+} influx across the membrane into the cell. A proper control of Ca^{2+} influx and release is important for the maintenance of Ca^{2+} homeostasis. Increase in cytosolic Ca^{2+} include plasma membrane channels which facilitate the influx of Ca^{2+} from the extracellular milieu, and channels located on the endoplasmic reticulum (ER) and sacroplasmic reticulum (SR) that regulate the release of Ca^{2+} from intracellular stores. At equilibrium, Ca^{2+} influx and release maintains the concentration of intracellular free Ca^{2+} ([Ca2+]i) at ~100nM or less, while extracellular Ca^{2+} concentration ($[Ca^{2+}]o$) is approximately 1–2mM (Mehta and Malik 2006, Sukriti et al. 2014, Bootman et al. 2001). Stimulation by an extracellular agonist or depolarization leads to an increase in $[Ca^{2+}]i$ globally of up to 1μM via Ca^{2+} influx through plasma membrane channels or Ca^{2+} release from stores .

The mechanism involved in Ca^{2+} influx into non-excitable cells is store operated Ca^{2+} entry (SOC). Following the depletion of intracellular stores, Ca^{2+} influx through SOC channels is fundamental for filling up the stores. Ca^{2+} influx is also important to maintain cytosolic Ca^{2+} concentrations for downstream signaling events **(Figure 5).**

Endothelial barrier function is vital in the regulation of tissue-fluid homeostasis, angiogenesis, and inflammation (Mehta and Malik 2006, Pober and Sessa 2007). Loss of endothelial barrier function following burn, trauma, or sepsis leads to acute lung injury (ALI), a life threatening condition due to respiratory failure (Matthay and Zemans 2011, Gonzales et al. 2014). A rise in intracellular free calcium concentration ($[Ca^{2+}]i$) caused by edemagenic agonists such as thrombin induces acto-myosin contraction in endothelial cells (ECs) leaving wide gaps between adjacent ECs (Mehta et al. 2003, Singh et al. 2007). These gaps, if not sealed, lead to elevated vascular permeability resulting in debilitating pulmonary edema. It is well-established that store-operated calcium entry (SOCE) activated upon depletion of Ca^{2+} from ER stores, plays a critical role in disrupting endothelial barrier function (Cioffi, Barry, and Stevens 2010, Moore et al. 2000).

STIM1 has been recently identified as a fundamental sensor of the Ca^{2+} concentration inside the ER lumen and thereby regulates SOCE in various cell types including ECs (Bird et al. 2009, Cheng et al. 2011, Hyser et al. 2013). It is a multi-domain protein containing a single transmembrane α-helix (Schindl et al. 2009). The N-terminus is located inside the ER lumen and consists of a Ca^{2+} binding EF hand and a sterile α-motif (or SAM domain) (Covington, Wu, and Lewis 2010, Zheng et al. 2008, Zheng et al. 2011). The transmembrane domain of STIM1 is flanked by an ezrin-radixin-moesin (ERM) motif known to interact with F-actin filaments (Ambily et al. 2014). STIM1's C-terminus is

composed of three coiled-coil (CC) domains, a COOH-terminal inhibitory domain (CTID), serine-proline rich (S/P) and threonine-arginine-isoleucine-proline (TRIP) regions and a lysine rich region (E-region) (Covington, Wu, and Lewis 2010). Mutational and molecular modeling analysis identified a stretch consisting of ~100 amino acids, from 340 to 440 aa, spanning the CC2 and CC3 domains, referred to as STIM1–Orai1 activating region (SOAR) (also known as CRAC activating domain, CAD or CCb9), as an essential domain for STIM1 oligomerization and activation of SOCE via Orai1 (Huang et al. 2006, Kawasaki, Lange, and Feske 2009, Korzeniowski et al. 2010, Yu et al. 2011).

Orai1 is the predominant pore-forming subunit in highly calcium-selective channels known as Ca^{2+}-release activated Ca^{2+} channels (CRAC) in various cell types including ECs (Abdullaev et al. 2008). Thus, the current model of SOCE activation by STIM1 indicates that upon store depletion, STIM1 undergoes conformational changes within its EF-SAM domains allowing long-range regulation within the CC1 domain that extends and organizes the SOAR domain to form discrete puncta. These puncta are then recruited towards the plasma membrane where STIM1 interacts with Orai1 to trigger SOCE (Putney 2005). The fundamental question whether the interaction between the STIM1 and Orai1 is regulated by intracellular signaling remains unanswered. STIM1 was discovered as a phosphoprotein. Studies so far have focused on the role of phosphorylation of serine residues located within the S/P stretch of STIM1 in dissociating STIM1 from microtubule end-binding protein as a mechanism of STIM1 modulation of Ca^{2+} entry and cell proliferation.

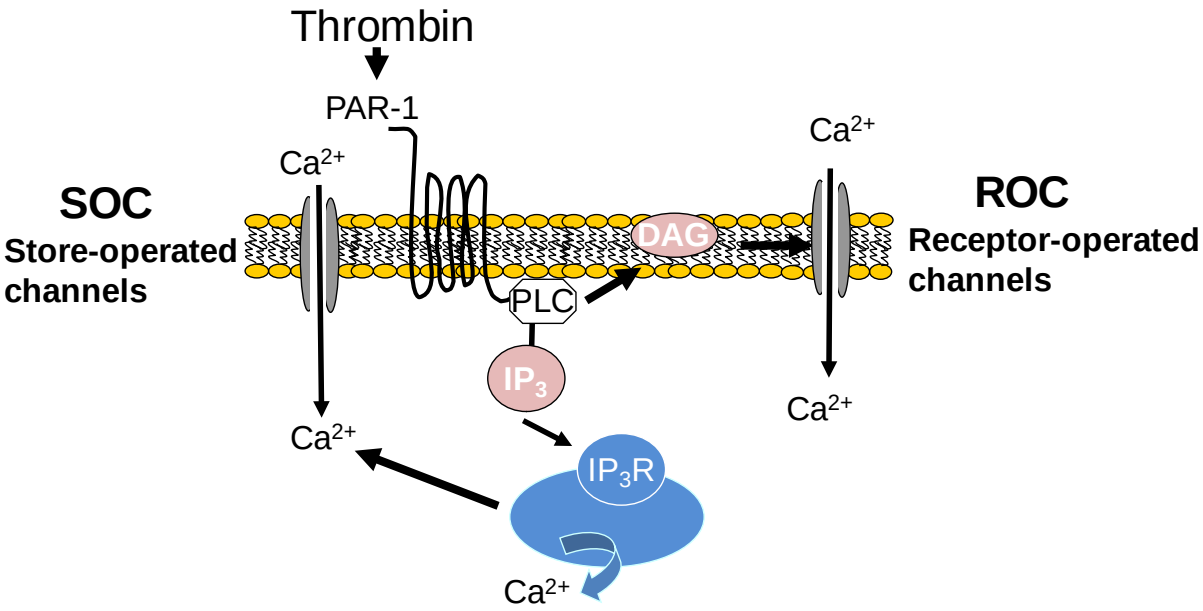

Figure 5. Schematic of Ca^{2+} signaling. Upon EC stimulation such as thrombin and activation of PLC, IP3 is generated and bound to IP_3R recptor on endoplasmic reticulum leading to Ca^{2+} store depletion and activation of SOCE and replenishing Ca^{2+} storage. PLC also generates diacyl glycerol to activate receptor operated channels to induce Ca^{2+} entry. Mehta D, Unpublished.

6. Cross-talk between FAK, S1PR1 and Ca^{2+} signaling

S1PR1 couples to $G_{i/o}$ alpha subunit of heterotrimeric G proteins, thus inhibiting adenylyl cyclase, resulting in attenuation of cAMP generation. S1PR1 signaling induces an increase in intracellular calcium, and can stimulate rat sarcoma (Ras) family of small GTPases and extracellular signal-regulated kinase (ERK) to induce proliferation and activation of phosphatidylinositide 3-kinase (PI3K)/Akt (protein kinase B) to inhibit apoptosis. FAK also regulate calcium signaling by suppressing RhoAGTPases (Knezevic et al. 2009). Schmidt et al. have demonstrated that loss of endothelial FAK alters the balance between RhoA and Rac1 small GTPases. One of the mechanisms by which RhoA gets activated is via increase in intracellular calcium concentration.

Mechanisms Regulating S1PR1

1. Post translational modification of S1PR1

Binding of S1P to S1PR1 causes receptor internalization and was reasoned to result in functional antagonism and/or constant signaling. Agonists binding to S1PR1 results in serine phosphorylation at the C terminus and subsequent internalization by β-arrestin pathway (Oo et al. 2011). Although S1P ligation results mostly in receptor internalization and recycling of S1PR1 back to the membrane, binding of pFTY720 to S1PR1 induces receptor internalization with subsequent WWP2 (a ubiquitin E3 ligase)-dependent degradation (Oo et al. 2007). Chavez et al. demonstrated a new mechanism of phosphorylation dependent regulation of S1PR1. They showed that Tyrosine phosphorylation at Y143 residue is important in maintaining cell surface receptor

expression. Rendering S1PR1 phosphor-defective by Y143->F substitution enhanced cell surface localization and persistent closure of endothelial junctions after S1P stimulation (Chavez et al. 2015).

2. Transcriptional regulation of S1PR1

The discovery of the orphan G-protein-coupled receptor initially identified as endothelial differentiation gene 1 (EDG1) paved the way to understand the biological functions of S1P (Hla and Maciag 1990). Endothelial cells express multiple S1PRs based on tissue distribution. In the lung, the predominant S1PR is S1PR1. S1P ligates with high affinity to S1PR1 to induce barrier protection by inducing Rac1-GTPases and cortical actin rearrangement (Mehta and Malik 2006, Dudek et al. 2004). Although S1PR2 and S1PR3 are expressed in endothelial cells, however, S1P mediated barrier enhancement is mediated through S1PR1. Studies have shown that knockdown of S1PR1 in human umbilical vein derived endothelial cells (HUVECs) induces adherens junction disruption and decrease in VE-cad expression after LPS or TNF-α stimulation (Krump-Konvalinkova et al. 2005). S1P/S1PR1 stimulation protects against vascular permeability and alveolar edema in preclinical mouse models of ARDS and ALI, suggesting that activating S1P/S1PR1 signaling would be beneficial in subjects of ALI and ARDS (Wang et al. 2014). Although S1PR1 transcription by signal transducer and activator of transcription factor a (STAT3) and Krüpple-like factor 2 (KLF2) is studied in immune cells (Bai et al. 2007, Lee et al. 2010), little is known about the transcriptional regulation of S1PR1 in endothelial cells. Cai et al. have shown that transcription factor forkhead box F1 (FOXF1) induces the transcriptional activity by binding to S1PR1 promoter in HUVECs (Cai et al.

2016). He et al. also demonstrated that Related Trancriptional Enhancer Factor 1 (RTEF-1) is capable of enhancing S1PR1 expression by binding to its promoter (He et al. 2014). Schmidt et al. have shown that FAK negatively regulates the activity of p38 MAPK by altering the balance between RhoA and Rac1 GTPase shifting towards Rac1 (Schmidt et al. 2013) and suppressing activating transcription factor 2 (ATF2) activitiy. It has been shown that KLF2 suppresses ATF2 activity by repressing its upstream activator p38 MAPK. Thus, we hypothesized that KLF2 could be a potential transcription factor that induces S1PR1 transcription in endothelial cells.

A. KLF2 as a key factor regulating EC barrier

1. Historical background

"Krüppel", the German word for "cripple" is a crucial transcription factor which contributes to the development of *Dosophila* (Jackle et al. 1985). This protein is named after *Drosophila* embryos lacking the protein Krüppel with malformed thoracic and abdominal segments where the legs should extend from, which results in lethality (Preiss et al. 1985). Mammalian nomenclature of Krüppel-like factor (KLF) family is derived from the homology to the DNA-binding domain of the *Drosophila* Krüppel. In 1993, erythroid Krüppel-like factor (EKLF/KLF1) was identified in red blood cells (Miller and Bieker 1993). It was shown to play a crucial role in β-globin gene synthesis and erythrocyte generation (Nuez et al. 1995, Perkins, Sharpe, and Orkin 1995). To date, there are about 17 mammalian Krüppels identified and named chronologically based on the discovery order (ie, KLF1-17). KLFs play a major role in regulating several cellular processes in various

cell types, as shown by gene knockout studies (Feinberg et al. 2004, Suzuki et al. 2005). Endothelial cells express KLF2, KLF4 and KLF6.

KLFs belong to zinc finger family of DNA-binding transcription factors (Suzuki et al. 2005). The C terminus of KLF protein harbors 3 Cys2/His2 zinc finger motifs, that binds the consensus sequence “CACCC” or the “GT box” at the promoter regions of its target genes (Dang, Pevsner, and Yang 2000). The inter-finger-space sequence contains a stretch of highly conserved 7-aa sequence, TGEKP(Y/F)X. Despite the similarity in the C terminus domains, KLFs have highly diverse N termini (Atkins and Jain 2007). The transactivation of KLFs to the target promoters is mediated by their multiple activation or repression domains residing in the N terminus (Atkins and Jain 2007) **(Figure 6).**

KLF2 was first cloned by the Lingrel group in 1995 (Anderson et al. 1995). This 354-aa protein was initially named as lung Kruppel-like factor (LKLF) because it is highly expressed in the lung tissue. Human KLF2 maps to chromosome 10p13.1 and has more than 85% sequence similarity to the mouse gene. Moreover, KLF2 promoter shares exact identity of 75-bp sequence conserved across species (Conkright, Wani, and Lingrel 2001). The N-terminal regulatory region includes the transcriptional activation domain (1-110 aa) and an inhibitory domain (110-267 aa) (Conkright, Wani, and Lingrel 2001, Wani, Wert, and Lingrel 1999). The activation domain interacts with coactivators such as p300/CBP, and the complex is capable of remodeling chromatin (Chen, Bacanamwo, and Harrison 2008). On the other hand, the inhibitory domain interacts with WW domain-containing E3 ubiquitin protein ligase 1 (WWP1), leading to ubiquitination and proteosomal degradation

of KLF2 (Conkright, Wani, and Lingrel 2001, Zhang, Srinivasan, and Lingrel 2004).

During embryonic development of mice, KLF2 is initially noted at embryonic day 7 (E7), then subsides by day 11 and reactivated at day 15 suggesting KLF2 plays an important role during embryo development and that its expression is regulated tightly (Anderson et al. 1995). The phenotype of KLF2 knockout mice exhibit abnormal blood vessel formation due to lack of smooth muscle cell recruitment, thus leading to embryonic hemorrhage and death between day 12.5 and 14.5 (Anderson et al. 1995, Wani, Means, and Lingrel 1998). KLF2 knockout mice also display an abnormal lung morphogenesis supporting the importance of this factor in lung development (Kuo et al. 1997, Wani, Means, and Lingrel 1998). EC specific KLF2 knock out mouse is embryonically lethal due to heart failure attributed to reduce vessel tone but not vascular defects (Lee et al. 2006). Van Thienen and colleagues showed that KLF2 expression is limited to the human aortic endothelial and that KLF2 expression is decreased at branch points which are shown to be prone to atherosclerosis in humans (van Thienen et al. 2006).

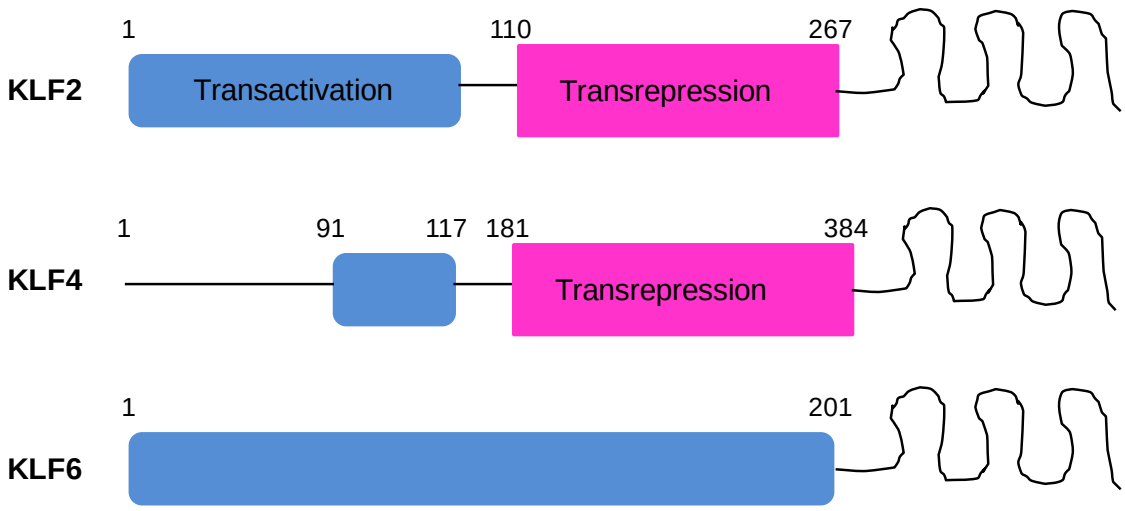

Figure 6. KLF family of transcription factors. The blue represents the activation domain of KLF and the pink is the repression domain. The C terminus is the zinc finger domain represented by the convoluted lines.

2. Role of KLF2 in endothelial cells

Dekker *et al*. in 2002 first showed that KLF2 knockdown inhibited flow-mediated induction of eNOS and flow-induced reduction of endothelin-1, which is the first evidence of KLF2 regulating flow-mediated effects in ECs (Dekker et al. 2002). Emerging studies demonstrates that KLF2 is a critical integrator of various endothelial functions (anti-inflammation, anti-angiogenesis, anti-thrombosis, vascular tone, blood vessel development). For example, KLF2 inhibits NFκB-dependent vascular cell adhesion molecule 1 (VCAM-1) and E-selectin expression in response to inflammatory cytokines (SenBanerjee et al. 2004). KLF2 also inhibits transforming growth factor (TGF)-β mediated signaling by suppressing the levels of phosphorylated activating transcription factor 2 (ATF-2) (Fledderus et al. 2007)**(Figure 7).**

3. Regulation of KLF2 expression in endothelial cells

a. Flow regulation of KLF2

Laminar flow is thought to be important for endothelial cells while disturbed flow contribute to atherogenesis in atheroprone regions. Using gene analysis profiling approach, Horrevoets identified that KLF2 is induced by prolonged laminar flow in cultured ECs (Dekker et al. 2002). Parmar et al. showed flow-dependent expression of endothelial KLF2 in vivo using *sih* zebrafish mutant, that lacks blood flow (Parmar et al. 2006). *In vitro* and *in vivo* experiments indicate that KLF2 exhibits sustained induction under laminar shear stress. Furthermore, Wang *et al*. noted that pulsatile flow induced sustained expression of KLF2, but the oscillatory flow caused suppression in ECs (Wang et al.

2006).

b. MEF2, a key transcription factor of KLF2

Many investigators used promoter analysis to elucidate the mechanism of flow-mediated KLF2 induction. In 2004, Huddleson et al. uncovered a 62-bp shear stress-responsive region in the KLF2 promoter region that harbors a 30-bp (-138 to -108 bp) palindrome motif (Huddleson et al. 2004). Deleting this site did not upregulate KLF2 expression by shear stress. The authors found a consensus myocyte enhancing factor 2 (MEF2) binding site (CTAAATTTAG) in this region. Chromatin immunoprecipitation (CHIP) experiments revealed both MEF2A and MEF2C bind to this region of KLF2 promoter in endothelial cells (Parmar et al. 2006).

MEF2 are members of the MADS box (MCM1, Agamous, Deficiens, Serum response factor) family of transcription factors that bind to A/T-rich sequences (McKinsey, Zhang, and Olson 2002, Naya and Olson 1999). MEF2 family of human transcription factors comprises of four proteins, MEF2A, -B, -C and –D, each has homolog in other vertebrates(Potthoff and Olson 2007). MEF2A and –C have very similar sequences (Wu et al. 2011). All MEF2 proteins have three domains: N-terminal DNA-binding MADS domain, central MEF2 region and a C-terminal transactivation domain (Potthoff and Olson 2007). MEF2 was initially identified as a key transcription factor that activates the expression of structural genes in skeletal and cardiac muscle cells (Black and Olson 1998). Recently, MEF2 transcription factor was found to be required for EC proliferation and viability and involved in the pathogenic mechanisms attributed to endothelial disorders (Olson 2004).

For instance, mutations in *mef2a* gene in humans have been observed in patients with inherited coronary artery disease (Lin et al. 1998, Olson 2004). mef2c knockout mouse is lethal with prominent cardiac and vascular defect due to impaired endothelial permeability and integrity (Bi, Drake, and Schwarz 1999).

The discovery of MEF2 factors as regulators of KLF2 expression provided a strong link to flow. Berk group, in 1999 identified ERK5 (also known as big mitogen-activated protein kinase 1) as a highly flow-induced factor (Yan et al. 1999). MEF2 is one of the well established targets of ERK5 (Kato et al. 1997, Yang et al. 1998). ERK5 is capable of greatly enhancing the transactivation activity of MEF2C by phosphorylating MEF2C at Ser 387 and Thr 300 and MEF2A at Ser 355, Thr 312 and Thr 319 both *in vitro* and *in vivo*. In Yeast 2-hybrid screening and co-immunoprecipitation experiments also revealed that ERK5 and MEF2C interact with each other. Furthermore, loss-of-function studies performed by the Winoto group showed that ERK5 is essential for embryonic KLF2 expression and that KLF2 transcription is driven by ERK5 by activating MEF2 transcription factors. Parmar et al. showed that overexpressing dominant-negative MEF2 or mutant MEK5 (an upstream activator of ERK5) prevented flow-mediated induction of KLF2 expression in endothelial cells. These results indicated that activation of a MEK5/ERK5/MEF2 pathway is attributed to mechanisms linking shear stress and KLF2 expression (Parmar et al. 2006).

Several transcription factors (TFs), in addition to MEF2 bind to the KLF2 promoter identified by using DNA affinity chromatography and mass spectrometry. These factors include p300/CBP-associated factor (PCAF), nucleolin and heterogeneous nuclear

ribonucleoprotein D (hnRNP D). Furthermore, these proteins were found to be required for the shear induction of KLF2 by chromatin immunoprecipitation and gel-shift analysis. Shear stress mediates the binding of this complex through a phosphoinositide-3 kinase (PI3K)-dependent/Akt-independent pathway (Pon and Marra 2016).

c. Post-transcriptional regulation of KLF2; Role of miRNA

MicroRNAs (miRNAs) have emerged as key regulators at the post transcriptional level. miRNAs are (20-23 nt), single stranded RNA molecules found endogenously that regulate gene expression by degradation of mRNA to prevent translation(Liu et al. 2012, Quarles et al. 2013). In humans, miRNAs are postulated to control more than 60% of all protein-coding gene activities and affect multiple cellular pathways such as cardiovascular diseases, cancer as well as development by binding to the 3'UTR regions of genes. Many miRNAs have exhibited their ability to regulate gene expression of KLF2. Among these miRNAs, miR17-92 family of miRNAs which are highly expressed in endothelial cells. Many investigators have shown that miR-92a is the major regulator of KLF2 expression in immune as well as endothelial cells. (Wu et al. 2011).

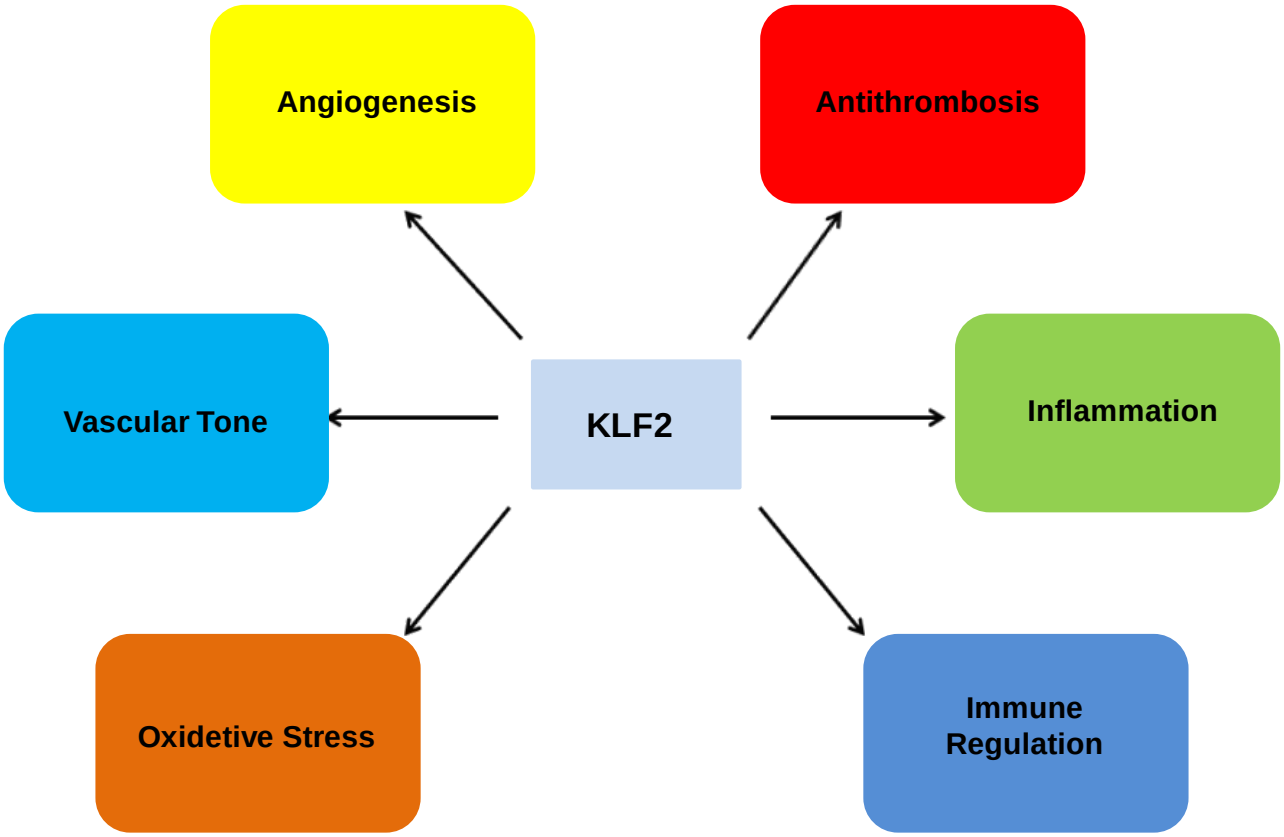

Figure 7. Role of KLF2 in endothelial cell biology. KLF2 plays a central role in suppressing inflammation, thrombosis and endothelial barrier disruption by promoting signaling pathways which protects and supports barrier integrity thus providing a critical mechanism to protect against acute lung injury and other vascular related anomalies.

B. DNA Methylation

Epigenetics is the study of mechanisms that can change DNA and pass to next generation without a change in DNA sequence. Sharma et al. provided a more precise definition which is: “The study of heritable changes in gene expression that occur independent of changes in the primary DNA sequence”. They described four major categories of epigenetics: covalent histone modifications, non-covalent mechanisms, DNA methylation, and non-coding RNAs (Castillo-Aguilera et al. 2017).

DNA methylation is catalyzed by DNA methyltransferases (Dnmts), is a mechanism that regulates the repertoire of progeny cells. This modification converts cytosine to 5’methyl-C, which is solely restricted to CpG dinucleotides in mammalian Gdna (genomic DNA). CpG islands are stretches of DNA with at least 500bp length, CG content of ≥55%. About half of the genes have CpG islands in their promoter region, and methylation of them is frequently associated with gene silencing (Bird 1986).

1. Basic functions of DNA methylation

Methylated cytosine was first reported in 1948 by using paper chromatography. Methylated CpGs are mainly located within repetitive elements such as SINEs, LINEs, LTR, etc and coding regions of genes (Bestor 2000). Mammals have several members of DNMTs, DNMT1, DNMT3a and DNMT3b with respective characteristics in catalyzing the attachment of methyl-group to the 5’-cytosine (Bestor 2000). All DNMTs are important for normal development. Mice lacking DNMTs die at fetal stage or early birth. DNMT3 family members are responsible for establishing initial CpG methylation patterns *de novo*,

whereas Dnmt1 is regarded as the maintenance enzyme with greater affinity for the hemi-methylated DNA. It maintains methylated patterns by working with proliferating cell nuclear antigen (PCNA) and the replication fork. The binding of DNMT1 with PCNA facilitates the different kinetics of the replication repertoire and DNA methylation, however, it is not absolutely require for methylation preservation.

In addition to DNMT3a and DNMT3b, the Dnmt3 family includes one regulatory factor, Dnmts-Like protein (Dnmt3L). Dnmt3a and Dnmt3b have similar domain structures **(Figure 8)** both contain a variable region at the N terminus, PWWP domain, a cystein rich Zn-binding domain (containing six CXXC motifs), and a C terminal catalytic domain. Dnmt3L is similar to the other DNMTs, but it lacks the conserved C-terminal catalytic domain (Lukasik et al. 2006). Most DNMT proteins share a common C-terminus that is responsible for the transferase activity, while the N-terminal of DNMT3A and DNMT3B consist of a cystein-rich domain and a tryptophan-rich (PWWP) domain which is required to direct the protein to major satellite repeats at pericentric heterochromatin (Lukasik et al. 2006). The N-termus of DNMT1 consists of different domains for its interaction with other proteins. There is a linker region between the N- and the C-terminus of the protein that is absent in other DNMT3's protein structure.

2. Recognition of methylation signals

Methyl-cytosine-binding proteins (MBPs) consist of three families of proteins which has high affinity for methylated CpGs: the MBD domain family, Kaiso and Kaiso-like proteins and SRA domain proteins. The MBD family is composed of methyl-CpG-binding

protein 2 (MeCP2), the methyl-CpG-binding-domain proteins MBD1, MBD2, MBD3 and MBD4 (Patel 2016). These proteins are involved in histone deacetylases and methyltransferases as transcriptional co-repressors. These proteins are expressed ubiquitously. MBD1 and MBD2 knockout mice are viable with mild phenotype, while MeCP2 knockout causes Rett syndrome, a neuro-developmental disorder. MeCP2 binds with high affinity to methylated CGs adjacent to four or more A/T bases. MBD1 also has high affinity to methylated CGs within TCGCA and TGCGCA sequences. Studies have shown that recognition of certain subsets of methylated regions for MBPs is dependent on their MBD domains and somehow has an overlapped target sites (Shimbo and Wade 2016).

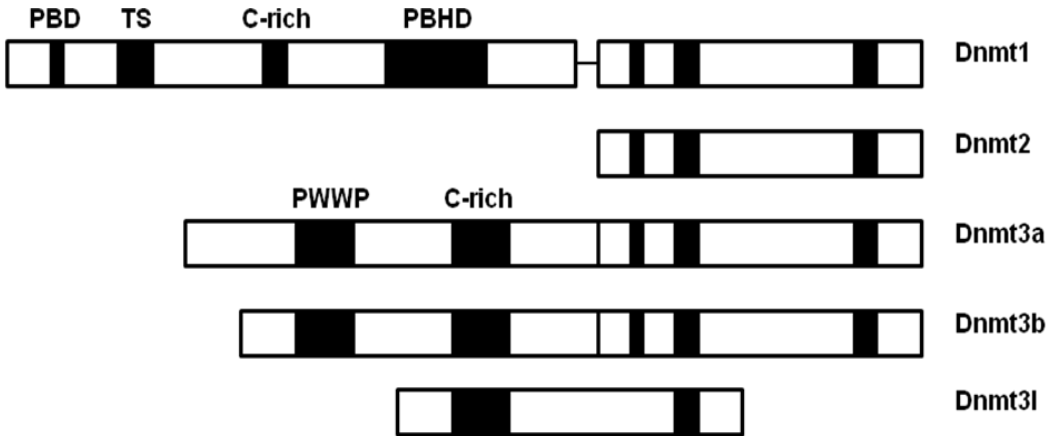

Figure 8. Structural differences of DNA methyltransferase. Most Dnmts have conserved C-terminus. The N-terminus of Dnmt1 has PCNA binding domain (PBD), a targeting sequence (TS), cysteine-rich region (C), a polybromo homology domain (PBHD); Dnmt3a and Dnmt3b contain a tryptophan-rich region (PWWP). There is a stretch of (GlyLys)6 repeat between the N- and C-terminus of Dnmt1.

II. EXPERIMENTAL DESIGN

Materials and methods used for experiments and results that are described in both sections of Chapter III.

A. Materials. Human pulmonary arterial endothelial cells (HPAECs), endothelial growth medium (EBM-2), Nucleofector kit, and Amaxa electroporation kit were obtained from Lonza. Alexa-fluor–568 and –488 conjugated secondary antibodies and ProLong Gold antifade were obtained from Invitrogen. Primary antibodies against FAK, Actin, and GFP were purchased from Santa Cruz Biotechnology. DNMT1 antibody was obtained from Active motif, DNMT3A was purchased from Cell Signaling and DNMT3B was purchased from Santa Cruz. S1PR1 antibody was obtained from Alomone lab (Jerusalem). SiRNA for FAK, Pyk2, and control siRNA were purchased from Dharmacon. S1P was purchased from Enzo Life Sciences. FUGENE transfection reagent was purchased from Promega (Madison, WI, USA). Primary antibodies against phospho-tyrosine (PY20, PY99, and PY350), Orai1, Stim1, GFP as well as A/G agarose beads were purchased from Santa Cruz Biotechnology (Santa Cruz, CA, USA). Phospho-Pyk2 and pan Pyk2 antibodies were purchased from Cell Signaling Technologies (Beverly, MA, USA). Thapsigargin was purchased from EMD Millipore (MA, USA). Paraformaldehyde was purchased from Fisher Scientific (Hampton, NH, USA). Fura 2-AM was purchased from Life Technologies (Carlsbad, CA, USA).

B. Animals. Generation and characterization of *EC-FAK*$^{-/-}$ is described earlier. All animal experiments were approved by the University of Illinois and Institutional Animal

Care and Use Committee. $FAK^{fl/fl}$ and *EC-FAK*$^{-/-}$ mice (6-7 week old) used in all experiments were C57blk/6J background. *EC-STIM1*$^{-/-}$ mice were generated by crossing $STIM1^{fl/fl}$ with Tie2-cre. C57BL/6J was purchased from Jackson's lab. All experiments were done on 6-8 weeks old mice.Liposomal delivery of cDNA into the mouse lung and lung vascular permeability measurements were performed in accordance with the IACUC.

C. Cell culture. Mouse lung endothelial cells (LECs) were isolated as described previously. Briefly, lungs from $FAK^{fl/fl}$ mice were harvested, minced and digested with collagenase for 60 min at 37°C with gentle rocking. Tissue was triturated using 15mm canula and centrifuged at 3000 rpm. The cell suspension was incubated with anti-mouse PECAM-1 (CD31) antibody (BD Pharminigen)-coated Dynabeads for 12 min with rocking at room temperature. Bead-cell complexes were washed multiple times to remove unbound cells. Cells were cultured with high glucose DMEM medium containing endothelial cell growth supplement. ECs were characterized by their cobblestone morphology, as well as VE-cadherin expression. Human pulmonary artery endothelial cellc (HPAECs) were cultured in a T-75 flask coated with 0.1% gelatin in EBM-2 medium containing 10% fetal bovine serum and endothelial cell growth supplements and maintained at 37°C in a humidified atmosphere of 5% CO2 and 95% air until they formed a confluent monolayer. Cells from the primary flask were detached using 0.05% Trypsin containing 0.02% EDTA and plated on appropriate tissue culture dishes for experiment. HPAECs between passages 6 and 8 were used. HPAE cells were transfected using Fugene (promega), santa cruz transfection or nucleofactor from

Lonza. . HEK cells were plated on 100 mm dishes and cultured using DMEM medium supplemented with 10% fetal bovine serum (FBS) till confluent.

D. Immunofuorescence staining. HPAECs transducing siSc or siFAK, or cells expressing indicated cDNA, were fixed, permeabilized, and stained with appropriate antibodies against FAK, CD31 and VE-cad (Santa Cruz). Nuclei were visualized using DAPI (life technologies). Immunostained ECs were visualized using a 63x 1.2 NA objective on a LSM confocal microscope (Carl Zeiss, Inc.). Inter-endothelial gap area was quantified using ImageJ software.

Cells seeded on 35 mm glass bottom dishes were co-transfected with Orai1-mCherry and YFP-STIM1 or YFP-STIM1-Y361F mutant using FUGENE. After 24 h, cells were serum starved for an hour in 0.1% FBS after which cells were treated with 2 μM thapsigargin for 5 min or left untreated. Cells were fixed with 4% formaldehyde and imaged using a LSM 880 inverted confocal microscope (Carl Zeiss) equipped with a Plan-Apochromat 63x/1.4 NA oil immersion objective, an Argon (λ=458, 488, 514nm) and diode-pumped solid-state laser (λ=561nm), 2 photomultiplier tubes and Gallium arsenide phosphide detector. EYFP images were acquired with λ=514-nm excitation and λ=519 – 583 nm emission; mCherry images were collected with λ=561 nm excitation and λ=583 – 696 emission.

The 16-bit images were analyzed with Metamorph (Molecular Devices, Sunnyvale, CA) and ImageJ (NIH) software. Projected images were generated by collecting maximum pixel intensity of the in-focus frames into a single frame. The

images were threshold to remove background fluorescence and used to create a mask image. Using the mask images, number of Orai1-mCherry and YFP-STIM1 clusters was scored with automatic “Analyze Particles” algorithm of ImageJ software and using cluster size of 3– 100 pixels and circularity 0.1 – 1.0. The data were expressed as the number of clusters per area (μm^2) of the cell.

Colocalization coefficient for Orai1-mCherry was determined using Z-stack images and Zen software (Carl Zeiss) according to the manufacturer’s instructions. Threshold images were used to set the vertical and horizontal crosshairs to separate clusters into quadrants. The colocalization coefficient was calculated as the sum of colocalized pixels divided by the total number of Orai1-mCherry clusters. All images were prepared for publication using Adobe Photoshop.

E. Liposomal delivery of cDNA in the mouse lung. Cationic liposomes were made using a mixture of dimethyldioctadecyl-ammonium bromide and cholesterol in chloroform (Tauseef et al. 2008). VE-cad-GFP, VE-cad -S1PR1-GFP, and (50-70µg) were mixed with 100 µL of liposomes. The mixture of liposomes and cDNA were injected intravenously (via retroorbital injection) into *FAK*$^{fl/fl}$ or *EC-FAK*$^{-/-}$ mice. Similarly, VE-cad-YFP, VE-cad-STIM1-YFP and VE-cad-Y361STIM1-YFP vectors were injected into WT, *STIM1*$^{fl/fl}$ or *EC-STIM1*$^{-/-}$ mice. After 48 h, mouse lungs were used for determining lung microvascular permeability or protein expression.

F. Immunoprecipitation. Cells were lysed in radioimmunoprecipitation buffer (50 mM Tris, pH 7.4, 1% deoxycholic acid, 150 mM NaCl, 0.25 mM EDTA, pH 8.0, 0.5%

Nonidet P-40, 0.1% SDS, 1mM NaF, 1 mM sodium orthovanadate,1 mM phenylmethylsulfonyl fluoride, and 2g/ml of (leupeptin, aprotinin, and pepstatin A) and were incubated with indicated antibodies overnight at 4 °C. After 24 h, lysates were coupled to protein A/G-agarose beads for 4 h at 4 °C. The beads were then collected by centrifugation at 3000 rpm for 3min and washed three times using detergent-free radioimmunoprecipitation buffer. Phosphotyrosine of STIM1 was detected using a mixture of anti-PY20, anti-PY99 and anti-PY350 in equal proportion.

G. Western blotting. For deletion of FAK, LECs were infected with 25 PFU/cell β-Gal (control) or Cre recombinase adenoviruses in 0.1% serum containing and antibiotic-free media for 6 h after which cells were refreshed with complete media containing growth factors, 20% serum and antibiotics. Experiments were performed 60-72 h post-infection when we observed maximal FAK deletion. HPAECs were transfected with scrambled or FAK siRNA (5'-GCAUGUGGCCUGCUAUGGA-5' sense and 5'-UCCAUAGCAGGCCACAUGC-3' antisense) or siPYK2, using Nucleofector kit and electroporation system from Lonza following manufacturer's protocol. Cell lysates assessed for FAK expression 24, 48, and 72 h post transfection showed maximal FAK knockdown at 72 h. performed at this time point. Pyk2 expression was determined after 48 hrs.

H. Quantitative Real-Time PCR. Total lung RNA was isolated with TRIzol reagent (Invitrogen) according to manufacturer's instructions and quantified spectrophotometrically. For qRT-PCR, RNA was reverse transcribed using a High Capacity cDNA reverse transcription kit based (Applied Biosystems). cDNA was used

for PCR amplification using the Applied Biosystems c DNA synthesis kit following manufacturer's protocol. All experiments were analyzed on Biosystems Sybr green and ABI Prism 7000 Sequence Detection System. For primer list see supplement S1. Gene expression was normalized using GAPDH as an internal control.

I. Bisulfite Conversion of DNA and methylation specific PCR (MS-PCR). DNA methylation was quantified at the promoter of KLF2 by bisulfite conversion of the DNA. EpiTect Plus Lyse All Bisulfite Kit (Qiagen, Valencia, CA, USA) was used for the bisulfate conversion. After sodium bisulfite conversion, DNA was collected into an EpiTect spin column and washed. The converted DNA was eluted following manufacturers protocol. PCR reaction was performed for methylated (M) and un-methylated (U) regions. Thermal cycling conditions included 94^0C for 5 minutes, 35 cycles of 94^0C for 1 minute, 55^0C for 30 seconds, 72^0C for 1 minute, and final extension at 72^0C for 10 minutes. The PCR products were analyzed on 2% agarose gel and the intensity of methylated bands to unmethylated bands were quantified using Image J, gel analyzing software.

J. Chromatin Immunoprecipitation (ChIP) Assay. Protein-DNA complex (100–120 µg) was immunoprecipitated with the antibody against MEF2 (MEF-2 (C-21): sc-313 (Santa Cruz Biotechnology, Santa Cruz, CA). DNA fragments were collected by phenol– chloroform–isoamyl alcohol extraction, followed by ethanol precipitation, and then resuspended in 14 µl water for PCR. Promoter region of KLF2 targeted a 169 bp fragment was quantified by Syber green-based real time quantitative PCR (q-PCR) using ViiA7 (Applied Biosystem, Foster City, CA). Normal rabbit IgG was used as

negative antibody control and DNA from the input (20–40 µg protein-DNA complexes) was exploited as an internal control.

K. Construction of VE-Cadherin promoter driven constructs. Full length human VE-Cadherin promoter, 3.5kb fragment of Human Chromosome 16 with GenBank Accession number NC_000016 from base pairs 66,397,084 to 66,400,592, was subcloned into PGL4.10 vector, a basic vector lacking a promoter while containing the luciferase reporter gene *luc 2* (Photinus pyralis) (Promega, Madison, WI) via restriction site *Sac I*. The human VE-Cadherin promoter was PCR-amplified from human genomic DNA, digested with *Sac I* restriction enzyme (NEB-New England Biolabs, Ipswich, MA), and ligated using T4 DNA Ligase (NEB) to PGL4.10 vector that was also digested with *Sac I* and treated with Calf Intestinal Alkaline Phosphatase (NEB). The ligated reaction was transformed into DH5α Subcloning Effiency Competent Cells (ThermoFisher Scientific, Grand Island, NY). The transformed cells were plated onto LB plates supplemented with 100 mg/ml Ampicillin (ThermoFisher). After overnight incubation at 37^{o}C, single colonies were cultured in LB with 100 mg/ml Ampicillin overnight. Plasmid DNA was obtained using GeneJet Plasmid Miniprep kit (ThermoFisher Scientific) and analyzed by restriction digestion to confirm the correct size of the VE-Cadherin promoter. Further amplification of the plasmid DNA was done using NucleoBond Xtra Midi Kit (Clontech Laboratories, Mountain View, CA). The resulting plasmid was verified for DNA purity and identity by DNA quantification, gel analysis, and sequencing analysis.

PGL4-VECP-GFP

GFP (Green Fluorescent Protein) was PCR-amplified using the pEGFP-N1 vector as the DNA template (Clontech Laboratories, Mountain View, CA). The GFP amplicon was digested and ligated to PGL4-VECP vector via *5'-Xho I* and *3'-Hind III* restriction sites The ligated reactions were transformed after which single colonies were screened and plasmid DNA was prepared as previously described. The GFP or YFP was engineered to be in frame and upstream of the luciferase reporter protein *luc 2* in the PGL4.10 vector. The primers used for amplifying GFP were GFP-start-*XhoI*-F: 5'-AAAAAA***CTCGAG***AGGCACCATGGTGAGCAAGG-3' and GFP-NoSTOP-*HindIII*-R: 5'-CCACCA***AAGCTT***GCTTGTACAGCTCGTCCAT-3'. In the primers, the bold and italicized base pairs indicated restriction sites.

PGL4-VECP-S1PR1-GFP

Human S1PR1-GFP was used as the DNA template to generate a PCR product containing flanking 5'-*Xho I* and 3'- *Hind III* restriction sites. The PCR product, S1PR1-GFP fusion with C-terminal tagged GFP, was then digested and ligated to PGL4-VECP vector via *5'-XhoI* and *3'-HindIII* restriction sites. The ligated reactions were transformed after which single colonies were screened and plasmid DNA was prepared as previously described. S1PR1-GFP fusion protein was engineered to be in frame and upstream of the luciferase reporter protein *luc 2* in the PGL4.10 vector. Primers used were S1PR1-Start-*XhoI*-F: AAAAAA*CTCGAG*AGGCACCATGGGGCCCAC -3' and GFP-NoStop-*HindIII*-R: 5'-CCACCA*AAGCTT*GCTTGTACAGCTCGTCCAT-3'.

PGL4-VECP-Y361F-STIM1-YFP

Generation of VE-cadherin promoter (VECP) driven control vector and Y361F-STIM1 mutant was performed as described (Prandini et al. 2005). Briefly, YFP- (Yellow Fluorescent Protein) was PCR-amplified using pEYFP-N1 as the DNA template (Clontech Laboratories, Mountain View, CA). YFP amplicon was digested and ligated to PGL4-VECP vector via *EcoRV*. The ligated reactions were transformed after which single colonies were screened and plasmid DNA was prepared as previously described. The YFP was engineered to be in frame and upstream of the luciferase reporter protein *luc2* in the PGL4.10 vector. The primers used for amplifying YFP were: YFP-ATG-*EcoRV*-F: 5'-TTTTTC*GATATC*AGCCACCATGGTGAGCAGCAAGGG-3' and YFP-NoSTOP-*EcoRV*-R: 5'-TTCTTC*GATATC*CTCTTGTACAGCTCGTCCATGCCG-3'; primers for amplifying YFP were YFP-start-*XhoI*-F: 5'-AAAAAA*CTCGAG*AGGCACCATGGTGAGCAAGG-3' was PCR-amplified using the pEGFP-N1 vector as the DNA template (Clontech Laboratories, Mountain View, CA). Primers used were STIM1-YFP-ATG-*EcoRV*-F: 5'-TTCTTC*GATATC*AGCCACCATGGATGTATGCGTCCG-3' and STIM1-YFP-NoStop-*EcoRV*-R: 5'-TTCTTC*GATATC*CTCTTGTACAGCTCGTCCATGCCG-3'.

L. Generation of pEGFP-C3-chFak-K454R. The mutation at K454R in chicken Fak was done using chFak as DNA template in a 2 step PCR. In the first PCR step, two sets of primers were used to generate DNA fragments "a" and "b" containing the K454R mutated site. In the second PCR step, the final DNA fragment "c" was generated by combining DNA fragments "a" and "b" in the PCR using a set of primers

that included the flanking 5'-*Xho I* and 3'-*Sac II* restriction sites. Primer sets used to generate fragment "a" were: chFak-ATG-XhoI-F: 5'-ATTA*CTCGAG*GGGGCCATGGAGCGAGT-3' and chFak-K454R-R: 5'-GTTTTTACATGTTCGGATTGCTACAGCCAT-3'; primer sets for fragment "b" were: chFak-K454R-F: 5'-GCTGTAGCAATCCGAACATGTAAAAACTGC-3' and chFak-Sac2-R: 5'-ATTA*CCGCGG*TTAGTGGGGCCTGGACTG-3'. Fragment "c" was generated by using primers chFak-ATG-XhoI-F and chFak-Sac2-R. In the primers, the bold and italicized base pairs indicated restriction sites while the underlined base pairs the mutated K454R. The final PCR product "c" was then digested with *Xho I* and *Sac II* and ligated to pEGFP-C3 vector also digested with the same restriction enzymes. The ligated reactions were transformed after which single colonies were screened and plasmid DNA was prepared as previously described. In this plasmid, the GFP was N-terminally tagged to chicken Fak similarly to the pEGFP-C3-chFak wild type plasmid.

M. Generation of Orai1-mCherry and STIM1 mutants. Human Orai1 cDNA was obtained from Addgene, after which it was subcloned into pAmCyan-N1 vector from Clontech via 5'-*XhoI* and *3'- BamHI*. Briefly, PCR primers were designed with flanking restriction sites, 5'-*XhoI* and *3'- BamHI,* to amplify the full length Orai1. The PCR fragment was then digested 5'-*XhoI* and *3'- BamHI* and ligated to the vector pAmCyan-N1 also digested at the same sites 5'-*XhoI* and *3'- BamHI.* The resulting plasmid is pAmCyan-N1-Orai1 with the Cyan tag at the C-terminus of Orai1. The subcloning of mCherry-Orai1 was done by digesting the pAmCyan tag out of the pAmCyan-N1-Orai1 plasmid, and insert into its place, the mCherry tag. To do so, PCR primers were

designed to amplify mCherry from mCherry plasmid, pmCherry-C1, cat #632524, Clontech, with flanking restriction sites, *5'- AgeI* and *3'- NotI.* The PCR fragment was digested with*5'- AgeI* and *3'- NotI*. The vector pAmCyan-N1-Orai1 was digested also at the same sites *5'- AgeI* and *3'- NotI* to release the pAmCyan tag. The digested PCR fragment was then ligated to the digested vector. The resulting plasmid was mCherry-N1-Orai11. The PCR primers used were: for pAmCyan-N1-Orai1: Orai1-ATG-*XhoI*-F: 5'-AAAAAA*CTCGAG*GCCACCATGCATCCGGAGCCC-3' and Orai1-noStop-*BamHI*-R: 5'-GAAAAA*GGATCC*AAGGCATAGTGGCTGCCG-3'; and for mCherry-N1-Orai1: mCherry-*AgeI*-ATG-F: 5'-AAAAAA*ACCGGT*CGCCACCATGGTGAGCAAGGGC-3' and mCherry-STOP-*NotI*- R: 5'-GAAAAAGCGGCCGCTTTACTTGTACAGCTCGTCCAT-3'. Multi-step PCR was done to mutate the amino acids of wild type human STIM1 (GenBank Accession number NM_003156) in pEYFP-N1 vector (C-terminal tagged YFP vector from BD Biosciences- Clontech, Palo Alto, CA). The Y316F and Y361F mutation was done using a two-step PCR subcloning method, using pEYFP-N1-STIM1-WT (wild-type STIM1) as the DNA template for PCR reactions. In the first PCR step, two sets of primers were used to generate PCR fragments "a" and "b" containing the YF mutated amino acid. In the second PCR step, the final PCR fragment "c" was generated by combining PCR fragments "a" and "b" in the PCR using a set of primers that included the flanking 5'-XhoI and 3'-Bam HI restriction sites. Primer sets used to generate fragment "a" were: 5'-GGAGTAACGGTTCTGGATAAAGGCAAACCAGCA-3' hSTIM1-Y316F-F: 5'-GCGGAGCCGCCAAAAATTTGCTGAGGAGGAG-3'and hSTIM1-Y316F-R 5'-CTCCAACTCCTCCTCAGCAAATTTTTGGCGGCT-3'and hSTIM1-Y361F-

F: 5'-GAGGTGGAGGTGCAATTTTACAACATCAAGAAGC-3' and hSTIM1-Y361F-R 5'-TGCTTCTTGATGTTGTAAAAATTGCACCTCCACC-3' and hSTIM1-Y361D-F: 5'-GAGGTGGAGGTGCAAGATTACAACATCAAGAAGC-3' and hSTIM1-Y361D-R: 5'-TGCTTCTTGATGTTGTAATCTTGCACCTCCACC-3'. Fragment "c" was generated by using primers **hSTIM1-*XhoI*-F and hSTIM1-*BamHI*-R.** In the primers, the bold and italicized base pairs indicated restriction sites while the underlined base pairs indicated the mutated amino acid. The final PCR product "c" was then digested with XhoI and BamHI and ligated to pEYFP-N1 vector also digested with the same restriction enzymes to generate the resulting plasmid pEYFP-N1-STIM1mutants. The ligated reactions were transformed into DH5α Subcloning Effiency Competent Cells (ThermoFisher Scientific, Grand Island, NY). The transformed cells were plated onto LB plates supplemented with 25μg/ml Kanamycin (ThermoFisher). After overnight incubation at 37^{o}C, single colonies were cultured in LB with 25μg/ml Kanamycin overnight. Plasmid DNA was obtained using GeneJet Plasmid Miniprep kit (ThermoFisher Scientific) and analyzed by restriction digestion to confirm the correct size of the vector (pEYFP-N1) and insert (STIM1). Further amplification of the plasmid DNA was done using NucleoBond Xtra Midi Kit (Clontech Laboratories, Mountain View, CA). The resulting plasmid was verified for DNA purity and identity by DNA quantification, gel analysis, and sequencing analysis.

N. PGL4-S1PR1-promoter-mutant. 1085 base pairs of murine S1PR1 promoter with GenBank Accession AC_000025.1 from base pairs 122149859 to 122148840 was subcloned into PGL4.10 via 5'-Kpn I and 3'-Xho I. In this region, 3 KLF2 binding sites

that had the motif CACCC or GGGTG (for the opposing DNA strand) in murine S1PR1 promoter were identified and mutated to either AAAAA from CACCC or TTTTT from GGGTG. The mutations were done by multi steps PCR using the mS1PR1 promoter as the DNA template. In the first round 3 PCR fragments (a, b, and c) were made. PCR fragment "a" was generated using primer pair mS1PR1-mt1-F: 5'-GAGGAGGGTACCAGGGGACTTTTTTTGAACCACTTTTT-3' and mS1PR1-mt2-R: 5'-AAGTGGCTTTCCCTTTTTCACGGTGAAGTG-3'; PCR fragment "b" with primer pairs mS1PR1-mt2-F: 5'-CACTTCACCGTGAAAAAGGGGAAAGCCACTT-3' and mS1PR1-mt3-R: 5'-CTCCTCTTCCTCAAAAACCTCCACTCCGA-3'; and PCR fragment "C" with primer pairs mS1PR1-mt3-F: 5'-TCGGAGTGGAGGTTTTTGAGGAAGAGGAG-3' and GL3-2R: 5'-TTGGCGTCTTCCATGGTGGC-3'. The underlined and bold base pairs in the primers indicated the KLF2 binding site mutations. In the second round of PCR, DNA fragment "d" was made by combining DNA fragments "a" and "b" with primer pairs mS1PR1-mt1-F and mS1PR1-mt3-R; DNA fragment "e" was made by combining DNA fragments "b" and "c" with primer pairs mS1PR1-mt2-F and GL3-2R. In the third and final round of PCR, DNA fragment "e" was made by combining DNA fragments "d" and "e" with primer pairs mS1PR1-mt1-F and GL3-2R. The final DNA fragment "f" was digested with *Kpn I* and *Xho I* and ligated to PGL4.10 vector via 5'- *KpnI* and 3'- *XhoI* restriction sites. Further downstream transformation and DNA plasmid preparation steps were as previously described. The final plasmid DNA was subjected to DNA sequencing for verification of the mutations that were made.

O. Calcium imaging. Intracellular Ca^{2+} increase was measured using the Ca^{2+}-sensitive fluorescent dye Fura 2-AM. Briefly, HPAE cells were transfected with control or FAK siRNA for 72h or indicated constructs for 24 h or Orai1, Pyk2 siRNA for 48 h respectively. Primary cells were isolated from 6-9 days old $FAK^{fl/fl}$ pups as previously described (Tauseef et al. 2008) . Cells were then loaded with Fura 2-AM dye for 20 min, rinsed twice with Ca^{2+} free HBSS media and stimulated with thapsigargin 2 μM or thrombin 50 nM to determine Ca^{2+} release. Only YFP transfected cells were selected for Ca^{2+} measurement. Ca^{2+} entry was determined following addition of 2 mM Ca^{2+}. In each experiment, at least 5 YFP-tagged cells were imaged for Ca^{2+} analysis.

P. Lung vascular permeability. $FAK^{fl/fl}$ and *EC-FAK*$^{-/-}$, WT or EC-*STIM1*$^{-/-}$ mice were anesthetized with an i.p. injection of ketamine (100 mg/kg) and xylazine (2.5 g/kg). PAR1 agonist peptide (TFLLRN-NH2) or control peptide (FTLLRN-NH2) (1 mg/kg body weight) were administered into WT or EC-*STIM1*$^{-/-}$ through retroorbital route. 1μM SIP was administered to $FAKfl^{/fl}$ and *EC-FAK*$^{-/-}$. After 30 min, left lungs were excised and completely dried in a 60°C oven overnight for determining lung wet–dry ratio. All animals used in this study were approved by the Institutional Animal Care and Use Committee of (IACUC) University of Illinois.

Q. Statistical analysis. Graphs were generated using GraphPad Prism (GraphPad Software, La Jolla, CA). Comparisons between experimental groups were made using one way ANOVA followed by *t*-test or Tukey test. Significance values are shown by *$p < 0.05$, **$p < 0.01$, and ***$p < 0.001$

III. RESULTS AND DISCUSSIONS

A. Endothelial focal adhesion kinase regulates S1PR1 transcription

1. Specific Aim 1

To determine the role of FAK in regulating S1P mediated annealing of EC barrier.

2. Results

a. Depletion of FAK impairs S1P-annealing of AJs

We have previously shown that loss of FAK in lung endothelial exhibits hemorrhage, leukocyte infiltration and edema in mice. We and others have also shown that S1P reverses increases in lung microvessel permeability due to inflammatory mediators. Therefore, we wondered whether S1P could enhance lung vascular barrier function in EC-FAK$^{-/-}$mice. FAK$^{fl/fl}$ and EC-FAK$^{-/-}$ mice were injected with 1 μM S1P for 30 min, after which we harvested the lungs and quantified lung fluid accumulation as an index of lung vascular permeability. We found that although S1P could slightly decrease endothelial permeability in EC-FAK$^{-/-}$mice, levels were still significantly higher than those seen in control lungs **(Figure 9A).** Similarly, Human pulmonary artery endothelial cells (HPAECs) transfected with control (siSC) and FAK specific siRNA (siFAK) were stimulated with S1P for indicated time points. Cell lysates were analyzed for VE-cadherin and FAK expression to confirm that the loss of S1P-induced junction assembly in FAK knockdown cells was not because of decreased AJ protein levels **(Figure 9B and C).** Changes in endothelial barrier integrity

were determined by quantifying interendothelial gap area in monolayers immunostained with anti-VE-cadherin antibody. Consistent with our previous studies, S1P rapidly increased VE-cadherin accumulation at cell-cell junctions in control cells, thus decreasing the amount of intercellular gap area assessed using ImajeJ **(Figure 9D).** FAK knockdown basally increased interendothelial gap area, and S1P could not promote junctional VE-cadherin organization to minimize intercellular gaps **(Figure 9D).**

To further corroborate above findings, changes in endothelial permeability were monitored by assessing the increase in transendothelial electrical resistance (TER) after S1P challenge. In control (siSc) transducing cells, S1P stimulation induces a rapid increase in endothelial monolayer resistances. However, in siFAK transducing HPAECs, S1P fails to induce any barrier strengthening effects **(Figure 9E).** Thus, endothelial FAK is required for S1P-induced strengthening on the lung vasculature. Therefore, we sought to determine how endothelial FAK was mediating S1P- induced strengthening of the endothelium.

b. Depletion of FAK suppresses S1PR1 expression

Because S1P induces endothelial barrier enhancement by primarily activating S1PR1, we reasoned if S1PR1 expression was impaired in the absence of FAK. We observed that depletion of FAK in HPAECs markedly reduced S1PR1 both at mRNA and protein level whereas S1PR2 expression was not altered. Surprisingly, we observed an increase at the mRNA level of S1PR3 in FAK depleted ECs **(Figure 10A)**. Similarly, we harvested the lungs from *FAK*$^{fl/fl}$ and *EC-FAK*$^{-/-}$ and looked at S1PR1 expression.

Surprisingly, S1PR1 expression was significantly lower in *EC-FAK*$^{-/-}$ lungs compared to control mice suggesting that FAK regulates S1PR1 transcriptionally **(Figure 10B)**. We also assessed S1PR1 expression in FAK depleted cells. We show that loss of FAK in HPAE reduces S1PR1 protein expression significantly compared to control siRNA **(Figure 10C)**.

If S1PR1 is solely responsible of enhancing EC barrier after S1P in FAK depleted cells, we predict that transducing S1PR1 in FAK depleted ECs should restore the barrier leak. We plated HPAEs on electrodes and using siRNA approach we knocked down FAK in endothelial cells with and without S1PR1 and stimulated the cells with S1P. The mRNA expression of S1PR1 in FAK depleted cells was about 10 fold. As expected, FAK depleted ECs failed to respond to S1P. However, S1PR1 transduced FAK depleted cells responded to S1P similarly to that of the control cells **(Figure 10D-E)**. To address if S1PR1 expression is required to restore S1P mediated barrier enhancement in the absence of FAK, we transduced VE-cad driven vector or S1PR1 in FAK null lung using liposomes. After 48h we determined lung edema formation in *FAK*$^{fl/fl}$ and *EC-FAK*$^{-/-}$ mice transduced with either vector or S1PR1. As shown in **(Figure 10F)**, transduction of S1PR1 in lungs significantly decreased lung edema formation in FAK null mice. These results indicate that FAK regulates S1PR1 expression transcriptionally.

c. FAK regulates S1PR1 via KLF2

To assess the transcription by which FAK regulates S1PR1 expression, we analyzed transcription factor binding sites at S1PR1 promoter. KLF2, a well established transcription factor as a central regulator of endothelial cell functions, including

angiogenesis and cell migration and maintenance of EC barrier may induce S1PR1 transcription. We found that the mRNA expression of KLF2 which binds DNA at the same motif (CACCC) was significantly reduced in FAK depleted cells, while other transcription factors such as SOX2 and ERTF-1 which are known to induce S1PR1 were not changed **(Figure 11A)**.

To address the functional relevance of KLF2 mediated S1PR1 expression, we plated HPAECs on electrodes and used both control and FAK siRNAs to deplete FAK in endothelial cells. We transduced KLF2 into FAK knock down cells and after 24hrs we stimulated the cells with S1P. The RNA expression level of KLF2 was increase in FAK depleted cells. S1PR1 mRNA level was increased by 5 fold. As expected, FAK depleted ECs failed to respond to S1P and thus enhance the barrier. However, KLF2 transduced FAK depleted cells restored their S1P response to control levels suggesting KLF2 restored S1PR1 expression in FAK depleted ECs **(Figure 11B-C)**.

d. KLF2 directly binds to and induces the transcriptional activity of S1PR1 promoter

Because lack of KLF2 was associated with decreased S1PR1 expression in vivo and in vitro, we investigated whether KLF2 directly regulated S1PR1 promoter. Three potential KLF2 binding sites were identified within -1kb promoter region of mouse *S1pr1* gene. KLF2 specifically binds to -941/-937 base pair (bp), -505/-501 base pair (bp) and -345/-341 base pair (bp) regions of *S1pr1* promoter that contain KLF2 binding sites **(Figure 12A)**. Endothelial cells transfected with KLF2 transcriptionally activated a mouse reporter

containing the *S1pr1* promoter fused with luciferase. However, KLF2 did not induce luciferase promoter activity in mutated *S1pr1* reporter promoter **(Figure 12B).** This data indicates that *S1pr1* is a direct transcriptional target of KLF2 in endothelial cell.

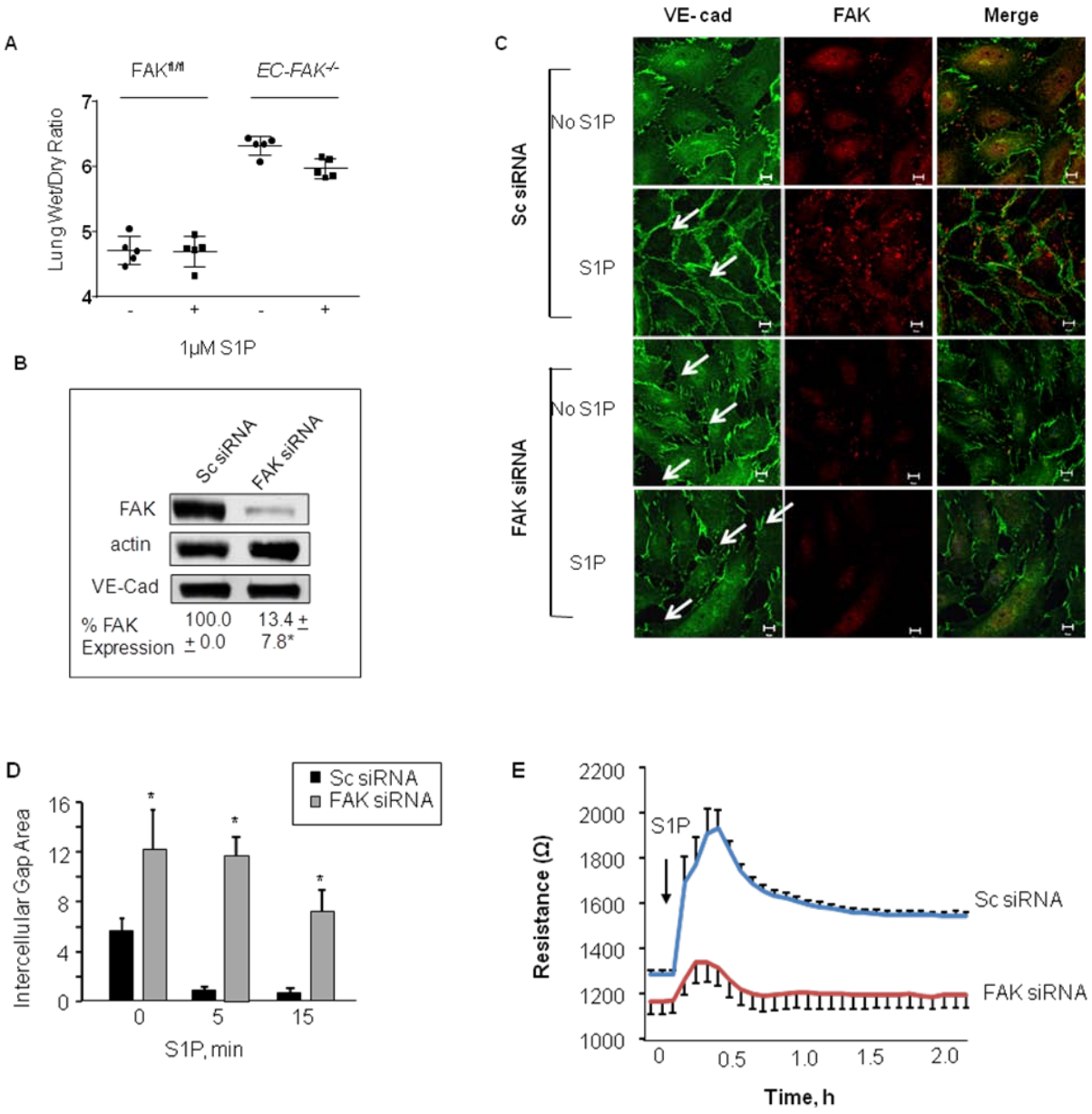
A
FAK^fl/fl
EC-FAK-/-
Lung Wet/Dry Ratio
7
6
5
4
- + - +
1μM S1P
B
Sc siRNA
FAK siRNA
FAK
actin
VE-Cad
% FAK Expression
100.0 ± 0.0
13.4 ± 7.8*
C
VE-cad
FAK
Merge
Sc siRNA
No S1P
S1P
FAK siRNA
No S1P
S1P
D
Sc siRNA
FAK siRNA
Intercellular Gap Area
16
12
8
4
0
0
5
15
S1P, min
E
Resistance (Ω)
2200
2000
1800
1600
1400
1200
1000
S1P
Sc siRNA
FAK siRNA
0
0.5
1.0
1.5
2.0
Time, h

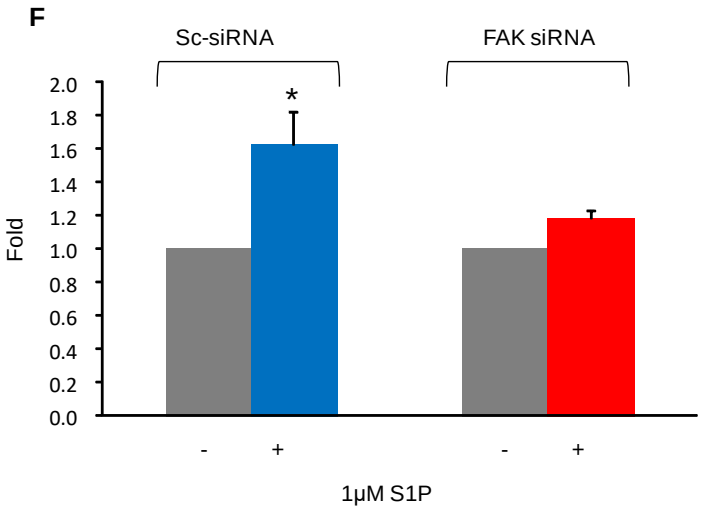

Figure 9. Depletion of FAK impairs S1P-annealing of AJs. (A) FAK$^{fl/fl}$ and *EC-FAK*$^{-/-}$ mice were injected with 1 μM S1P or PBS retroorbitally 30 min prior to sacrifice. Lungs were harvested and wet/dry ratio was measured. **(B)** Inst of lysates was immunoblotted with anti-FAK and VE-cad antibodies. Anti-actin antibody was used to normalize for protein loading**. (C)** HPAE cells transiently transfected with either siSc or siFAK for 72 hr, were stimulated with 1 μM S1P for 15 min, fixed and stained with anti-FAK antibody to assess FAK knockdown as well as VE-cadherin antibody. **(D)** Quantification of gap formation. **(E-F)** Basal TER values of siSc and siFAK expressing cells were recorded to compare the effect of 1 μM S1P on the endothelial barrier. * $p < 0.05$

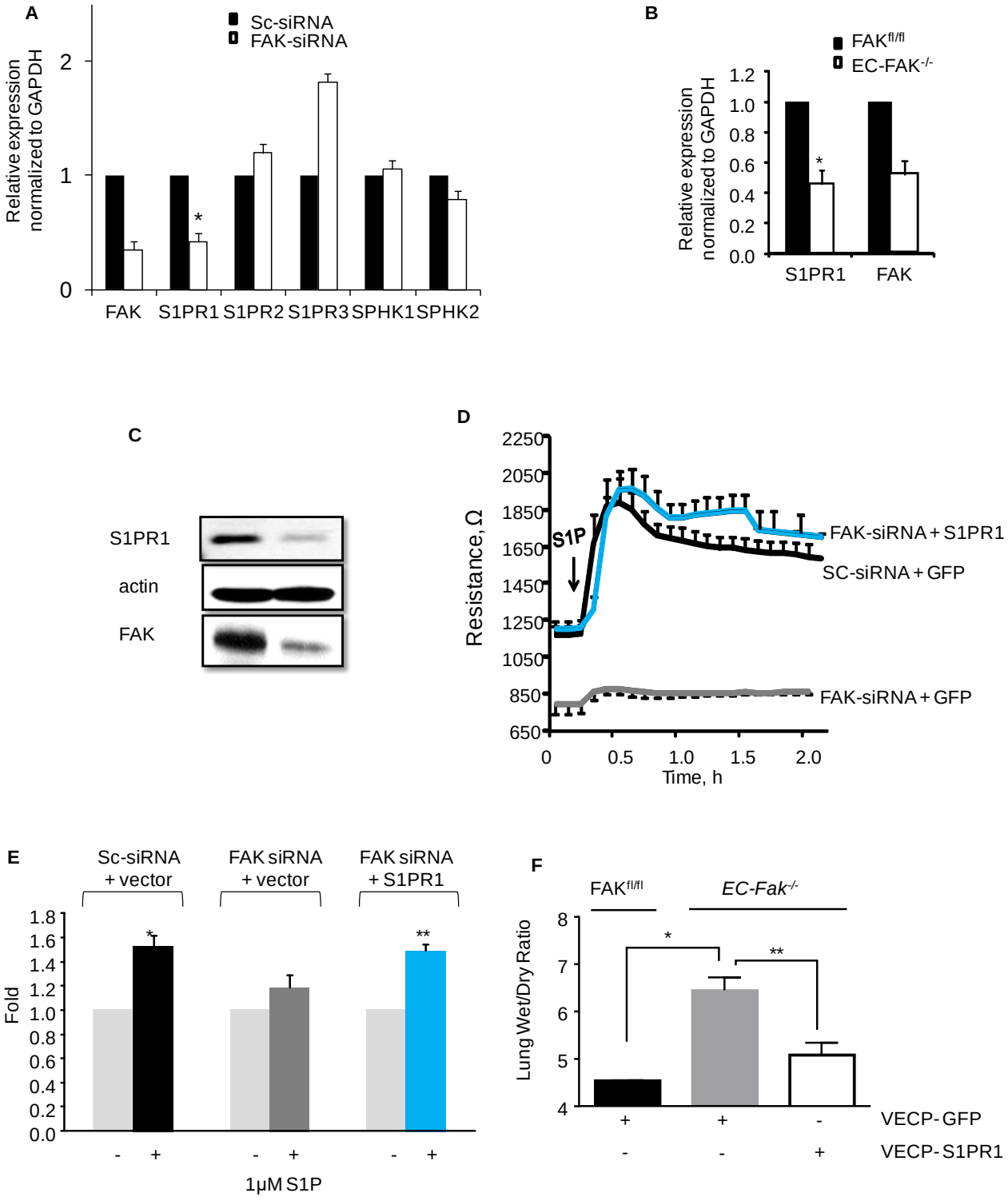
A
Sc-siRNA
FAK-siRNA
Relative expression normalized to GAPDH
FAK
S1PR1
S1PR2
S1PR3
SPHK1
SPHK2
B
FAKfl/fl
EC-FAK-/-
Relative expression normalized to GAPDH
S1PR1
FAK
C
S1PR1
actin
FAK
D
Resistance, Ω
S1P
FAK-siRNA + S1PR1
SC-siRNA + GFP
FAK-siRNA + GFP
Time, h
E
Sc-siRNA + vector
FAK siRNA + vector
FAK siRNA + S1PR1
Fold
1μM S1P
F
FAKfl/fl
EC-Fak-/-
Lung Wet/Dry Ratio
VECP- GFP
VECP- S1PR1

Figure 10. Depletion of FAK suppresses S1PR1 expression. (A) HPAEC transfected with FAK siRNA and control siRNA for 72 hr, RNA was isolated using TriZol and q-PCR was performed to show the gene expression of S1PRs and SPHKs after FAK knock down using GAPDH as internal control. **(B)** Lungs from EC-FAK null as well as $FAK^{fl/fl}$ were harvested, RNA was isolated using TriZol and q-PCR was done to show the gene expression of S1PR1 after FAK deletion. **(C)** Protein from FAK and comtrol siRNA was extracted using RIPA buffer and SDS-PAGE was run and immunobloted for S1PR1 and FAK using actin as a loading control. **(D-E)** HPAECs were transfected with control or FAK siRNA without or with S1PR1 cDNA. TER values of siSc and siFAK expressing cells were normalized to compare the effect of 1 μM S1P on the endothelial barrier. **(F)** $FAK^{fl/fl}$ or *EC-FAK* $^{-/-}$ mice expressing indicated constructs were assessed for lung edema formation by determining lung wet-to-dry weight ratios. Graph represents means +/- SD. Experiments repeated 3 times. **Significance from GFP or GFP-S1PR1 transducing *EC-FAK* $^{-/-}$ lungs and FAK knock down cells. * $p<0.05$

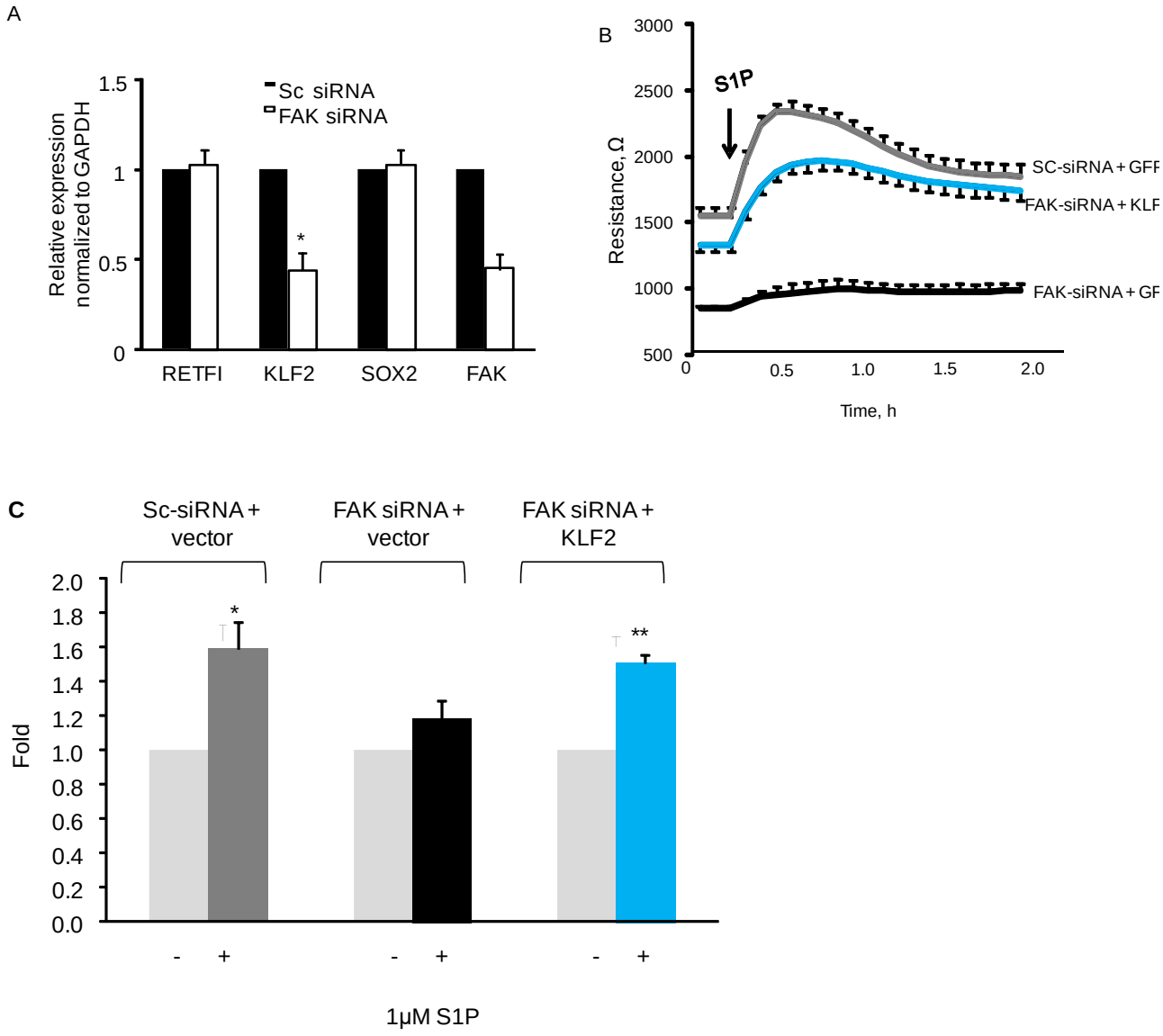

Figure 11. FAK regulates S1PR1 via KLF2. (A) Using TriZol, RNA was isolated using Qiagen RNA isolation kit from control and FAK siRNA transfected HPAECs. cDNA was synthesized using applied biosystems Universal cDNA synthesis kit and q-PCR was performed using FAK , RTEFII, SOX2 and KLF2 primers.GAPDH was used as internal control. **(B-C)** HPAECs were transfected with control or FAK siRNA without or with KLF2 cDNA. Basal TER values of siSc and siFAK expressing cells were recorded to compare the effect of 1 μM S1P on the endothelial barrier. * $p<0.05$. **Significance from GFP or GFP-KLF2 transducing FAK knock down cells.

e. FAK downregulates endothelial KLF2 expression via DNA methylation

Recently, lots of studies have focused on unraveling epigenetic mechanisms by which genes have been regulated. There is evidence in literature that KLF2 promoter is regulated epigenetically via DNA methylation (Kumar et al. 2013). DNA methylation plays a critical role in modulating the expression of various genes. To address if this mechanism is relevant in cells lacking FAK, we knocked down FAK in endothelial cells and did the bisulfate conversion assay where we show that cells lacking FAK exhibit high methylation profile as compared to control cells **(Figure 13A)**. To corroborate this finding, we performed ChIP analysis on KLF2 promoter to assess if binding of MEF2, a critical transcription factor that is known to synthesize KLF2, has been altered. Surprisingly, we saw 70% decrease in MEF2 binding on KLF2 promoter in FAK depleted ECs as compared to control cells **(Figure 13B top)**. We also ran agarose gel to validate the above finding **(Figure 13B bottom)**. This data suggests that loss of FAK has led to the activation of epigenetic machinery to regulate KLF2 expression. To extrapolate this finding, we opt to assess DNA methylase activity in FAK depleted cells. We transfected control and FAK siRNA in HPAE cells and after 72h we harvested the nucelii and looks at DNMT activity using ELISA kit. As expected, enzyme activity was significantly elevated in FAK depleted ECs as compared to control or untransfected cells **(Figure 13C)**.

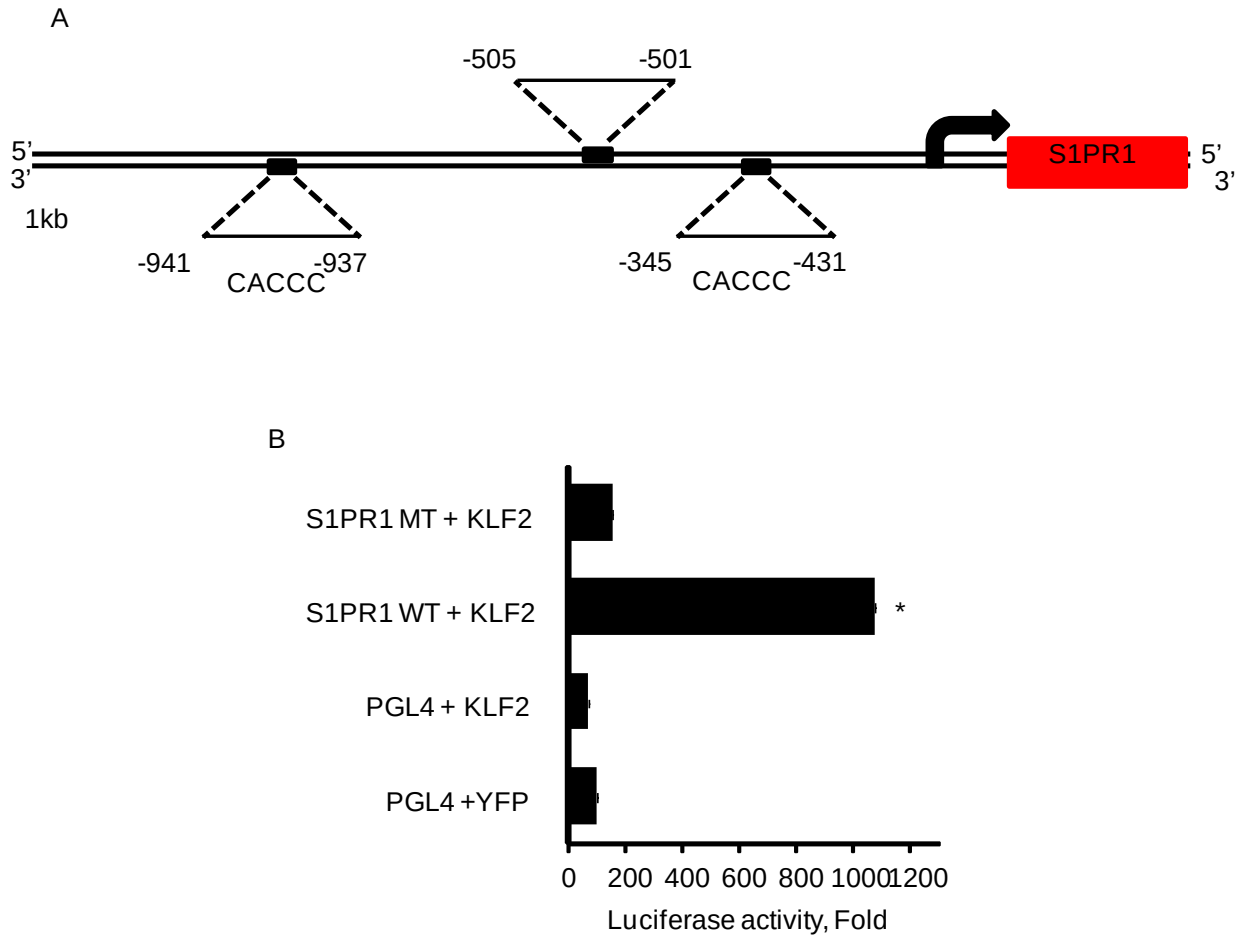

Figure 12: KLF2 directly binds to and induces the transcriptional activity of S1PR1 promoter. (A) Schematic diagram illustrating S1PR1 promoter with KLF2 binding site. **(B)** HPAE cells transfected with PGL4 control vector as well as WT-S1PR1 and MT-S1PR1 luciferase vector for 24hrs and measured the luciferase activity using Promega dual luciferase kit according to the manufacturer's protocol. * $p<0.05$

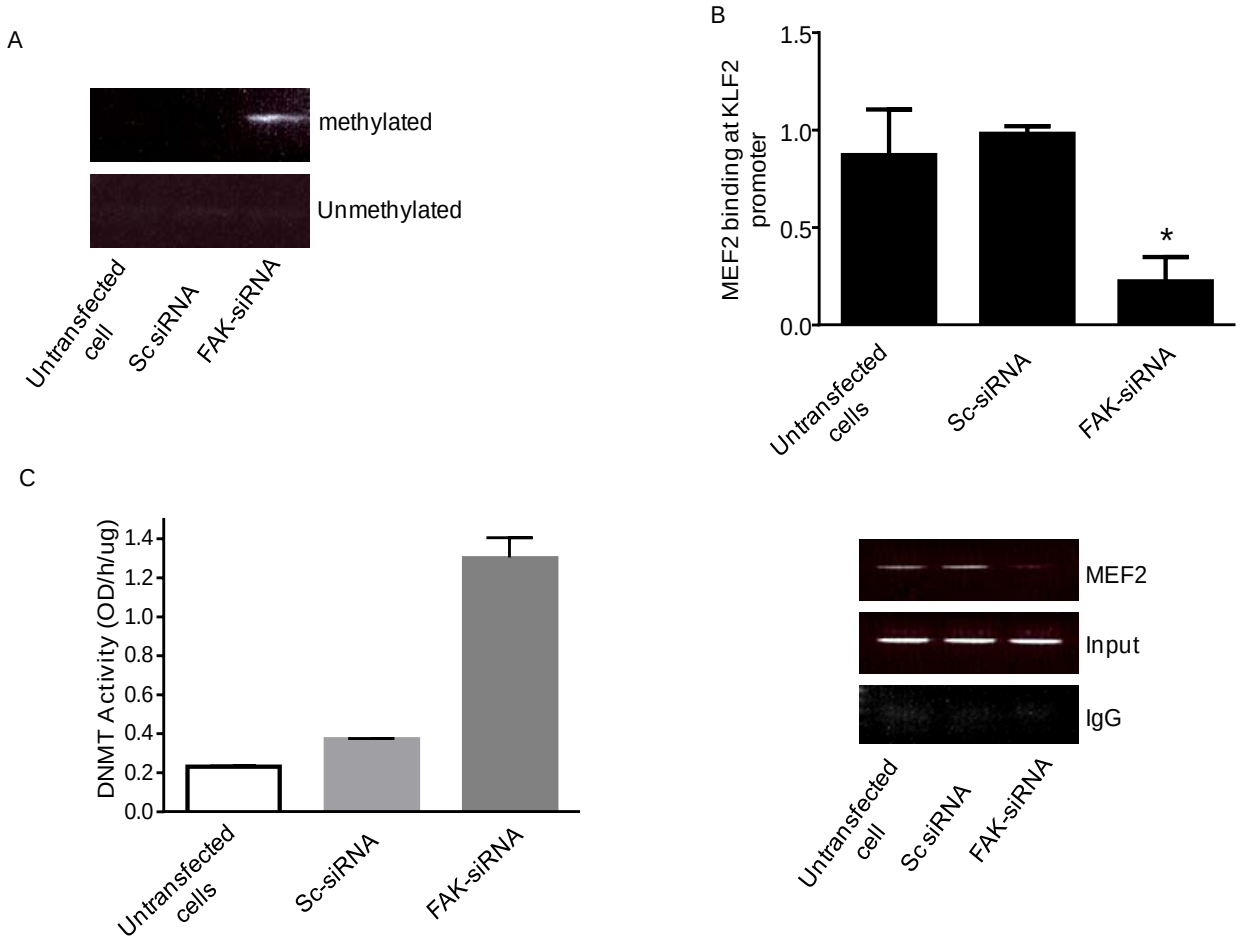

Figure 13: Loss of FAK activates KLF2 DNA methylation: (A) HPAE cells were transfected with control and FAK siRNA. After 72h bisulfite reaction was performed using EpiTect Plus Lyse All Bisulfite Kit (Qiagen, Valencia, CA, USA) and DNA was applied to an EpiTect spin column and washed to remove traces of sodium bisulfite. DNA was eluted and PCR was performed for methylated and unmethylated regions. **(B)** HPAE cells were transfected with control and FAK siRNA for 72 h. Protein-DNA complex (100–120 µg) was immunoprecipitated with the antibody against MEF2. DNA fragments were recovered by phenol– chloroform–isoamyl alcohol extraction, followed by ethanol precipitation, and then resuspended in 14 µl water for PCR. Promoter region of KLF2 targeted a 169 bp fragment was quantified by Sybr green-based real time quantitative PCR (q-PCR). Normal rabbit IgG was used as negative antibody control and DNA from the input (20–40 µg protein-DNA complex) was exploited as an internal control. **(C)** FAK regulates DNMT activity. Nuclei from control and FAK depleted ECs was harvested and ELISA was performed to assess methylase activity. * $p<0.05$

3. Discussion

We have shown that loss of FAK in endothelial cells increased endothelial permeability due to an imbalance between RhoA and Rac1 GTPase activties (Schmidt et al. 2013) . These monomeric RhoGTPases, RhoA and Rac1, play a critical role in regulating AJs in endothelial cells (Mehta and Malik 2006). Mediators that rapidly activate RhoA facilitate stress fiber formation and disrupt AJs while Rac1 induces protrusion that seals the gap (Carbajal and Schaeffer 1999, Holinstat et al. 2006, Knezevic et al. 2009, Radeva and Waschke 2017). The importance of endothelial FAK in the vasculature is demonstrated by the fact that FAK depletion in mouse models resulted in embryonic lethality due to vascular defect and edema formation (Shen et al. 2005).

S1P activates FAK and induces its translocation to the focal adhesion (Wang et al. 2015). We show that FAK depletion increased basal endothelial monolayer permeability. This data suggests that FAK expression is required to maintain and preserve endothelial barrier function and thereby protects against lung vascular leak. S1P is a potent barrier enhancing agonist that opposes LPS mediated barrier disruption (Tauseef et al. 2008). Surprisingly, S1P failed to restore lung edema in *EC-FAK*$^{-/-}$ null mice lungs suggesting that FAK is required for S1P mediated barrier enhancement. Similarly, S1P failed to enhance endothelial barrier in FAK knock down as compared to control cells. Because S1P mediates barrier protection through S1PR1 (Tauseef et al. 2008, McVerry and Garcia 2005, Singleton et al. 2005, Mehta et al. 2005) we wondered if S1PR1 is altered in the absence of FAK. Since FAK can phopsphorylate S1PR1 we wondered if FAK phosphorylated S1PR1 and thereby regulated S1P responses. However, we showed that

phosphorylation of S1PR1 imapired S1P-enhancement of barrier function (Chavez et al. 2015) ruling out the possibility of FAK phosphorylation of S1PR1 is responsible for altered S1PR1 function. Thus, we focused on its transcriptional regulation. We found that the expression of S1PR1 was significantly reduced both at mRNA and protein levels suggesting FAK regulates S1PR1 at the level of transcription. In order to restore lung vascular leak, we transduced S1PR1 via liposomes and assessed lung edema formation. Interestingly, S1PR1 transduced FAK null lungs restored their edema to the level of controls.

Several transcription factors have been reported to induce the transcription of S1pr1in various immune cell types. One of the key transcription factor that we found common in endothelial cell is KLF2 (Lee et al. 2015, Skon et al. 2013). To investigate the key transcription factor that may induce S1PR1 expression in endothelial cell, we looked within 1kb region downstream of endothelial S1PR1 transcript site and identified few potential transcription factors that are present in endothelial cells and assessed their expression in the absence of FAK. We identified KLF2 as a potential transcription factor which was down-regulated in the absence of FAK while other transcription factors such as Sox2 and RTEF-1 were not changed. KLF2 is a zinc finger transcription factor, the expression of which is increased by laminar SS in endothelium (Dekker et al. 2002). Intriguingly, rescuing KLF2 restored basal barrier leak in FAK depleted ECs and resumed S1P mediated barrier protection. S1PR1 promoter showed 3 binding sites for KLF2 within 1kb region downstream of transcript site. We showed 2 of these sites were important since their mutation suppressed luciferase activity. These data demonstrates that KLF2 binds

S1PR1 to induce its transcription.

DNA methylation plays an important role in regulating the expression of multiple genes (Kumar et al. 2013). Methylases, such as DNMT1, DNMT3a and DNMT3b mark the CpG islands of many genes preventing transcription factors, activators and enhancers to bind to the promoter region, thus inhibiting the transcription of several genes. KLF2 has a stretch of CpG islands within its promoter region suggesting that KLF2 is tightly regulated (Kumar et al. 2013). Thus, we surmised that FAK may regulate KLF2 methylation. Infact, bisulfate conversion assay showed that KLF2 promoter was highly methylated as compared to control cells. To further investigate this paradigm, we performed ChiP analysis on control and FAK depleted ECs. Surprisingly, we found that MEF2, a key transcription factor that binds and synthesizes KLF2 (Kumar et al. 2005, Parmar et al. 2006, Xu et al. 2015) was 70% reduced at KLF2 promoter in FAK depleted ECs. We also assessed DNMT enzyme activity by using ELISA. We show that FAK depleted ECs has 3.5 fold increase in DNMT activity over control cells.

In summary, we have identified a novel mechanism by which FAK regulates EC barrier function. We show that FAK is required to maintain S1PR1 via KLF2. We propose a model where FAK suppresses DNMT to facilitate MEF2 binding on KLF2 promoter to synthesize KLF2 which in turn binds S1PR1 and induces its transcription **(Figure 14)**. Together, these events provide a novel touch of FAK mediated epigenetic modulation of S1PR1 via KLF2. Mechanisms preserving FAK expression could lead to therapeutic strategies to prevent against leaky vessel syndrome.

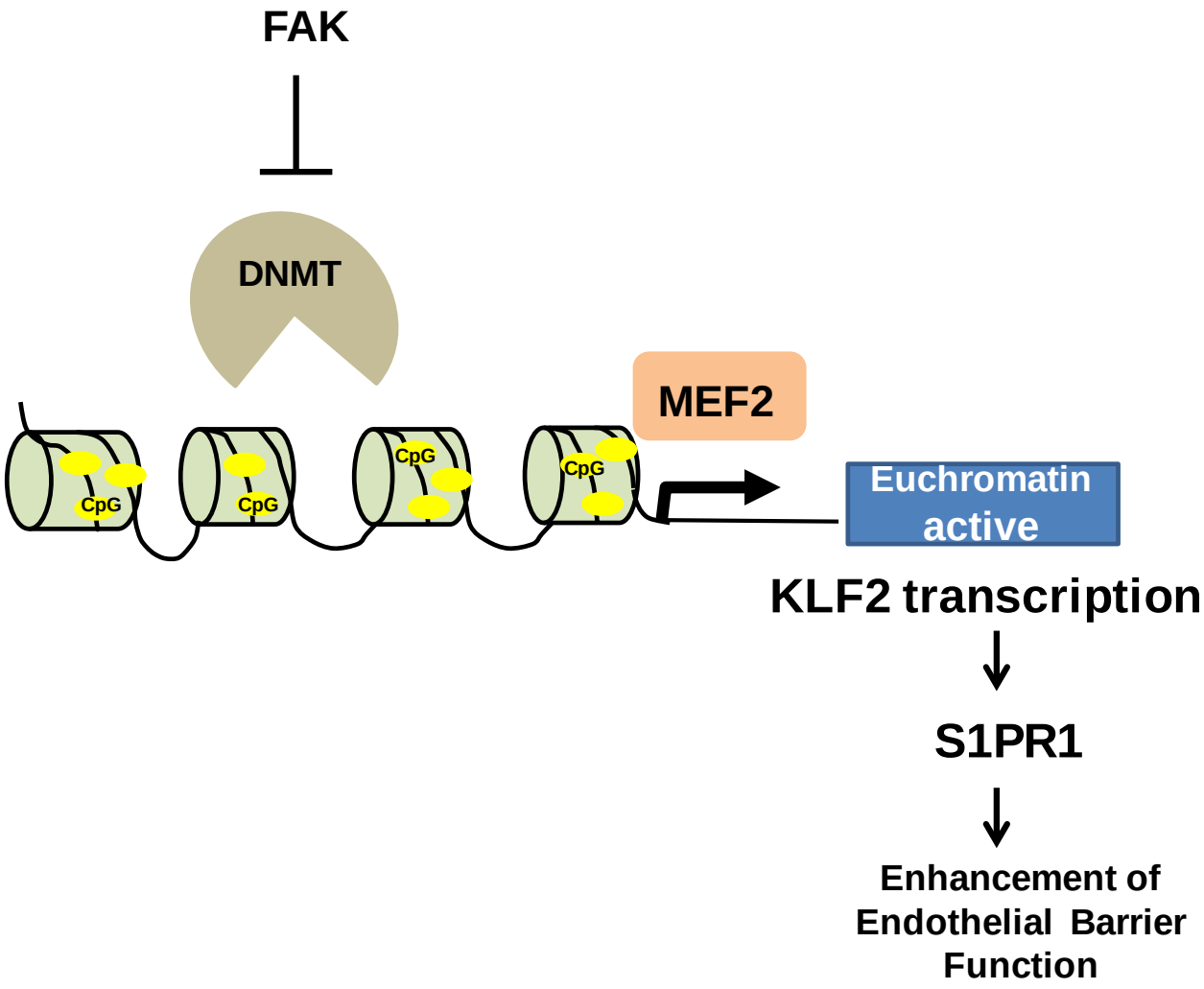

Figure 14. Model of endothelial FAK-mediated regulation of S1PR1: Our studies show that FAK regulates DNMT activity by unknown mechanism which in turn facilitates MEF2 transcription factor to bind to KLF2 promoter to induce its transcription. Additionally, we show that S1PR1, a major receptor in endothelial cell that induces barrier enhancement is regulated transcriptionally by KLF2. Thus, negative regulation of DNA methylation downstream of FAK provides a noval strategy to prevent acute lung injury.

B. Focal adhesion kinase regulation of store operated calcium entry

1. Specific Aim 2

To determine if FAK regulation of Ca^{2+} signaling downstream of RhoA leading to epigenetic switch-on.

2. Results

a. FAK depletion augments Ca^{2+} entry

Schmidt et al. have shown that loss of FAK in endothelial cells induces small GTPase RhoA activity (Schmidt et al. 2013). RhoA is known to induce disassembly of endothelial cell AJs in response to stimuli like thrombin or bradykinin (Sukriti et al. 2014). Inhibition of Rho kinase, a known downstream effecter of RhoA normalized EC barrier in the absence of FAK. We have questioned whether Ca^{2+} signaling, a downstream affecter of RhoA has contributed to the leaky phenotype in cells lacking FAK (Chitaley, Weber, and Webb 2001). We knocked down FAK in endothelial cells and stimulated ECs with thapsigargin in Ca^{2+} free media to induce Ca^{2+} release from ER (first peak) followed by repletion of 2mM extracellular Ca^{2+} to activate SOCE (second peak) in response to thapsigargin. We found that FAK depleted ECs exhibited higher Ca^{2+} entry in response to 2mM Ca^{2+} as compared to control cells **(Figure 15A).** To further corroborate our findings, we isolated cells from $FAK^{fl/fl}$ and infected with β-Gal (control) or Cre recombinase adenovirus. After 60-72 h post-infection, when we observed maximal depletion, we assessed cytosolic Ca^{2+} mobilization in response to thapsigargin in Ca^{2+} free media to induce Ca^{2+} release from ER (first peak) followed by repletion of 2mM extracellular Ca^{2+} to

activate SOCE (second peak) in response to thapsigargin **(Figure 15B)**. We found that FAK depleted lung endothelial cells (LECs) exhibited higher Ca^{2+} entry compared to control cells. To exclude the possibility that Ca^{2+} entry is mediated via receptor operated channels (ROC), we stimulated control and FAK knock down cells with HYP9, an activator of TRPC6 (Montecinos-Oliva et al. 2014), and found no difference in the entry levels between control and FAK depleted ECs **(Figure 15C)**. These data suggests that loss of FAK has led to activation of SOCE.

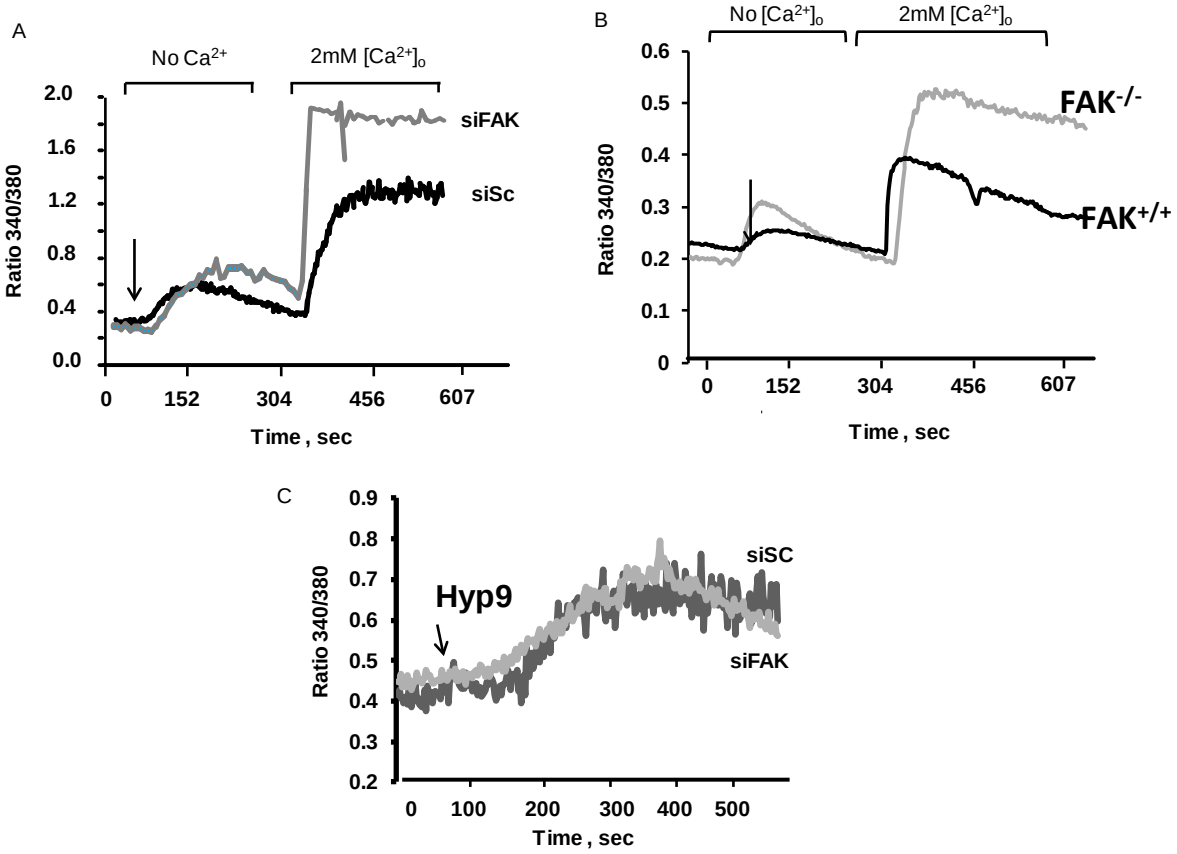

Figure 15. Depletion of FAK augments Ca^{2+} entry. (A) HPAE cells transfected with control and FAK siRNA for 72hr. Cells were loaded with Fura 2AM. Cells were washed and stimulated with thapsigargin in Ca^{2+}-free medium followed by addition of 2 mM Ca^{2+}.**(B)** Cells from $FAK^{fl/fl}$ pups were isolated and treated with control or cre virus to induce FAK deletion. Cells were loaded with Fura 2AM, washed and stimulated with thapsigargin in Ca^{2+}-free medium followed by addition of 2 mM Ca^{2}. **(C)** Control or FAK depleted HPAE cells were treated with HYP9 1μM in Ca^{2+} containing media.

b. Phosphorylation of STIM1 at Y361 is required to trigger SOCE

STIM1 contains a number of tyrosine residues (Lopez et al. 2012) two of which lie within SOAR domain but the role of these potential phosphorylation sites in regulating SOCE remains unclear. Here, we addressed the question whether thapsigargin, an indirect activator of SOCE through ER store depletion, induces tyrosine phosphorylation of STIM1. Human pulmonary aortic endothelial (HPAE) cells were stimulated with thapsigargin at the indicated time points (**Figure 16A**) and STIM1 was immunoprecipitated from the cell lysates using an anti-STIM1 antibody. Immunocomplexes were then probed with anti-phosphotyrosine (anti-PY) antibodies to detect tyrosine phosphorylation. We observed that STIM1 was minimally phosphorylated on tyrosine residues in naïve HPAE monolayers whereas thapsigargin promptly stimulated the phosphorylation of STIM1 within 2.5 min. The phosphorylation levels peaked (4-fold increase) at 5 min (**Figure 16A bottom**). Hence, our data demonstrate that STIM1 undergoes phosphorylation on tyrosine residues, which coincides with Ca^{2+} release from ER stores.

The phosphopeptide analysis of STIM1 (http://www.cbs.dtu.dk/services/NetPhos-2.0/) predicted phosphorylation of six tyrosine residues (**Figure 16B, yellow circles**). Intriguingly, Y361 and another residue, Y316, located within the second α-helix (also known as Cα2) of the coil-coil domains were predicted to be two key residues (**Figure 16B**). Thus, to investigate whether phosphorylation of either Y316 or Y361 is required for SOCE, we introduced a single point mutation at Y316 or Y361 by substitution of phenylalanine (316Y->316F; 361Y->361F) to generate phospho-defective STIM1 mutants and tagged them with YFP. We first stimulated ECs with thapsigargin in Ca^{2+} free media to induce Ca^{2+} release from ER (first peak) followed by repletion of 2mM extracellular Ca^{2+} to

activate SOCE (second peak). Overexpression of STIM1-WT or the phospho-defective STIM1-Y316F mutant had no effect on Ca^{2+} release or SOCE as compared to cells expressing control vector (**Figures 16C-D**). Intriguingly, overexpression of the phospho-defective STIM1-Y361F mutant did not alter Ca^{2+} release but suppressed Ca^{2+} entry by ~85% (**Figures 16C-D**) indicating that tyrosine phosphorylation of STIM1 at Y361 plays a key role in regulating SOCE. To confirm that Y361 in STIM1 is a primary phosphorylation site, we overexpressed STIM1-WT and the STIM1-Y361F mutant in human embryonic kidney (HEK) cells and determined whether mutation at Y361 alters STIM1 phosphorylation in response to thapsigargin. Again, we detected the phosphorylation of WT-STIM1 but modest phosphorylation in cells transfected with STIM1-Y316F mutant with anti-PY antibodies indicating that Y361 is the main tyrosine phosphorylation site in cells expressing WT STIM1. We concluded, therefore, that STIM1 undergoes transient phosphorylation on its Y361 residue, which in turn, promotes SOCE.

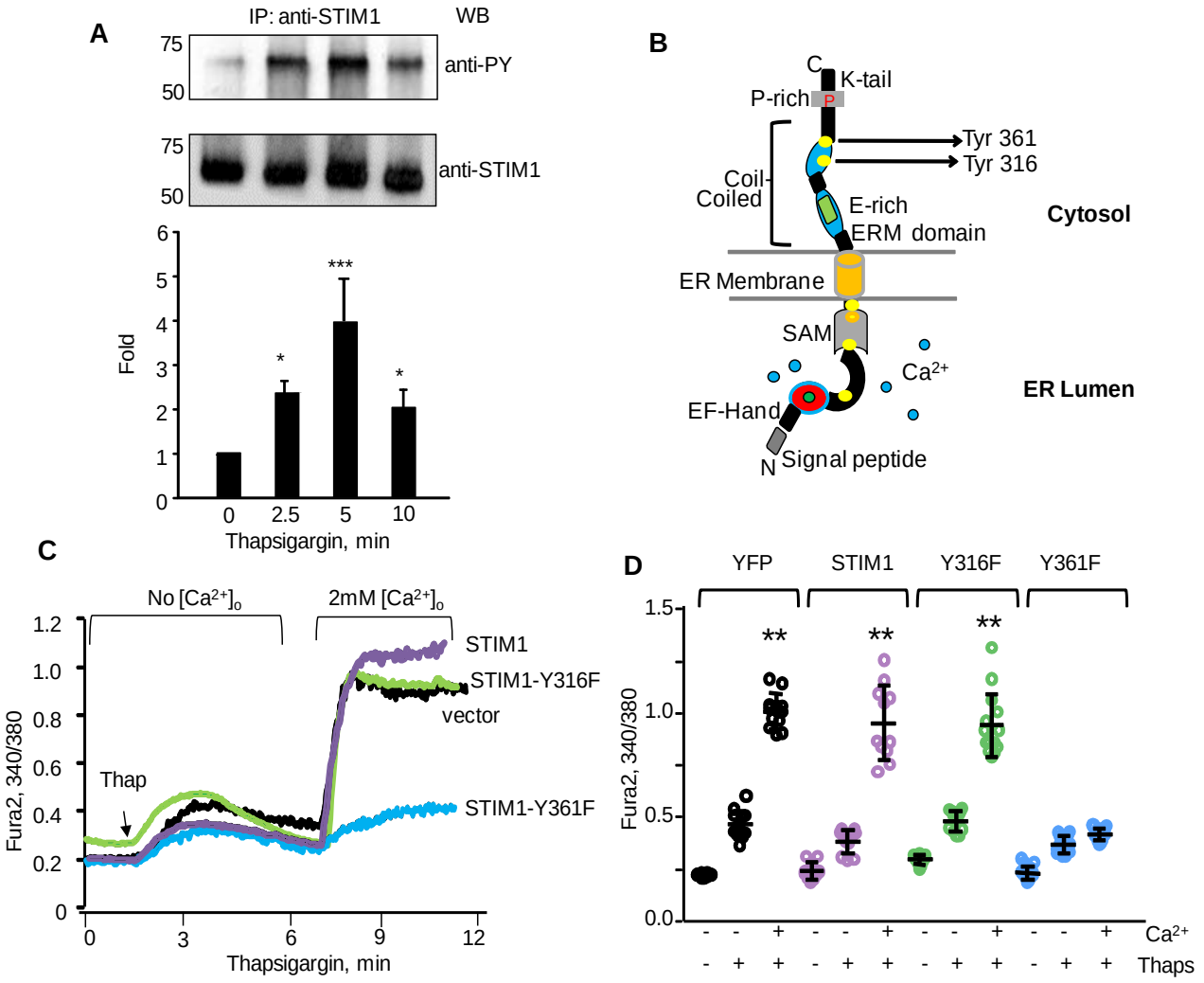

Figure 16. Phosphorylation of STIM1 at Y361 is required to trigger SOCE. **(A**) STIM1 was immunoprecipitated (IP) with anti-STIM1 antibodies from lysates of HPAE cell treated with 2 μM thapsigargin for indicated times. Resulting precipitates were probed with the phosphotyrosine antibodies. A representative immunoblot (top) and densitometry of bar graph of mean ± SD (bottom) demonstrate transient changes in STIM1 phosphorylation on tyrosine residues at various times after thapsigargin stimulation. Fold change was expressed as a ratio between phosphotyrosine and total STIM1 density normalized to 0 times. Data are from 3 independent experiments. * p<0.05, and ***, p<0.001 indicates significant increase as compared to 0 times. **(B**) Schematic representation of STIM1 domains and putative tyrosine phosphorylation sites. Note, Y316 and 361 are located in Cα2 and SOAR domains, respectively. (**C-D**) Phosphorylation of STIM1-Y361 residue is required for inducing Ca^{2+} entry. HPAE cells were transfected with vector (YFP), WT-STIM1, Y316F-STIM1 or Y361F-STIM1 mutants. Cells were stimulated with thapsigargin in Ca^{2+}-free medium followed by addition of 2 mM Ca^{2+} at ~300s. (**C**) A prepresentative trace. (**D)** Individual data points (from 5-10 cells) and mean ± SD are plotted from 3

independent experiments. ** p<0.01 compared to unstimulated cells or cells stimulated with thapsigargin in Ca^{2+}-free medium (Yazbeck et al. 2017).

c. FAK depletion induces Pyk2 phosphorylation

STIM1 contains multiple tyrosine sites and we have shown that thapsigargin, an activator of SOCE induces STIM1 phosphorylation. Pyk2 is a Ca^{2+} dependent tyrosine kinase. It shares 70% homology with FAK. We rationaled if Pyk2 is activated in the absence of FAK to induce phosphorylation of STIM1 and inducing SOCE. We knock down FAK in endothelial cells and assessed Pyk2 phosphorylation. Surprisingly, Pyk2 phosphorylation was significantly increased in comparison to control cells **(Figure 17)**. This data suggests that Pyk2 could be the tyrosine kinase that phosphorylates STIM1 to induce SOCE.

d. Pyk2 phosphorylates STIM1

Next, we sought to determine the kinase responsible for STIM1 tyrosine phosphorylation. Proline-rich tyrosine kinase 2 (Pyk2) is regulated by intracellular Ca^{2+} in several cell types including ECs. We, therefore, assessed if thapsigargin induces Pyk2 activity, which in turn, regulates tyrosine phosphorylation of STIM1. Using a Pyk2 phospho-Y402-specific antibody, we demonstrated that thapsigargin rapidly activated Pyk2 in ECs (**Figure 18A**). However, thapsigargin did not activate other tyrosine kinases such as p60Src (data not shown). To establish the role of Pyk2 in inducing STIM1 phosphorylation and thereby SOCE, we depleted Pyk2 using siRNA. Additionally, we assessed if rescuing STIM1 phosphorylation at Y361 in Pyk2-depleted ECs rescues SOCE. We found that depletion of Pyk2 markedly suppressed STIM1 phosphorylation in ECs in response to thapsigargin **(Figure 18B).** Depletion of Pyk2 also reduced SOCE (**Figures 18C-D**) mimicking findings in cells transducing the STIM1-Y361F mutant. Furthermore, SOCE was restored in Pyk2 depleted cells by rescuing STIM1 phosphorylation through overexpression of the phospho-mimetic STIM1-Y361D mutant (**Figures 18C-D**). These data suggest that Pyk2 induces phosphorylation of STIM1 on its Y361 residue, which is required for triggering SOCE.

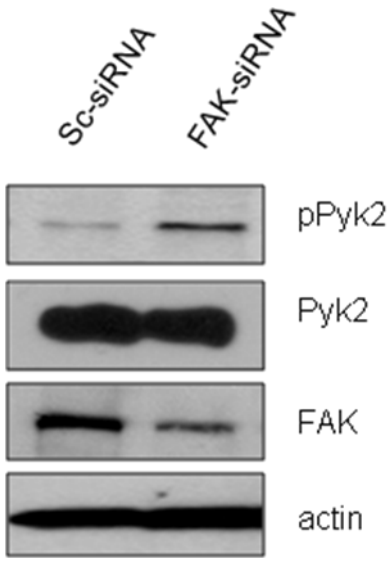

Figure 17. FAK depletion induces Pyk2 phosphorylation. HPAE cells were transfected with control and FAK siRNA for 72h. Cells were lysed with RIPA buffer and proteins were loaded on SDS-PAGE. Membrane was probed using phospho-Pyk2 (Tyr-402) and total Pyk2. FAK antibody was used to confirm deletion. Actin was used as an internal control.

e. STIM1 phosphorylation of Y361 is required for STIM1-Orai1 interaction and recruitment of Orai1 to STIM1 puncta

Studies show that upon store depletion, STIM1 appears in discrete puncta within the ER membrane that recruit Orai1 following translocation to ER-PM junctions. Because Y361 residues are critically positioned within the STIM1 dimer, we asked if phosphorylation of STIM1 might be required to induce conformational changes within STIM1 to trigger STIM1 multi-dimerization or interaction with Orai1. To test this possibility, we analyzed the intracellular distribution of both WT-STIM1 and the phospho-defective Y361F-STIM1 mutant with respect to WT-Orai1 in ECs following thapsigargin stimulation. Interestingly, thapsigargin increased puncta formation both in cells expressing WT-STIM1 and those expressing the STIM1-Y361F mutant, suggesting that phosphorylation of the Y361 residue is not required for STIM1 multi-dimerization (**Figures 19A and B**). In contrast, increase in the number of Orai1puncta by thapsigargin was significantly reduced in cells expressing the STIM1-Y361F mutant (**Figures 19A and C**). Also, Orai1 failed to co-localize with the STIM1-Y361F mutant (**Figures 19A and D**) suggesting that STIM1 phosphorylation dynamically regulates recruitment of Orai1 to the STIM1 puncta where they can interact.

To further corroborate the role of STIM1 phosphorylation on Y361 in inducing interaction with Orai1, we performed immunoprecipitation of Orai1 in HEK cells expressing either WT, phospho-defective (STIM1-Y361F), or phospho-mimetic (STIM1-Y361D) mutants. We found that thapsigargin induced the interaction of Orai1 with WT-STIM1 (**Figure 20A**). However, thapsigargin failed to induce an interaction between Orai1 and the STIM1-Y361F mutant (**Figure 20A**). Cells transducing the Y361D-STIM1 mutant behaved similarly to WT-STIM1 expressing cells, i.e. we did not observe any greater interaction of this mutant with Orai1basally **(Figure 20A)**. Next, we depleted Orai1 in ECs, which reduced Orai1 expression by more than 90% **(Figure 20B)**. We then expressed WT-STIM1 or the phospho-mimetic STIM1 mutant (Y361D-STIM1 mutant) into Orai1 depleted cells and imaged YFP-tagged cells to establish the

role of STIM1 activation of Orai1 as a requisite for SOCE. We found that both WT-STIM1 and the Y361D-STIM1 mutant failed to rescue SOCE in Orai1 depleted ECs (**Figure 20C-D**) supporting the contention that phosphorylation of STIM1 at Y361 induces STIM1-Orai1 interaction and Orai1 gating.

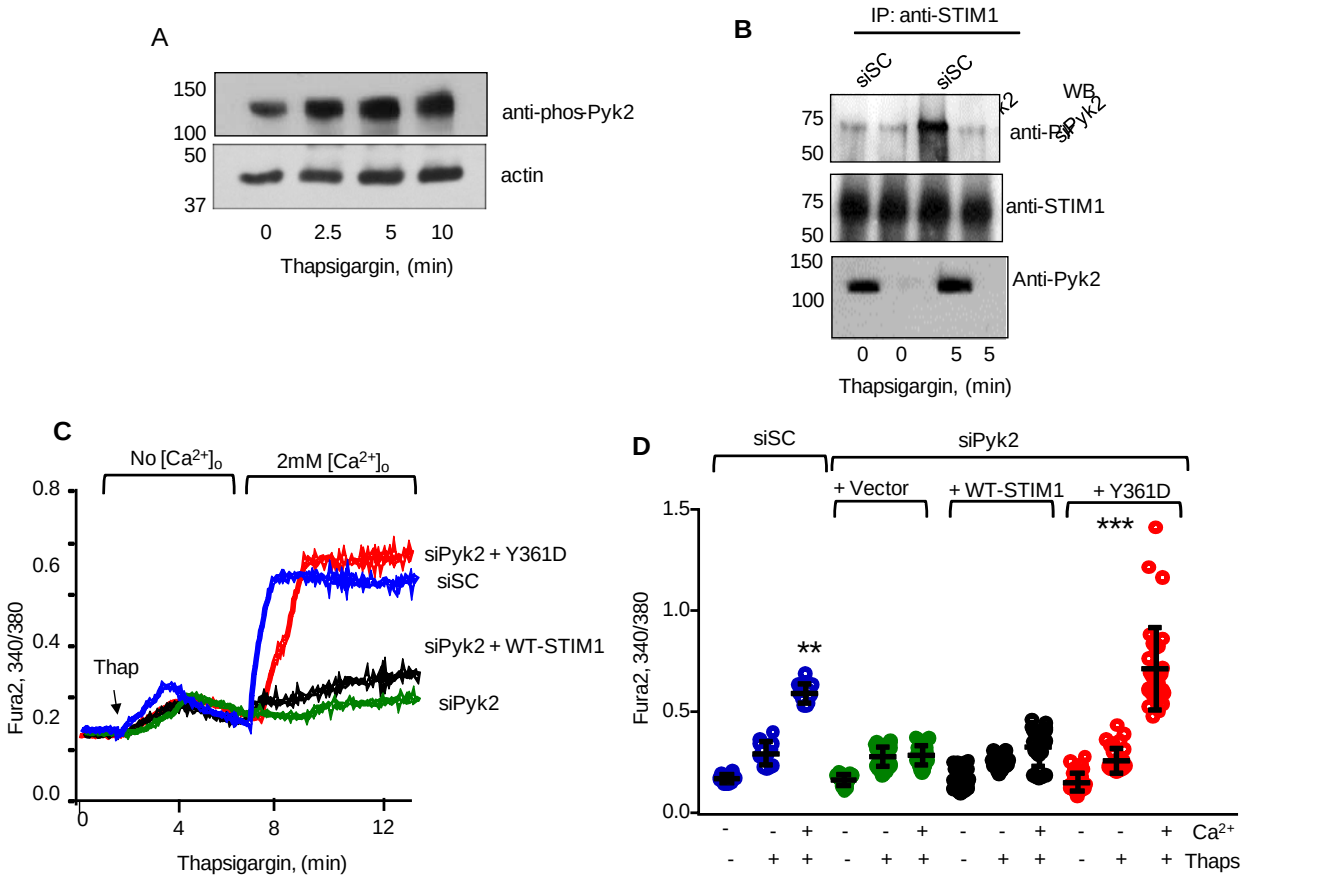

Figure 18. Pyk2 phosphorylates STIM1. (**A)** Western blot analysis of a time-course of Pyk2 phosphorylation using anti-Y-402-phospho-Pyk2 in HPAE cells treated with thapsigargin at indicated times. Note, Pyk2 undergoes phosphorylation after treatment with thapsigargin**.** A representative blot is shown from experiments that were repeated at least three times. **(B)** Depletion of Pyk2 blocks STIM1 tyrosine phosphorylation. Western blot analysis of STIM1 phosphorylation (as described in Fig. 1a) in HPAE cells depleted of Pyk2 and treated with thapsigargin at indicated times. Western blot with anti-Pyk2 was used to determine efficiency of Pyk2 depletion. siSC, scramble siRNA; siPyk2, Pyk2-targeting siRNA. A representative blot is shown from experiments that were repeated at least three times. (**C-D)** Overexpression of phospho-mimetic Y361D-STIM1 mutant but not WT-STIM1 or phosho-defective Y361F-STIM1 mutant rescues SOCE in Pyk2-depleted cells. Effect of Pyk2 depletion on SOCE was assessed as in Figure 19. A representative trace (**C**). (**D**) Summary results. Individual data points (from 5-10 cells) and mean ± SD are plotted from 3 independent experiments. ** p<0.01, *** p<0.001 compared to unstimulated cells or cells stimulated with thapsigargin in Ca^{2+}-free medium (Yazbeck et al. 2017).

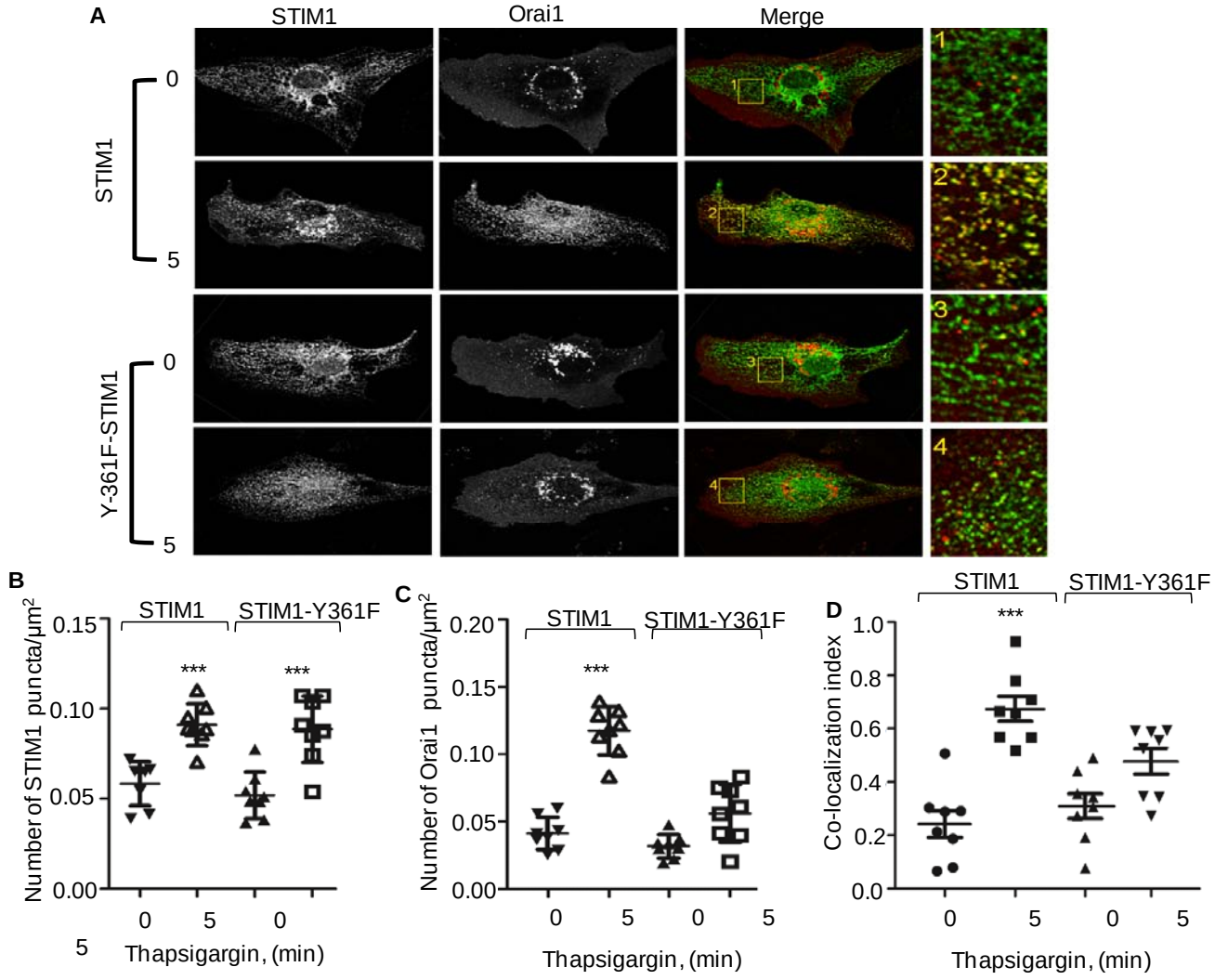

Figure 19. STIM1 phosphorylation at Y361 is required for STIM1-Orai1 interaction and recruitment of Orai1 to STIM1 puncta. (A-D) HPAE cells co-expressing either WT-YFP-STIM1 and mCherry-Orai1 or Y361F-YFP-STIM1 and mCherry-Orai1 were stimulated with 2 μM thapsigargin for the indicated times, fixed and visualized with confocal LSM 880 microscope. Images showing STIM1 puncta and recruitment of Orai1 to STIM1 puncta **(A)**, number of STIM1 **(B)** and Orai1 clusters **(C)**, colocalization index for Orai1 **(D)**. Individual data points (from 5-10 cells) and mean ± SD are plotted. *** $p<0.001$ compared to unstimulated cells **(B-D)** or thapsigargin stimulated STIM1-Y361F mutant expressing cells **(C-D)** (Yazbeck et al. 2017).

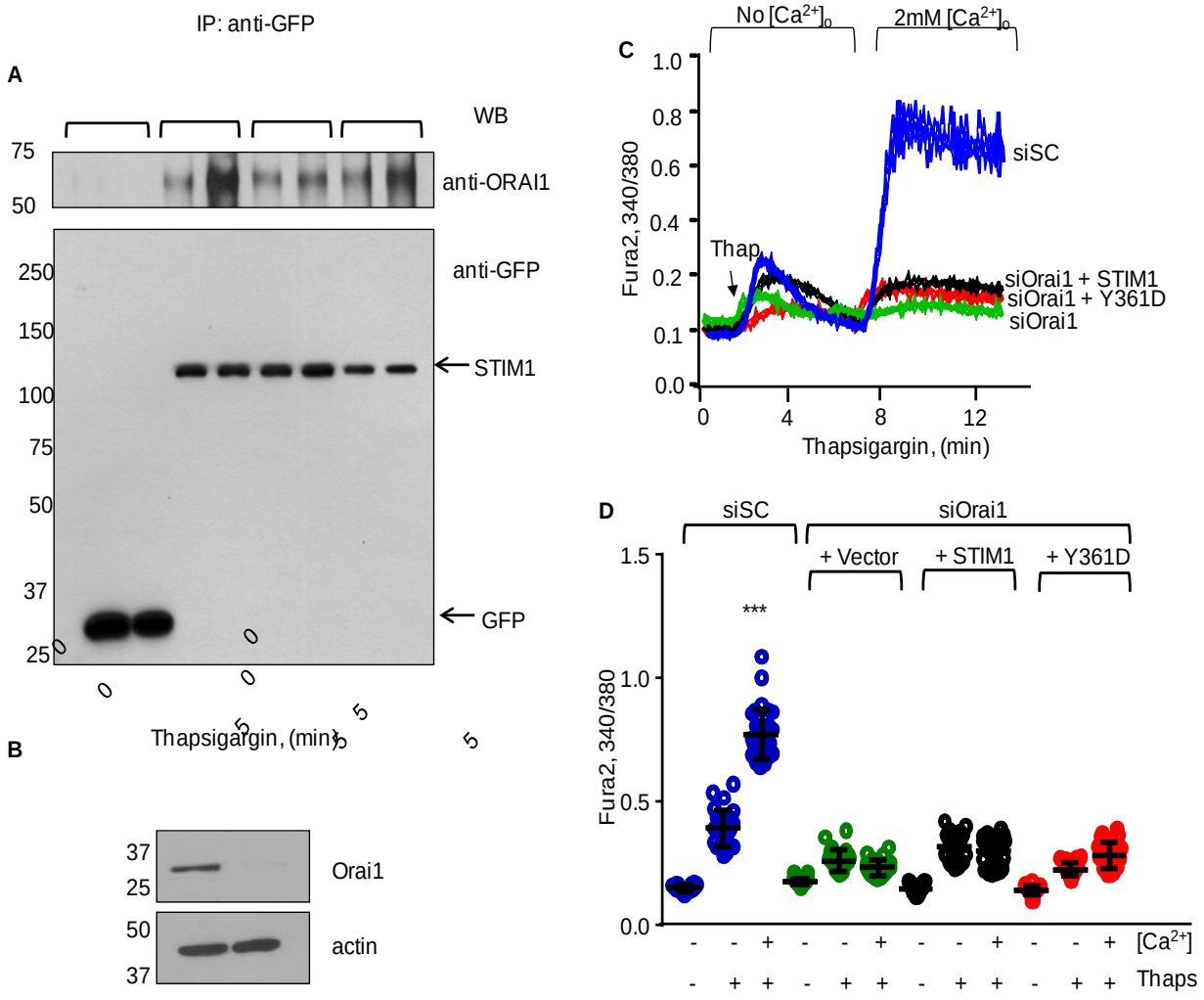

Figure 20. Tyrosine phosphorylation of STIM1 at Y361 residue mediates STIM1-Orai1 interaction and activation of Orai1. **(A)** HEK cells co-expressing YFP, WT-YFP-STIM1, or YFP-Y361F-STIM1, YFP-Y361D-STIM1 mutant together with mCherry-Orai1 were stimulated with thapsigargin for 5 min or left unstimulated. Exogenous STIM1 was immunoprecipitated with anti-GFP antibodies followed by immunoblotting using both anti-Orai1 and anti-GFP antibodies. A representative blot is shown from experiments that were repeated multiple times. (**B)** Western blot analysis of Orai1 expression in HPAE cells depleted of Orai1. A representative blot is shown from experiments that were repeated multiple times. siSC, scramble siRNA; siOrai1, Orai1-targeting siRNA. **(C-D)** Overexpression of Y361D-STIM1 mutant rescues SOCE in Orai1 depleted ECs. Effect of Orai1 depletion on SOCE was assessed as in Figure 1 c-d; Summary results. Individual data points (from 10-15 cells) and mean ± SD are plotted from 3 independent experiments. *** p<0.001 compared to unstimulated cells or thapsigargin stimulated cells as indicated **(C-D)** (Yazbeck et al. 2017).

f. STIM1 phosphorylation at Y361 residue is required for increasing vascular permeability

We next addressed the physiological significance of STIM1 phosphorylation on its Y361 residue in regulating increased endothelial permeability. We first determined whether inhibition of STIM1 phosphorylation altered SOCE secondary to activation of the G-protein coupled receptor PAR1. Similar to thapsigargin, activation of PAR1 with thrombin also increased Pyk2 and STIM1 phosphorylation in a time dependent manner **(Figures 21A-B)**. As expected, thrombin induced SOCE in cells transducing WT-STIM1 or control vector (data not shown) but not in cells transducing the phospho-defective STIM1-Y361F mutant (**Figures 21C-D**). Next, we transiently expressed the phospho-defective STIM1-Y361F mutant in pulmonary endothelium of mice using liposome-based delivery to assess the role of STIM1 phosphorylation in increasing pulmonary vascular permeability. Thus, we prepared liposomes containing vectors driven by the VE-cadherin promoter for YFP (empty vector control), WT, or the STIM1-Y361F mutant and injected them intravenously into mice. As expected, a selective PAR1 agonist peptide increased lung vascular permeability in mice transducing vector alone or WT-STIM1 (**Figure 21E)**. However, the PAR1-agonist peptide failed to increase vascular permeability in mice transducing the STIM1-Y361F mutant (**Figure 21E**). In other studies, we assessed vascular permeability in response to PAR1 activation in mice lacking STIM1 only in ECs **(Figure 21E)**. We found that PAR1 peptide increased vascular permeability in STIM1-floxed control mice to a level similar to WT mice receiving liposomes containing YFP or WT-STIM1 vectors (**Figure 21E**). However, activation of PAR1 failed to increase vascular permeability in mice lacking STIM1 in ECs (*EC-Stim1$^{-/-}$ mice;* **Figure 21E**). The block of vascular permeability increase in mice transducing the phospho-defective STIM1-Y361F mutant was similar to that in mice lacking STIM1 in ECs (*EC-Stim1$^{-/-}$ mice*). These findings thereby demonstrate a pivotal role of STIM1 phosphorylation on Y361 in mediating the lung vascular permeability response.

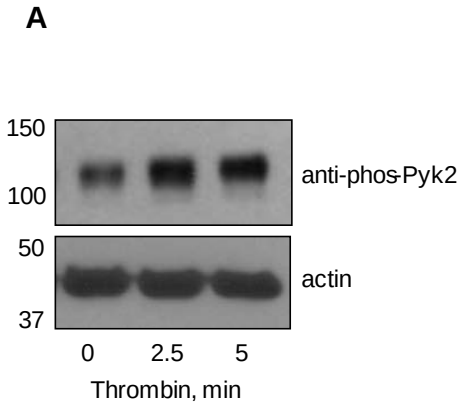
A
150
100
50
37
anti-phos-Pyk2
actin
0
2.5
5
Thrombin, min

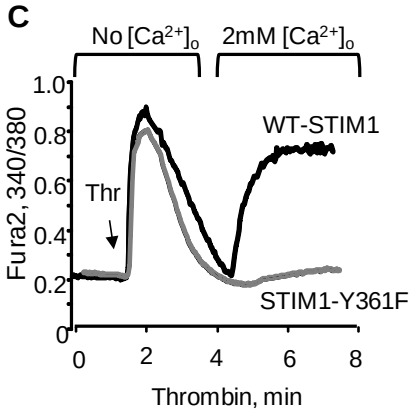
C
No [Ca2+]o
2mM [Ca2+]o
Fura2, 340/380
1.0
0.8
0.6
0.4
0.2
0
Thr
WT-STIM1
STIM1-Y361F
0
2
4
6
8
Thrombin, min

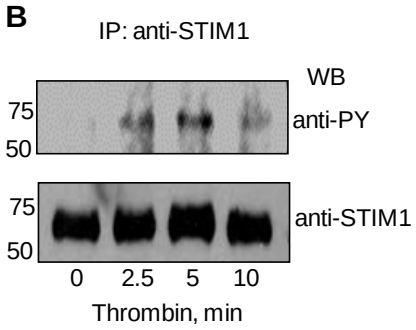
B
IP: anti-STIM1
WB
75
50
anti-PY
75
50
anti-STIM1
0
2.5
5
10
Thrombin, min

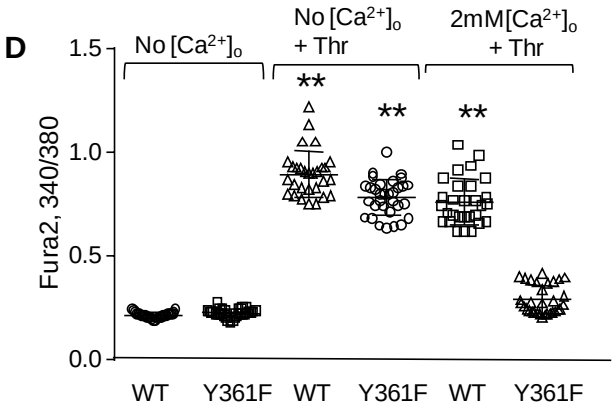
D
No [Ca2+]o
No [Ca2+]o
+ Thr
2mM[Ca2+]o
+ Thr
Fura2, 340/380
1.5
1.0
0.5
0.0
**
**
**
WT
Y361F
WT
Y361F
WT
Y361F

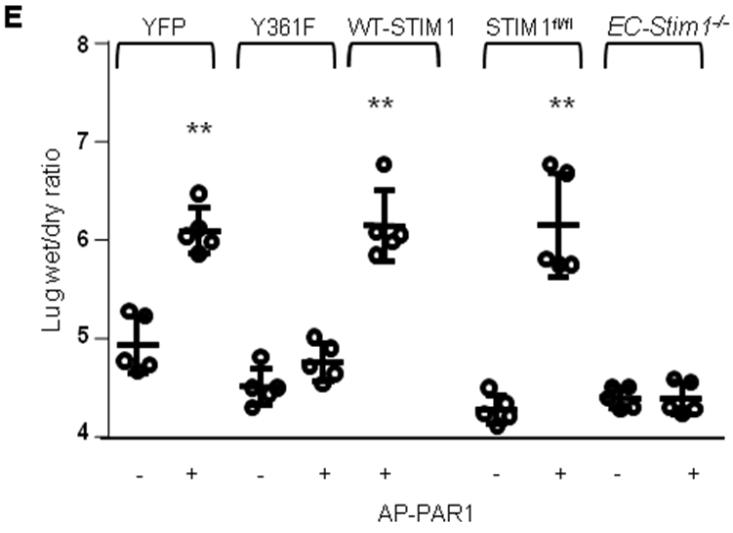
E
YFP
Y361F
WT-STIM1
STIM1fl/fl
EC-Stim1-/-
Lung wet/dry ratio
8
7
6
5
4
**
**
**
- + - + + - + - +
AP-PAR1

Figure 21. STIM1 phosphorylation at Y361 residue contributes to increased lung vascular permeability. (**A)** Western blot analysis of a time-course of Pyk2 phosphorylation using anti-Y-402-phospho-Pyk2 in HPAE cells treated with thrombin as determined in Figure 1. Image shown are cropped. Full immunoblot is uploaded in Supplementary Figure S3. A representative blot is shown from experiments that were repeated multiple times (**B)** Thrombin induces tyrosine phosphorylation of STIM1. Lysates were IP with anti-STIM1 antibody. Resulting precipitates were probed with the phosphotyrosine antibodies. A representative blot is shown from experiments that were repeated multiple times. (**C-D)** Phosphorylation of STIM1 on Y361 is required for α-thrombin-induced SOCE. A representative trace **(C).** (**D**) Individual data points (from 10-15 cells) and mean ± SD are plotted from 3 independent experiments. ** $p<0.01$ compared to unstimulated cells or thrombin stimulated STIM1-Y361F mutant expressing cells. (**E**) Liposomes containing either YFP, WT-STIM1 or Y361F-STIM1 were injected in WT mouse ice through retroorbital sinus 40 h prior to experiments. In parallel experiment, $STIM^{fl/fl}$ and *EC-Stim1*$^{-/-}$ were used. To induce vascular permeability, PAR1 agonist peptide was given i.v. 30 min prior to harvesting lungs for measurement of lung wet/dry ratio. Individual data points and mean ± SD are plotted from 5 mice. Experiments were repeated two times. ** $p<0.01$ compared to mice receiving control peptide or PAR1 activated mice expressing STIM1-Y361F mutant (Yazbeck et al. 2017).

3. Discussion

In this study, we have uncovered a novel regulatory mechanism that primes STIM1 to interact with the Ca^{2+}-selective Orai1 channel inducing SOCE. In this context, Pyk2-dependent phosphorylation of the Y361 residue within STIM1 induces SOCE. Our data showed that phosphorylation of the Y361 residue does not interfere with STIM1 puncta formation but controls recruitment of Orai1 to STIM1 puncta enabling STIM1-Orai1 interaction and Ca^{2+} entry through Orai1 channels. Furthermore, we established the physiological role of STIM1 tyrosine phosphorylation in regulating endothelial permeability *in vivo* by demonstrating that transduction of the phospho-defective STIM1-Y361F mutant in pulmonary endothelium of WT mice blocked the increase in endothelial permeability associated with activation of PAR1 signaling.

Both STIM1 and Orai1 are integral components of SOCE in ECs (Abdullaev et al. 2008, Varnai, Hunyady, and Balla 2009). STIM1 binds Ca^{2+} ions in the ER lumen through its EF hand motif under basal conditions (Huang et al. 2009, Stathopulos et al. 2008). Several inflammatory mediators such as thrombin, histamine, and growth factors initiate ER-Ca^{2+}depletion, which is followed by Ca^{2+} entry through SOCE (Moccia, Berra-Romani, and Tanzi 2012). Ca^{2+} entry is a multistep process, which requires sensing of the Ca^{2+} concentration within the ER, establishment of ER- plasmalemmal (PM) junctions, and activation of plasmalemmal Ca^{2+}channels. STIM1 plays a critical role in each of these steps (Stathopulos et al. 2006) . It functions as a sensor for Ca^{2+} concentration inside the ER lumen. Following agonist-induced depletion of the ER-Ca^{2+} store, STIM1 oligomerizes to form numerous puncta within the ER membrane (Shim, Tirado-Lee, and Prakriya 2015). These puncta then translocate to the ER-PM junctions where STIM1 interacts with plasmalemmal Ca^{2+} channels such as Orai1 channels to activate SOCE (Cheng et al. 2013).

In the present study, we showed that Pyk2-dependent tyrosine phosphorylation of STIM1 at Y361 within SOAR domain of STIM1 is an integral step in activating Ca^{2+} entry through Orai1

channels. We showed that Pyk2 but not p60Src is rapidly activated following stimulation of ECs with the SERCA inhibitor thapsigargin or thrombin. Depletion of Pyk2 inhibited both STIM1 phosphorylation and Ca^{2+} entry in ECs, demonstrating that Pyk2 mediates phosphorylation of STIM1. We showed that, while the expression of the phospho-defective STIM1-Y361F mutant markedly suppressed Ca^{2+} entry in ECs in response to either thapsigargin or thrombin, expression of the phospho-mimetic STIM1-Y361D mutant was sufficient to restore SOCE in Pyk2-depleted ECs, thus indicating that activation of Pyk2 through Ca^{2+} mobilization from ER stores provides a positive feedback mechanism for Ca^{2+} entry by phosphorylating STIM1.

Our findings also showed that the phospho-defective STIM1-Y361F mutant exhibited a dominant negative effect through inactivation of endogenous STIM1. We speculate that the ectopically-expressed STIM1-Y361F mutant blocks SOCE by forming dysfunctional STIM1 oligomers with endogenous STIM1 protein upon ER-Ca^{2+} depletion. This impairs recruitment of Orai1 into STIM1 puncta, limiting formation of functional Orai1 channels. Our findings also showed that recruitment of Orai1 into STIM1 puncta is a critical step in inducing Ca^{2+} entry via the SOCE, since expression of the STIM1-Y361F mutant or depletion of Orai1 in ECs inhibited SOCE to a similar degree.

Crystal structure analysis revealed that the STIM1 dimer forms a V-shaped structure in which the Y361 residue from each monomer meet at the angle of the “V” shaped structure (Feske and Prakriya 2013). We therefore surmised that phosphorylation of Y361 might be required for generation of repulsive forces within the “V” shaped structure, inducing both STIM1 puncta formation and interaction with Orai1. To our surprise, phosphorylation of Y361 was not required for STIM1 dimerization since a loss-of-function of STIM1 (Y361F-STIM1 mutant) did not alter the number of STIM1 puncta as compared to WT-STIM1 upon thapsigargin stimulation. However, phosphorylation of Y361 was found to be required for recruiting and ’trapping’ Orai1 by STIM1 puncta at the plasma membrane (Hodeify et al. 2015). These findings support a

recently described ‘trafficking trap’ hypothesis in which cortical STIM1 puncta govern Orai1 recycling at the plasma membrane. Interestingly, our data also showed that a gain-of-function STIM1 mutation *per se* did not increase STIM1’s interaction with Orai1, basically indicating that phosphorylation of STIM1 alone is not sufficient to promote STIM1 and Orai1 interaction at the ER membrane and that consequently, STIM1 reorganization into puncta is a prerequisite for this interaction. We, therefore, conclude from these findings that recruitment of Orai1 into STIM1 puncta is an independent step requiring STIM1 phosphorylation by Pyk2.

How phosphorylation of Y361 regulates STIM1’s interaction with Orai1 remains to be parsed out but some speculation may be offered. Studies have identified SOAR as the minimal domain required for both STIM1 puncta formation and activation of Orai1 channels (Feske and Prakriya 2013, Stathopulos et al. 2008, Zhou et al. 2015). However, full-length STIM1 is inactive as steric hindrance from its CC1 domain prevents unfolding of the STIM1-SOAR domain (Fahrner et al. 2013). Structural studies showed that the SOAR domain interacts with Orai1’s C-terminus through the STIM1-Orai1 association pocket (SOAP) (Derler, Jardin, and Romanin 2016, Shim, Tirado-Lee, and Prakriya 2015). This pocket is formed through coupling of several positively charged lysine residues from the STIM1-CC2 domain with negatively charged (D284, D287, D291) residues on Orai1 (Stathopulos et al. 2013). It is possible; therefore, that STIM1 phosphorylation on Y361 may expose positively charged lysine residues in STIM1 enabling recruitment and interaction of Orai1 with STIM1.

Activation of SOCE by STIM1 plays a key role in regulating endothelial permeability (Cioffi and Stevens 2006, DebRoy et al. 2014, Gudermann and Steinritz 2013). We showed that PAR1 activation caused an increase in endothelial permeability in the lungs of WT mice expressing either the YFP empty vector or WT-STIM1. However, expression of the phospho-defective mutant (Y361F-STIM1 mutant) prevented the increase in vascular permeability by PAR1 much like the findings in mice lacking STIM1 in ECs. These data establish the critical role of the

STIM1 phospho-switch in disrupting endothelial barrier function. Together, our data suggest a model in which phosphorylation of STIM1 on its Y361 residue represents an independent and obligatory step linking STIM1 puncta to gating of Orai1 channels and thereby Ca^{2+} entry and increased endothelial barrier permeability **(Figure 22)**. This step is required for recruitment of Orai1 into STIM1 puncta and STIM1-Orai1 interaction. Our observations provide the first direct evidence for tyrosine phosphorylation-dependent activation of SOAR that mediates recruitment of Orai1 to STIM1 puncta. This phospho-switch is essential for activation of Ca^{2+} entry through Orai1 and disruption of endothelial barrier function in lungs, which leads to several pathologic disorders including lung injury. In this sense, STIM1 phsophorylation at Y361 represents a novel target for preventing diseases associated with leaky blood vessels.

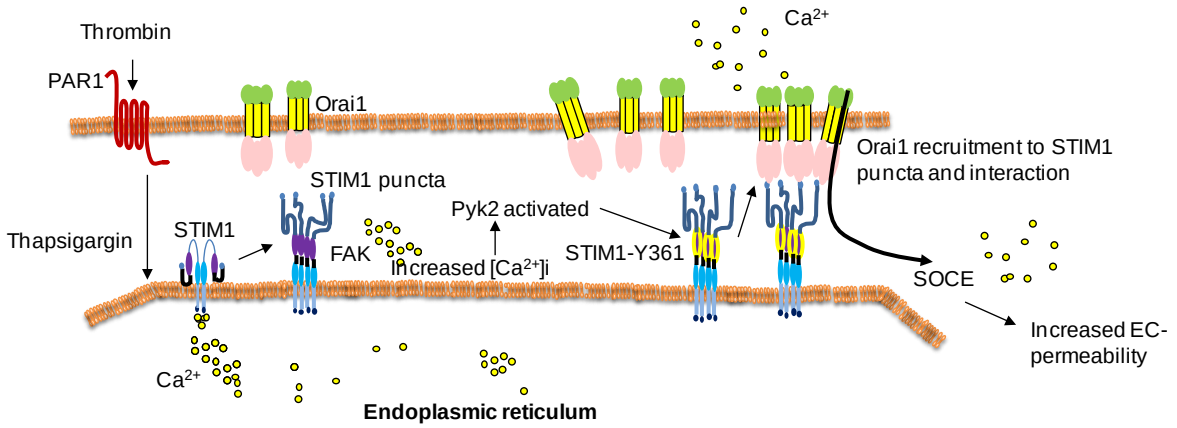

Figure 22. Model of FAK regulation of SOCE. Thrombin induces depletion of Ca^{2+} stored from the ER leading or oligomerization of STIM1 proteins. Released cytosolic Ca^{2+} in turn activates Proline rich tyrosine kinase Pyk2 to phosphorylate STIM1 at Y361 resisue to allow STIM1-Orai1 interaction, puncta formation and SOCE. Mehta D. Unpublished

IV. SUMMARY AND CONCLUSIONS

In this study, we have uncovered a novel regulatory mechanism that primes STIM1 to interact with the Ca^{2+}-selective Orai1 channel inducing SOCE. We showed that FAK regulates Pyk2 activity and that Pyk2 is highly phosphorylated in the absence of FAK. In this context, Pyk2-dependent phosphorylation of the Y361 residue within STIM1 induces SOCE. Our data showed that phosphorylation of the Y361 residue does not interfere with STIM1 puncta formation but controls recruitment of Orai1 to STIM1 puncta enabling STIM1-Orai1 interaction and Ca^{2+} entry through Orai1 channels. Furthermore, we established the physiological role of STIM1 tyrosine phosphorylation in regulating endothelial permeability *in vivo* by demonstrating that transduction of the phospho-defective STIM1-Y361F mutant in pulmonary endothelium of WT mice blocked the increase in endothelial permeability associated with activation of PAR1 signaling. In summary, STIM1 phosophorylation at Y361 represents a novel target for preventing diseases associated with leaky blood vessels.

V. FUTURE DIRECTIONS

This work has identified a novel mechanism by which FAK epigenetically regulates S1PR1 expression. We have shown that DNMT activity was significantly increased in FAK depleted cells compared to control cells. Although we identified DNMT3A as a mechanism of regulation of KLF2, we still need thorough analysis of this regulation. Altering DNMT3A activity using pharmacological inhibitor such as 5'Aza or knock down approach should restore KLF2 and S1PR1 expression in FAK depleted ECs. Recent studies have shown that cellular tension modulates gene expression by inducing epigenetic machinery. Schmidt et al. have shown that loss of endothelial FAK has altered the balance between RhoA and Rac1 GTPases favoring RhoA and inducing cellular tension. We speculate that RhoA activation in the absence of FAK provides a mechanism by which FAK regulates DNMT activity. This hypothesis needs to be tested rigorously. Restoring cellular balance between RhoA and Rac1 by dn RhoA, RhoA inhibitor or Knocking down RhoA should suppress DNMT3A activity in FAK depleted or null ECs. Although we have shown that FAK is responsible for modulating KLF2 expression and thus S1PR1 transcription, we still need to identify the role of kinase vs non-kinase function of FAK in this process. Loss of FAK has led to increase in SOCE. We showed that Pyk2, a Ca^{2+} dependent kinase is phosphorylated in the absence of FAK. How FAK maintains pyk2 and SOCE needs further investigation. FAK regulation of SOCE and DNMT to regulate barrier function could be distinct or merged pathways (Figure 23). Thorough investigation is needed to assess these two pathways.

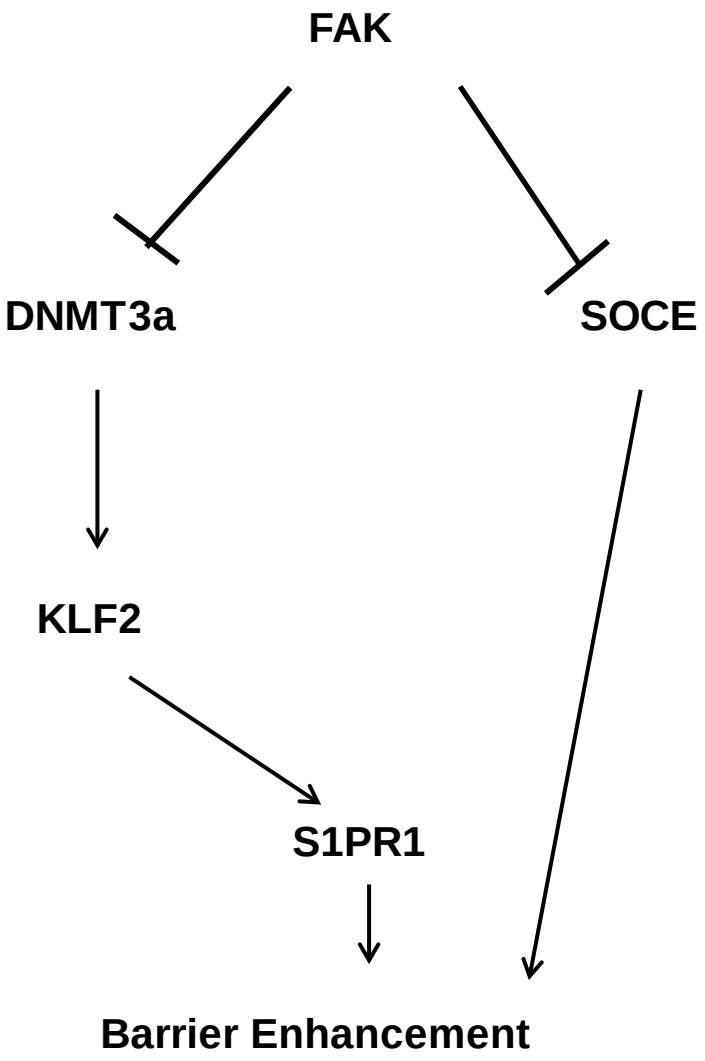

Figure 23. Model of FAK regulation of EC barrier: FAK suppresses DNMT3A activity to maintain KLF2 promoter and facilitate the transcription of S1PR1 to enhance EC barrier. Also FAK suppresses SOCE by regulating STIM1 phosphorylation and STIM1-Orai1 coupling to prevent Ca^{2+} influx and maintain EC barrier.

VI. Appendices

Appendix A

Figures by Yazbeck et al. under Creative Commons Attribution (CC BY) Scientific Reports. No permission is required.

Results and Discussions from Chapter III section B is copy paste from Yazbeck et al. under Creative Commons Attribution, Scientific Reports. No permission is required.

VII. CITED LITERATURE

Abdullaev, I. F., J. M. Bisaillon, M. Potier, J. C. Gonzalez, R. K. Motiani, and M. Trebak. 2008. "Stim1 and Orai1 mediate CRAC currents and store-operated calcium entry important for endothelial cell proliferation." *Circ Res* 103 (11):1289-99. doi: 10.1161/01.RES.0000338496.95579.56.

Ambily, A., W. J. Kaiser, C. Pierro, E. V. Chamberlain, Z. Li, C. I. Jones, N. Kassouf, J. M. Gibbins, and K. S. Authi. 2014. "The role of plasma membrane STIM1 and Ca(2+)entry in platelet aggregation. STIM1 binds to novel proteins in human platelets." *Cell Signal* 26 (3):502-11. doi: 10.1016/j.cellsig.2013.11.025.

Ancellin, N., C. Colmont, J. Su, Q. Li, N. Mittereder, S. S. Chae, S. Stefansson, G. Liau, and T. Hla. 2002. "Extracellular export of sphingosine kinase-1 enzyme. Sphingosine 1-phosphate generation and the induction of angiogenic vascular maturation." *J Biol Chem* 277 (8):6667-75. doi: 10.1074/jbc.M102841200.

Anderson, K. P., C. B. Kern, S. C. Crable, and J. B. Lingrel. 1995. "Isolation of a gene encoding a functional zinc finger protein homologous to erythroid Kruppel-like factor: identification of a new multigene family." *Mol Cell Biol* 15 (11):5957-65.

Anliker, B., and J. Chun. 2004. "Cell surface receptors in lysophospholipid signaling." *Semin Cell Dev Biol* 15 (5):457-65. doi: 10.1016/j.semcdb.2004.05.005.

Atkins, G. B., and M. K. Jain. 2007. "Role of Kruppel-like transcription factors in endothelial biology." *Circ Res* 100 (12):1686-95. doi: 10.1161/01.RES.0000267856.00713.0a.

Bai, A., H. Hu, M. Yeung, and J. Chen. 2007. "Kruppel-like factor 2 controls T cell trafficking by activating L-selectin (CD62L) and sphingosine-1-phosphate receptor 1 transcription." *J Immunol* 178 (12):7632-9.

Bassi, R., V. Anelli, P. Giussani, G. Tettamanti, P. Viani, and L. Riboni. 2006. "Sphingosine-1-phosphate is released by cerebellar astrocytes in response to bFGF and induces astrocyte proliferation through Gi-protein-coupled receptors." *Glia* 53 (6):621-30. doi: 10.1002/glia.20324.

Bestor, T. H. 2000. "The DNA methyltransferases of mammals." *Hum Mol Genet* 9 (16):2395-402.

Bi, W., C. J. Drake, and J. J. Schwarz. 1999. "The transcription factor MEF2C-null mouse exhibits complex vascular malformations and reduced cardiac expression of angiopoietin 1 and VEGF." *Dev Biol* 211 (2):255-67. doi: 10.1006/dbio.1999.9307.

Bird, A. P. 1986. "CpG-rich islands and the function of DNA methylation." *Nature* 321 (6067):209-13. doi: 10.1038/321209a0.

Bird, G. S., S. Y. Hwang, J. T. Smyth, M. Fukushima, R. R. Boyles, and J. W. Putney, Jr. 2009. "STIM1 is a calcium sensor specialized for digital signaling." *Curr Biol* 19 (20):1724-9. doi: 10.1016/j.cub.2009.08.022.

Black, B. L., and E. N. Olson. 1998. "Transcriptional control of muscle development by myocyte enhancer factor-2 (MEF2) proteins." *Annu Rev Cell Dev Biol* 14:167-96. doi: 10.1146/annurev.cellbio.14.1.167.

Blaho, V. A., and T. Hla. 2011. "Regulation of mammalian physiology, development, and disease by the sphingosine 1-phosphate and lysophosphatidic acid receptors." *Chem Rev* 111 (10):6299-320. doi: 10.1021/cr200273u.

Bootman, M. D., T. J. Collins, C. M. Peppiatt, L. S. Prothero, L. MacKenzie, P. De Smet, M. Travers, S. C. Tovey, J. T. Seo, M. J. Berridge, F. Ciccolini, and P. Lipp. 2001. "Calcium signalling--an overview." *Semin Cell Dev Biol* 12 (1):3-10. doi: 10.1006/scdb.2000.0211.

Braren, R., H. Hu, Y. H. Kim, H. E. Beggs, L. F. Reichardt, and R. Wang. 2006. "Endothelial FAK is essential for vascular network stability, cell survival, and lamellipodial formation." *J Cell Biol* 172 (1):151-62. doi: 10.1083/jcb.200506184.

Cai, Y., C. Bolte, T. Le, C. Goda, Y. Xu, T. V. Kalin, and V. V. Kalinichenko. 2016. "FOXF1 maintains endothelial barrier function and prevents edema after lung injury." *Sci Signal* 9 (424):ra40. doi: 10.1126/scisignal.aad1899.

Carbajal, J. M., and R. C. Schaeffer, Jr. 1999. "RhoA inactivation enhances endothelial barrier function." *Am J Physiol* 277 (5 Pt 1):C955-64.

Castillo-Aguilera, O., P. Depreux, L. Halby, P. B. Arimondo, and L. Goossens. 2017. "DNA Methylation Targeting: The DNMT/HMT Crosstalk Challenge." *Biomolecules* 7 (1). doi: 10.3390/biom7010003.

Chavez, A., T. T. Schmidt, P. Yazbeck, C. Rajput, B. Desai, S. Sukriti, K. Giantsos-Adams, N. Knezevic, A. B. Malik, and D. Mehta. 2015. "S1PR1 Tyr143 phosphorylation downregulates endothelial cell surface S1PR1 expression and responsiveness." *J Cell Sci* 128 (5):878-87. doi: 10.1242/jcs.154476.

Chen, H. C., P. A. Appeddu, J. T. Parsons, J. D. Hildebrand, M. D. Schaller, and J. L. Guan. 1995. "Interaction of focal adhesion kinase with cytoskeletal protein talin." *J Biol Chem* 270 (28):16995-9.

Chen, W., M. Bacanamwo, and D. G. Harrison. 2008. "Activation of p300 histone acetyltransferase activity is an early endothelial response to laminar shear stress and is essential for stimulation of endothelial nitric-oxide synthase mRNA transcription." *J Biol Chem* 283 (24):16293-8. doi: 10.1074/jbc.M801803200.

Cheng, K. T., H. L. Ong, X. Liu, and I. S. Ambudkar. 2011. "Contribution of TRPC1 and Orai1 to Ca(2+) entry activated by store depletion." *Adv Exp Med Biol* 704:435-49. doi: 10.1007/978-94-007-0265-3_24.

Cheng, K. T., H. L. Ong, X. Liu, and I. S. Ambudkar. 2013. "Contribution and regulation of TRPC channels in store-operated Ca2+ entry." *Curr Top Membr* 71:149-79. doi: 10.1016/B978-0-12-407870-3.00007-X.

Chitaley, K., D. Weber, and R. C. Webb. 2001. "RhoA/Rho-kinase, vascular changes, and hypertension." *Curr Hypertens Rep* 3 (2):139-44.

Cioffi, D. L., C. Barry, and T. Stevens. 2010. "Store-operated calcium entry channels in pulmonary endothelium: the emerging story of TRPCS and Orai1." *Adv Exp Med Biol* 661:137-54. doi: 10.1007/978-1-60761-500-2_9.

Cioffi, D. L., and T. Stevens. 2006. "Regulation of endothelial cell barrier function by store-operated calcium entry." *Microcirculation* 13 (8):709-23. doi: 10.1080/10739680600930354.

Conkright, M. D., M. A. Wani, and J. B. Lingrel. 2001. "Lung Kruppel-like factor contains an autoinhibitory domain that regulates its transcriptional activation by binding WWP1, an E3 ubiquitin ligase." *J Biol Chem* 276 (31):29299-306. doi: 10.1074/jbc.M103670200.

Covington, E. D., M. M. Wu, and R. S. Lewis. 2010. "Essential role for the CRAC activation domain in store-dependent oligomerization of STIM1." *Mol Biol Cell* 21 (11):1897-907. doi: 10.1091/mbc.E10-02-0145.

Dang, D. T., J. Pevsner, and V. W. Yang. 2000. "The biology of the mammalian Kruppel-like family of transcription factors." *Int J Biochem Cell Biol* 32 (11-12):1103-21.

DebRoy, A., S. M. Vogel, D. Soni, P. C. Sundivakkam, A. B. Malik, and C. Tiruppathi. 2014. "Cooperative signaling via transcription factors NF-kappaB and AP1/c-Fos mediates endothelial cell STIM1 expression and hyperpermeability in response to endotoxin." *J Biol Chem* 289 (35):24188-201. doi: 10.1074/jbc.M114.570051.

Dekker, R. J., S. van Soest, R. D. Fontijn, S. Salamanca, P. G. de Groot, E. VanBavel, H. Pannekoek, and A. J. Horrevoets. 2002. "Prolonged fluid shear stress induces a distinct set of endothelial cell genes, most specifically lung Kruppel-like factor (KLF2)." *Blood* 100 (5):1689-98. doi: 10.1182/blood-2002-01-0046.

Derler, I., I. Jardin, and C. Romanin. 2016. "Molecular mechanisms of STIM/Orai communication." *Am J Physiol Cell Physiol* 310 (8):C643-62. doi: 10.1152/ajpcell.00007.2016.

Dudek, S. M., J. R. Jacobson, E. T. Chiang, K. G. Birukov, P. Wang, X. Zhan, and J. G. Garcia. 2004. "Pulmonary endothelial cell barrier enhancement by sphingosine 1-phosphate: roles for cortactin and myosin light chain kinase." *J Biol Chem* 279 (23):24692-700. doi: 10.1074/jbc.M313969200.

Edsall, L. C., and S. Spiegel. 1999. "Enzymatic measurement of sphingosine 1-phosphate." *Anal Biochem* 272 (1):80-6. doi: 10.1006/abio.1999.4157.

Ezratty, E. J., M. A. Partridge, and G. G. Gundersen. 2005. "Microtubule-induced focal adhesion disassembly is mediated by dynamin and focal adhesion kinase." *Nat Cell Biol* 7 (6):581-90. doi: 10.1038/ncb1262.

Fahrner, M., I. Derler, I. Jardin, and C. Romanin. 2013. "The STIM1/Orai signaling machinery." *Channels (Austin)* 7 (5):330-43. doi: 10.4161/chan.26742.

Feinberg, M. W., Z. Lin, S. Fisch, and M. K. Jain. 2004. "An emerging role for Kruppel-like factors in vascular biology." *Trends Cardiovasc Med* 14 (6):241-6. doi: 10.1016/j.tcm.2004.06.005.

Feske, S., and M. Prakriya. 2013. "Conformational dynamics of STIM1 activation." *Nat Struct Mol Biol* 20 (8):918-9. doi: 10.1038/nsmb.2647.

Fledderus, J. O., J. V. van Thienen, R. A. Boon, R. J. Dekker, J. Rohlena, O. L. Volger, A. P. Bijnens, M. J. Daemen, J. Kuiper, T. J. van Berkel, H. Pannekoek, and A. J. Horrevoets. 2007. "Prolonged shear stress and KLF2 suppress constitutive proinflammatory transcription through inhibition of ATF2." *Blood* 109 (10):4249-57. doi: 10.1182/blood-2006-07-036020.

Fu, P., D. L. Ebenezer, E. V. Berdyshev, I. A. Bronova, M. Shaaya, A. Harijith, and V. Natarajan. 2016. "Role of Sphingosine Kinase 1 and S1P Transporter Spns2 in HGF-mediated Lamellipodia Formation in Lung Endothelium." *J Biol Chem* 291 (53):27187-27203. doi: 10.1074/jbc.M116.758946.

Garcia, J. G., F. Liu, A. D. Verin, A. Birukova, M. A. Dechert, W. T. Gerthoffer, J. R. Bamberg, and D. English. 2001. "Sphingosine 1-phosphate promotes endothelial cell barrier integrity by Edg-dependent cytoskeletal rearrangement." *J Clin Invest* 108 (5):689-701. doi: 10.1172/JCI12450.

Goetzl, E. J., and G. Tigyi. 2004. "Lysophospholipids and their G protein-coupled receptors in biology and diseases." *J Cell Biochem* 92 (5):867-8. doi: 10.1002/jcb.20186.

Gonzales, J. N., B. Gorshkov, M. N. Varn, M. A. Zemskova, E. A. Zemskov, S. Sridhar, R. Lucas, and A. D. Verin. 2014. "Protective effect of adenosine receptors against lipopolysaccharide-induced acute lung injury." *Am J Physiol Lung Cell Mol Physiol* 306 (6):L497-507. doi: 10.1152/ajplung.00086.2013.

Guan, J. L., and D. Shalloway. 1992. "Regulation of focal adhesion-associated protein tyrosine kinase by both cellular adhesion and oncogenic transformation." *Nature* 358 (6388):690-2. doi: 10.1038/358690a0.

Guan, J. L., J. E. Trevithick, and R. O. Hynes. 1991. "Fibronectin/integrin interaction induces tyrosine phosphorylation of a 120-kDa protein." *Cell Regul* 2 (11):951-64.

Gudermann, T., and D. Steinritz. 2013. "STIMulating stress fibers in endothelial cells." *Sci Signal* 6 (267):pe8. doi: 10.1126/scisignal.2004051.

Hanks, S. K., M. B. Calalb, M. C. Harper, and S. K. Patel. 1992. "Focal adhesion protein-tyrosine kinase phosphorylated in response to cell attachment to fibronectin." *Proc Natl Acad Sci U S A* 89 (18):8487-91.

He, P., M. J. Philbrick, X. An, J. Wu, A. F. Messmer-Blust, and J. Li. 2014. "Endothelial differentiation gene-1, a new downstream gene is involved in RTEF-1 induced angiogenesis in endothelial cells." *PLoS One* 9 (2):e88143. doi: 10.1371/journal.pone.0088143.

Hens, M. D., and D. W. DeSimone. 1995. "Molecular analysis and developmental expression of the focal adhesion kinase pp125FAK in Xenopus laevis." *Dev Biol* 170 (2):274-88. doi: 10.1006/dbio.1995.1214.

Hildebrand, J. D., M. D. Schaller, and J. T. Parsons. 1993. "Identification of sequences required for the efficient localization of the focal adhesion kinase, pp125FAK, to cellular focal adhesions." *J Cell Biol* 123 (4):993-1005.

Hla, T. 2003. "Signaling and biological actions of sphingosine 1-phosphate." *Pharmacol Res* 47 (5):401-7.

Hla, T., and T. Maciag. 1990. "An abundant transcript induced in differentiating human endothelial cells encodes a polypeptide with structural similarities to G-protein-coupled receptors." *J Biol Chem* 265 (16):9308-13.

Hodeify, R., S. Selvaraj, J. Wen, A. Arredouani, S. Hubrack, M. Dib, S. N. Al-Thani, T. McGraw, and K. Machaca. 2015. "A STIM1-dependent 'trafficking trap' mechanism regulates Orai1 plasma membrane residence and Ca(2)(+) influx levels." *J Cell Sci* 128 (16):3143-54. doi: 10.1242/jcs.172320.

Holinstat, M., N. Knezevic, M. Broman, A. M. Samarel, A. B. Malik, and D. Mehta. 2006. "Suppression of RhoA activity by focal adhesion kinase-induced activation of p190RhoGAP: role in regulation of endothelial permeability." *J Biol Chem* 281 (4):2296-305. doi: 10.1074/jbc.M511248200.

Huang, G. N., W. Zeng, J. Y. Kim, J. P. Yuan, L. Han, S. Muallem, and P. F. Worley. 2006. "STIM1 carboxyl-terminus activates native SOC, I(crac) and TRPC1 channels." *Nat Cell Biol* 8 (9):1003-10. doi: 10.1038/ncb1454.

Huang, Y., Y. Zhou, H. C. Wong, Y. Chen, Y. Chen, S. Wang, A. Castiblanco, A. Liu, and J. J. Yang. 2009. "A single EF-hand isolated from STIM1 forms dimer in the absence and presence of Ca2+." *FEBS J* 276 (19):5589-97. doi: 10.1111/j.1742-4658.2009.07240.x.

Huddleson, J. P., S. Srinivasan, N. Ahmad, and J. B. Lingrel. 2004. "Fluid shear stress induces endothelial KLF2 gene expression through a defined promoter region." *Biol Chem* 385 (8):723-9. doi: 10.1515/bc.2004.088.

Hyser, J. M., B. Utama, S. E. Crawford, J. R. Broughman, and M. K. Estes. 2013. "Activation of the endoplasmic reticulum calcium sensor STIM1 and store-operated calcium entry by rotavirus requires NSP4 viroporin activity." *J Virol* 87 (24):13579-88. doi: 10.1128/JVI.02629-13.

Igarashi, Y., and Y. Yatomi. 1998. "Sphingosine 1-phosphate is a blood constituent released from activated platelets, possibly playing a variety of physiological and pathophysiological roles." *Acta Biochim Pol* 45 (2):299-309.

Ilic, D., Y. Furuta, S. Kanazawa, N. Takeda, K. Sobue, N. Nakatsuji, S. Nomura, J. Fujimoto, M. Okada, and T. Yamamoto. 1995. "Reduced cell motility and enhanced focal adhesion contact formation in cells from FAK-deficient mice." *Nature* 377 (6549):539-44. doi: 10.1038/377539a0.

Jackle, H., U. B. Rosenberg, A. Preiss, E. Seifert, D. C. Knipple, A. Kienlin, and R. Lehmann. 1985. "Molecular analysis of Kruppel, a segmentation gene of Drosophila melanogaster." *Cold Spring Harb Symp Quant Biol* 50:465-73.

Kato, Y., V. V. Kravchenko, R. I. Tapping, J. Han, R. J. Ulevitch, and J. D. Lee. 1997. "BMK1/ERK5 regulates serum-induced early gene expression through transcription factor MEF2C." *Embo j* 16 (23):7054-66. doi: 10.1093/emboj/16.23.7054.

Kawasaki, T., I. Lange, and S. Feske. 2009. "A minimal regulatory domain in the C terminus of STIM1 binds to and activates ORAI1 CRAC channels." *Biochem Biophys Res Commun* 385 (1):49-54. doi: 10.1016/j.bbrc.2009.05.020.

Knezevic, N., M. Tauseef, T. Thennes, and D. Mehta. 2009. "The G protein betagamma subunit mediates reannealing of adherens junctions to reverse endothelial permeability increase by thrombin." *J Exp Med* 206 (12):2761-77. doi: 10.1084/jem.20090652.

Kornberg, L. J., H. S. Earp, C. E. Turner, C. Prockop, and R. L. Juliano. 1991. "Signal transduction by integrins: increased protein tyrosine phosphorylation caused by clustering of beta 1 integrins." *Proc Natl Acad Sci U S A* 88 (19):8392-6.

Korzeniowski, M. K., I. M. Manjarres, P. Varnai, and T. Balla. 2010. "Activation of STIM1-Orai1 involves an intramolecular switching mechanism." *Sci Signal* 3 (148):ra82. doi: 10.1126/scisignal.2001122.

Krump-Konvalinkova, V., S. Yasuda, T. Rubic, N. Makarova, J. Mages, W. Erl, C. Vosseler, C. J. Kirkpatrick, G. Tigyi, and W. Siess. 2005. "Stable knock-down of the sphingosine 1-phosphate receptor S1P1 influences multiple functions of human endothelial cells." *Arterioscler Thromb Vasc Biol* 25 (3):546-52. doi: 10.1161/01.ATV.0000154360.36106.d9.

Kumar, A., S. Kumar, A. Vikram, T. A. Hoffman, A. Naqvi, C. M. Lewarchik, Y. R. Kim, and K. Irani. 2013. "Histone and DNA methylation-mediated epigenetic downregulation of endothelial Kruppel-like factor 2 by low-density lipoprotein cholesterol." *Arterioscler Thromb Vasc Biol* 33 (8):1936-42. doi: 10.1161/ATVBAHA.113.301765.

Kumar, A., Z. Lin, S. SenBanerjee, and M. K. Jain. 2005. "Tumor necrosis factor alpha-mediated reduction of KLF2 is due to inhibition of MEF2 by NF-kappaB and histone deacetylases." *Mol Cell Biol* 25 (14):5893-903. doi: 10.1128/MCB.25.14.5893-5903.2005.

Kuo, C. T., M. L. Veselits, K. P. Barton, M. M. Lu, C. Clendenin, and J. M. Leiden. 1997. "The LKLF transcription factor is required for normal tunica media formation and blood vessel stabilization during murine embryogenesis." *Genes Dev* 11 (22):2996-3006.

Lee, H., J. Deng, M. Kujawski, C. Yang, Y. Liu, A. Herrmann, M. Kortylewski, D. Horne, G. Somlo, S. Forman, R. Jove, and H. Yu. 2010. "STAT3-induced S1PR1 expression is crucial for persistent STAT3 activation in tumors." *Nat Med* 16 (12):1421-8. doi: 10.1038/nm.2250.

Lee, J. S., Q. Yu, J. T. Shin, E. Sebzda, C. Bertozzi, M. Chen, P. Mericko, M. Stadtfeld, D. Zhou, L. Cheng, T. Graf, C. A. MacRae, J. J. Lepore, C. W. Lo, and M. L. Kahn. 2006. "Klf2 is an essential regulator of vascular hemodynamic forces in vivo." *Dev Cell* 11 (6):845-57. doi: 10.1016/j.devcel.2006.09.006.

Lee, J. Y., C. N. Skon, Y. J. Lee, S. Oh, J. J. Taylor, D. Malhotra, M. K. Jenkins, M. G. Rosenfeld, K. A. Hogquist, and S. C. Jameson. 2015. "The transcription factor KLF2 restrains CD4(+) T follicular helper cell differentiation." *Immunity* 42 (2):252-64. doi: 10.1016/j.immuni.2015.01.013.

Lin, Q., J. Lu, H. Yanagisawa, R. Webb, G. E. Lyons, J. A. Richardson, and E. N. Olson. 1998. "Requirement of the MADS-box transcription factor MEF2C for vascular development." *Development* 125 (22):4565-74.

Liu, X., S. He, G. Skogerbo, F. Gong, and R. Chen. 2012. "Integrated sequence-structure motifs suffice to identify microRNA precursors." *PLoS One* 7 (3):e32797. doi: 10.1371/journal.pone.0032797.

Lopez, E., I. Jardin, A. Berna-Erro, N. Bermejo, G. M. Salido, S. O. Sage, J. A. Rosado, and P. C. Redondo. 2012. "STIM1 tyrosine-phosphorylation is required for STIM1-Orai1 association in human platelets." *Cell Signal* 24 (6):1315-22. doi: 10.1016/j.cellsig.2012.02.012.

Lu, Q., and S. Rounds. 2012. "Focal adhesion kinase and endothelial cell apoptosis." *Microvasc Res* 83 (1):56-63. doi: 10.1016/j.mvr.2011.05.003.

Lukasik, S. M., T. Cierpicki, M. Borloz, J. Grembecka, A. Everett, and J. H. Bushweller. 2006. "High resolution structure of the HDGF PWWP domain: a potential DNA binding domain." *Protein Sci* 15 (2):314-23. doi: 10.1110/ps.051751706.

Lulo, J., S. Yuzawa, and J. Schlessinger. 2009. "Crystal structures of free and ligand-bound focal adhesion targeting domain of Pyk2." *Biochem Biophys Res Commun* 383 (3):347-52. doi: 10.1016/j.bbrc.2009.04.011.

Matthay, M. A., and R. L. Zemans. 2011. "The acute respiratory distress syndrome: pathogenesis and treatment." *Annu Rev Pathol* 6:147-63. doi: 10.1146/annurev-pathol-011110-130158.

McKinsey, T. A., C. L. Zhang, and E. N. Olson. 2002. "MEF2: a calcium-dependent regulator of cell division, differentiation and death." *Trends Biochem Sci* 27 (1):40-7.

McVerry, B. J., and J. G. Garcia. 2005. "In vitro and in vivo modulation of vascular barrier integrity by sphingosine 1-phosphate: mechanistic insights." *Cell Signal* 17 (2):131-9. doi: 10.1016/j.cellsig.2004.08.006.

Mehta, D. 2012. "Focal adhesion kinase regulation of endothelial barrier function, apoptosis, and neovascularization." *Microvasc Res* 83 (1):1-2. doi: 10.1016/j.mvr.2011.10.001.

Mehta, D., G. U. Ahmmed, B. C. Paria, M. Holinstat, T. Voyno-Yasenetskaya, C. Tiruppathi, R. D. Minshall, and A. B. Malik. 2003. "RhoA interaction with inositol 1,4,5-trisphosphate receptor and transient receptor potential channel-1 regulates Ca2+ entry. Role in signaling increased endothelial permeability." *J Biol Chem* 278 (35):33492-500. doi: 10.1074/jbc.M302401200.

Mehta, D., M. Konstantoulaki, G. U. Ahmmed, and A. B. Malik. 2005. "Sphingosine 1-phosphate-induced mobilization of intracellular Ca2+ mediates rac activation and adherens junction assembly in endothelial cells." *J Biol Chem* 280 (17):17320-8. doi: 10.1074/jbc.M411674200.

Mehta, D., and A. B. Malik. 2006. "Signaling mechanisms regulating endothelial permeability." *Physiol Rev* 86 (1):279-367. doi: 10.1152/physrev.00012.2005.

Meyer zu Heringdorf, D., H. Lass, R. Alemany, K. T. Laser, E. Neumann, C. Zhang, M. Schmidt, U. Rauen, K. H. Jakobs, and C. J. van Koppen. 1998. "Sphingosine kinase-mediated Ca2+ signalling by G-protein-coupled receptors." *Embo j* 17 (10):2830-7. doi: 10.1093/emboj/17.10.2830.

Miller, I. J., and J. J. Bieker. 1993. "A novel, erythroid cell-specific murine transcription factor that binds to the CACCC element and is related to the Kruppel family of nuclear proteins." *Mol Cell Biol* 13 (5):2776-86.

Mitra, S. K., D. A. Hanson, and D. D. Schlaepfer. 2005. "Focal adhesion kinase: in command and control of cell motility." *Nat Rev Mol Cell Biol* 6 (1):56-68. doi: 10.1038/nrm1549.

Moccia, F., R. Berra-Romani, and F. Tanzi. 2012. "Update on vascular endothelial Ca(2+) signalling: A tale of ion channels, pumps and transporters." *World J Biol Chem* 3 (7):127-58. doi: 10.4331/wjbc.v3.i7.127.

Montecinos-Oliva, C., A. Schuller, J. Parodi, F. Melo, and N. C. Inestrosa. 2014. "Effects of tetrahydrohyperforin in mouse hippocampal slices: neuroprotection, long-term potentiation and TRPC channels." *Curr Med Chem* 21 (30):3494-506.

Moolenaar, W. H. 1995. "Lysophosphatidic acid signalling." *Curr Opin Cell Biol* 7 (2):203-10.

Moore, T. M., N. R. Norwood, J. R. Creighton, P. Babal, G. H. Brough, D. M. Shasby, and T. Stevens. 2000. "Receptor-dependent activation of store-operated calcium entry increases endothelial cell permeability." *Am J Physiol Lung Cell Mol Physiol* 279 (4):L691-8.

Naya, F. J., and E. Olson. 1999. "MEF2: a transcriptional target for signaling pathways controlling skeletal muscle growth and differentiation." *Curr Opin Cell Biol* 11 (6):683-8.

Nuez, B., D. Michalovich, A. Bygrave, R. Ploemacher, and F. Grosveld. 1995. "Defective haematopoiesis in fetal liver resulting from inactivation of the EKLF gene." *Nature* 375 (6529):316-8. doi: 10.1038/375316a0.

Olson, E. N. 2004. "Undermining the endothelium by ablation of MAPK-MEF2 signaling." *J Clin Invest* 113 (8):1110-2. doi: 10.1172/jci21497.

Oo, M. L., S. H. Chang, S. Thangada, M. T. Wu, K. Rezaul, V. Blaho, S. I. Hwang, D. K. Han, and T. Hla. 2011. "Engagement of S1P(1)-degradative mechanisms leads to vascular leak in mice." *J Clin Invest* 121 (6):2290-300. doi: 10.1172/JCI45403.

Oo, M. L., S. Thangada, M. T. Wu, C. H. Liu, T. L. Macdonald, K. R. Lynch, C. Y. Lin, and T. Hla. 2007. "Immunosuppressive and anti-angiogenic sphingosine 1-phosphate receptor-1 agonists induce ubiquitinylation and proteasomal degradation of the receptor." *J Biol Chem* 282 (12):9082-9. doi: 10.1074/jbc.M610318200.

Parekh, A. B., and J. W. Putney, Jr. 2005. "Store-operated calcium channels." *Physiol Rev* 85 (2):757-810. doi: 10.1152/physrev.00057.2003.

Parmar, K. M., H. B. Larman, G. Dai, Y. Zhang, E. T. Wang, S. N. Moorthy, J. R. Kratz, Z. Lin, M. K. Jain, M. A. Gimbrone, Jr., and G. Garcia-Cardena. 2006. "Integration of flow-dependent endothelial phenotypes by Kruppel-like factor 2." *J Clin Invest* 116 (1):49-58. doi: 10.1172/JCI24787.

Parsons, J. T. 2003. "Focal adhesion kinase: the first ten years." *J Cell Sci* 116 (Pt 8):1409-16.

Patel, D. J. 2016. "A Structural Perspective on Readout of Epigenetic Histone and DNA Methylation Marks." *Cold Spring Harb Perspect Biol* 8 (3):a018754. doi: 10.1101/cshperspect.a018754.

Perkins, A. C., A. H. Sharpe, and S. H. Orkin. 1995. "Lethal beta-thalassaemia in mice lacking the erythroid CACCC-transcription factor EKLF." *Nature* 375 (6529):318-22. doi: 10.1038/375318a0.

Petit, V., and J. P. Thiery. 2000. "Focal adhesions: structure and dynamics." *Biol Cell* 92 (7):477-94.

Pober, J. S., and W. C. Sessa. 2007. "Evolving functions of endothelial cells in inflammation." *Nat Rev Immunol* 7 (10):803-15. doi: 10.1038/nri2171.

Pon, J. R., and M. A. Marra. 2016. "MEF2 transcription factors: developmental regulators and emerging cancer genes." *Oncotarget* 7 (3):2297-312. doi: 10.18632/oncotarget.6223.

Potthoff, M. J., and E. N. Olson. 2007. "MEF2: a central regulator of diverse developmental programs." *Development* 134 (23):4131-40. doi: 10.1242/dev.008367.

Prandini, M. H., I. Dreher, S. Bouillot, S. Benkerri, T. Moll, and P. Huber. 2005. "The human VE-cadherin promoter is subjected to organ-specific regulation and is activated in tumour angiogenesis." *Oncogene* 24 (18):2992-3001. doi: 10.1038/sj.onc.1208483.

Preiss, A., U. B. Rosenberg, A. Kienlin, E. Seifert, and H. Jackle. 1985. "Molecular genetics of Kruppel, a gene required for segmentation of the Drosophila embryo." *Nature* 313 (5997):27-32.

Prutzman, K. C., G. Gao, M. L. King, V. V. Iyer, G. A. Mueller, M. D. Schaller, and S. L. Campbell. 2004. "The focal adhesion targeting domain of focal adhesion kinase contains a hinge region that modulates tyrosine 926 phosphorylation." *Structure* 12 (5):881-91. doi: 10.1016/j.str.2004.02.028.

Putney, J. W., Jr. 2005. "Capacitative calcium entry: sensing the calcium stores." *J Cell Biol* 169 (3):381-2. doi: 10.1083/jcb.200503161.

Quadri, S. K., M. Bhattacharjee, K. Parthasarathi, T. Tanita, and J. Bhattacharya. 2003. "Endothelial barrier strengthening by activation of focal adhesion kinase." *J Biol Chem* 278 (15):13342-9. doi: 10.1074/jbc.M209922200.

Quadri, S. K., and J. Bhattacharya. 2007. "Resealing of endothelial junctions by focal adhesion kinase." *Am J Physiol Lung Cell Mol Physiol* 292 (1):L334-42. doi: 10.1152/ajplung.00228.2006.

Quarles, K. A., D. Sahu, M. A. Havens, E. R. Forsyth, C. Wostenberg, M. L. Hastings, and S. A. Showalter. 2013. "Ensemble analysis of primary microRNA structure reveals an extensive capacity to deform near the Drosha cleavage site." *Biochemistry* 52 (5):795-807. doi: 10.1021/bi301452a.

Radeva, M. Y., and J. Waschke. 2017. "Mind the gap: mechanisms regulating the endothelial barrier." *Acta Physiol (Oxf)*. doi: 10.1111/apha.12860.

Rajput, C., V. Kini, M. Smith, P. Yazbeck, A. Chavez, T. Schmidt, W. Zhang, N. Knezevic, Y. Komarova, and D. Mehta. 2013. "Neural Wiskott-Aldrich syndrome protein (N-WASP)-mediated p120-catenin interaction with Arp2-Actin complex stabilizes endothelial adherens junctions." *J Biol Chem* 288 (6):4241-50. doi: 10.1074/jbc.M112.440396.

Sanllehi, P., J. L. Abad, J. Casas, and A. Delgado. 2016. "Inhibitors of sphingosine-1-phosphate metabolism (sphingosine kinases and sphingosine-1-phosphate lyase)." *Chem Phys Lipids* 197:69-81. doi: 10.1016/j.chemphyslip.2015.07.007.

Scheswohl, D. M., J. R. Harrell, Z. Rajfur, G. Gao, S. L. Campbell, and M. D. Schaller. 2008. "Multiple paxillin binding sites regulate FAK function." *J Mol Signal* 3:1. doi: 10.1186/1750-2187-3-1.

Schindl, R., M. Muik, M. Fahrner, I. Derler, R. Fritsch, J. Bergsmann, and C. Romanin. 2009. "Recent progress on STIM1 domains controlling Orai activation." *Cell Calcium* 46 (4):227-32. doi: 10.1016/j.ceca.2009.08.003.

Schmidt, T. T., M. Tauseef, L. Yue, M. G. Bonini, J. Gothert, T. L. Shen, J. L. Guan, S. Predescu, R. Sadikot, and D. Mehta. 2013. "Conditional deletion of FAK in mice endothelium disrupts lung vascular barrier function due to destabilization of RhoA and Rac1 activities." *Am J Physiol Lung Cell Mol Physiol* 305 (4):L291-300. doi: 10.1152/ajplung.00094.2013.

SenBanerjee, S., Z. Lin, G. B. Atkins, D. M. Greif, R. M. Rao, A. Kumar, M. W. Feinberg, Z. Chen, D. I. Simon, F. W. Luscinskas, T. M. Michel, M. A. Gimbrone, Jr., G. Garcia-Cardena, and M. K. Jain. 2004. "KLF2 Is a novel transcriptional regulator of endothelial proinflammatory activation." *J Exp Med* 199 (10):1305-15. doi: 10.1084/jem.20031132.

Shen, T. L., A. Y. Park, A. Alcaraz, X. Peng, I. Jang, P. Koni, R. A. Flavell, H. Gu, and J. L. Guan. 2005. "Conditional knockout of focal adhesion kinase in endothelial cells reveals its role in angiogenesis and vascular development in late embryogenesis." *J Cell Biol* 169 (6):941-52. doi: 10.1083/jcb.200411155.

Shim, A. H., L. Tirado-Lee, and M. Prakriya. 2015. "Structural and functional mechanisms of CRAC channel regulation." *J Mol Biol* 427 (1):77-93. doi: 10.1016/j.jmb.2014.09.021.

Shimbo, T., and P. A. Wade. 2016. "Proteins That Read DNA Methylation." *Adv Exp Med Biol* 945:303-320. doi: 10.1007/978-3-319-43624-1_13.

Singh, I., N. Knezevic, G. U. Ahmmed, V. Kini, A. B. Malik, and D. Mehta. 2007. "Galphaq-TRPC6-mediated Ca2+ entry induces RhoA activation and resultant endothelial cell shape change in response to thrombin." *J Biol Chem* 282 (11):7833-43. doi: 10.1074/jbc.M608288200.

Singleton, P. A., S. M. Dudek, E. T. Chiang, and J. G. Garcia. 2005. "Regulation of sphingosine 1-phosphate-induced endothelial cytoskeletal rearrangement and barrier enhancement by S1P1 receptor, PI3 kinase, Tiam1/Rac1, and alpha-actinin." *FASEB J* 19 (12):1646-56. doi: 10.1096/fj.05-3928com.

Skon, C. N., J. Y. Lee, K. G. Anderson, D. Masopust, K. A. Hogquist, and S. C. Jameson. 2013. "Transcriptional downregulation of S1pr1 is required for the establishment of resident memory CD8+ T cells." *Nat Immunol* 14 (12):1285-93. doi: 10.1038/ni.2745.

Spiegel, S., and S. Milstien. 2003. "Sphingosine-1-phosphate: an enigmatic signalling lipid." *Nat Rev Mol Cell Biol* 4 (5):397-407. doi: 10.1038/nrm1103.

Spiering, D., and L. Hodgson. 2011. "Dynamics of the Rho-family small GTPases in actin regulation and motility." *Cell Adh Migr* 5 (2):170-80.

Stathopulos, P. B., G. Y. Li, M. J. Plevin, J. B. Ames, and M. Ikura. 2006. "Stored Ca2+ depletion-induced oligomerization of stromal interaction molecule 1 (STIM1) via the EF-SAM region: An initiation mechanism for capacitive Ca2+ entry." *J Biol Chem* 281 (47):35855-62. doi: 10.1074/jbc.M608247200.

Stathopulos, P. B., R. Schindl, M. Fahrner, L. Zheng, G. M. Gasmi-Seabrook, M. Muik, C. Romanin, and M. Ikura. 2013. "STIM1/Orai1 coiled-coil interplay in the regulation of store-operated calcium entry." *Nat Commun* 4:2963. doi: 10.1038/ncomms3963.

Stathopulos, P. B., L. Zheng, G. Y. Li, M. J. Plevin, and M. Ikura. 2008. "Structural and mechanistic insights into STIM1-mediated initiation of store-operated calcium entry." *Cell* 135 (1):110-22. doi: 10.1016/j.cell.2008.08.006.

Sukriti, S., M. Tauseef, P. Yazbeck, and D. Mehta. 2014. "Mechanisms regulating endothelial permeability." *Pulm Circ* 4 (4):535-51. doi: 10.1086/677356.

Suzuki, T., K. Aizawa, T. Matsumura, and R. Nagai. 2005. "Vascular implications of the Kruppel-like family of transcription factors." *Arterioscler Thromb Vasc Biol* 25 (6):1135-41. doi: 10.1161/01.atv.0000165656.65359.23.

Takabe, K., R. H. Kim, J. C. Allegood, P. Mitra, S. Ramachandran, M. Nagahashi, K. B. Harikumar, N. C. Hait, S. Milstien, and S. Spiegel. 2010. "Estradiol induces export of sphingosine 1-phosphate from breast cancer cells via ABCC1 and ABCG2." *J Biol Chem* 285 (14):10477-86. doi: 10.1074/jbc.M109.064162.

Takabe, K., S. W. Paugh, S. Milstien, and S. Spiegel. 2008. ""Inside-out" signaling of sphingosine-1-phosphate: therapeutic targets." *Pharmacol Rev* 60 (2):181-95. doi: 10.1124/pr.107.07113.

Tauseef, M., V. Kini, N. Knezevic, M. Brannan, R. Ramchandaran, H. Fyrst, J. Saba, S. M. Vogel, A. B. Malik, and D. Mehta. 2008. "Activation of sphingosine kinase-1 reverses the increase in lung vascular permeability through sphingosine-1-phosphate receptor signaling in endothelial cells." *Circ Res* 103 (10):1164-72. doi: 10.1161/01.res.0000338501.84810.51.

van Thienen, J. V., J. O. Fledderus, R. J. Dekker, J. Rohlena, G. A. van Ijzendoorn, N. A. Kootstra, H. Pannekoek, and A. J. Horrevoets. 2006. "Shear stress sustains atheroprotective endothelial KLF2 expression more potently than statins through mRNA stabilization." *Cardiovasc Res* 72 (2):231-40. doi: 10.1016/j.cardiores.2006.07.008.

Varnai, P., L. Hunyady, and T. Balla. 2009. "STIM and Orai: the long-awaited constituents of store-operated calcium entry." *Trends Pharmacol Sci* 30 (3):118-28. doi: 10.1016/j.tips.2008.11.005.

Venkataraman, K., Y. M. Lee, J. Michaud, S. Thangada, Y. Ai, H. L. Bonkovsky, N. S. Parikh, C. Habrukowich, and T. Hla. 2008. "Vascular endothelium as a contributor of plasma sphingosine 1-phosphate." *Circ Res* 102 (6):669-76. doi: 10.1161/circresaha.107.165845.

Wang, L., R. Bittman, J. G. Garcia, and S. M. Dudek. 2015. "Junctional complex and focal adhesion rearrangement mediates pulmonary endothelial barrier enhancement by FTY720 S-phosphonate." *Microvasc Res* 99:102-9. doi: 10.1016/j.mvr.2015.03.007.

Wang, L., S. Sammani, L. Moreno-Vinasco, E. Letsiou, T. Wang, S. M. Camp, R. Bittman, J. G. Garcia, and S. M. Dudek. 2014. "FTY720 (s)-phosphonate preserves sphingosine 1-phosphate receptor 1 expression and exhibits superior barrier protection to FTY720 in acute lung injury." *Crit Care Med* 42 (3):e189-99. doi: 10.1097/CCM.0000000000000097.

Wang, N., H. Miao, Y. S. Li, P. Zhang, J. H. Haga, Y. Hu, A. Young, S. Yuan, P. Nguyen, C. C. Wu, and S. Chien. 2006. "Shear stress regulation of Kruppel-like factor 2 expression is flow pattern-specific." *Biochem Biophys Res Commun* 341 (4):1244-51. doi: 10.1016/j.bbrc.2006.01.089.

Wani, M. A., R. T. Means, Jr., and J. B. Lingrel. 1998. "Loss of LKLF function results in embryonic lethality in mice." *Transgenic Res* 7 (4):229-38.

Wani, M. A., S. E. Wert, and J. B. Lingrel. 1999. "Lung Kruppel-like factor, a zinc finger transcription factor, is essential for normal lung development." *J Biol Chem* 274 (30):21180-5.

Whitney, G. S., P. Y. Chan, J. Blake, W. L. Cosand, M. G. Neubauer, A. Aruffo, and S. B. Kanner. 1993. "Human T and B lymphocytes express a structurally conserved focal adhesion kinase, pp125FAK." *DNA Cell Biol* 12 (9):823-30. doi: 10.1089/dna.1993.12.823.

Wu, W., S. de Folter, X. Shen, W. Zhang, and S. Tao. 2011. "Vertebrate paralogous MEF2 genes: origin, conservation, and evolution." *PLoS One* 6 (3):e17334. doi: 10.1371/journal.pone.0017334.

Xu, Z., T. Yoshida, L. Wu, D. Maiti, L. Cebotaru, and E. J. Duh. 2015. "Transcription factor MEF2C suppresses endothelial cell inflammation via regulation of NF-kappaB and KLF2." *J Cell Physiol* 230 (6):1310-20. doi: 10.1002/jcp.24870.

Yan, C., M. Takahashi, M. Okuda, J. D. Lee, and B. C. Berk. 1999. "Fluid shear stress stimulates big mitogen-activated protein kinase 1 (BMK1) activity in endothelial cells. Dependence on tyrosine kinases and intracellular calcium." *J Biol Chem* 274 (1):143-50.

Yang, C. C., O. I. Ornatsky, J. C. McDermott, T. F. Cruz, and C. A. Prody. 1998. "Interaction of myocyte enhancer factor 2 (MEF2) with a mitogen-activated protein kinase, ERK5/BMK1." *Nucleic Acids Res* 26 (20):4771-7.

Yazbeck, P., M. Tauseef, K. Kruse, M. R. Amin, R. Sheikh, S. Feske, Y. Komarova, and D. Mehta. 2017. "STIM1 Phosphorylation at Y361 Recruits Orai1 to STIM1 Puncta and Induces Ca2+ Entry." *Sci Rep* 7:42758. doi: 10.1038/srep42758.

Young, N., and J. R. Van Brocklyn. 2006. "Signal transduction of sphingosine-1-phosphate G protein-coupled receptors." *ScientificWorldJournal* 6:946-66. doi: 10.1100/tsw.2006.182.

Yu, F., L. Sun, R. Courjaret, and K. Machaca. 2011. "Role of the STIM1 C-terminal domain in STIM1 clustering." *J Biol Chem* 286 (10):8375-84. doi: 10.1074/jbc.M110.188789.

Yuan, S. Y., Q. Shen, R. R. Rigor, and M. H. Wu. 2012. "Neutrophil transmigration, focal adhesion kinase and endothelial barrier function." *Microvasc Res* 83 (1):82-8. doi: 10.1016/j.mvr.2011.06.015.

Zebda, N., O. Dubrovskyi, and K. G. Birukov. 2012. "Focal adhesion kinase regulation of mechanotransduction and its impact on endothelial cell functions." *Microvasc Res* 83 (1):71-81. doi: 10.1016/j.mvr.2011.06.007.

Zhang, X., S. V. Srinivasan, and J. B. Lingrel. 2004. "WWP1-dependent ubiquitination and degradation of the lung Kruppel-like factor, KLF2." *Biochem Biophys Res Commun* 316 (1):139-48. doi: 10.1016/j.bbrc.2004.02.033.

Zheng, L., P. B. Stathopulos, G. Y. Li, and M. Ikura. 2008. "Biophysical characterization of the EF-hand and SAM domain containing Ca2+ sensory region of STIM1 and STIM2." *Biochem Biophys Res Commun* 369 (1):240-6. doi: 10.1016/j.bbrc.2007.12.129.

Zheng, L., P. B. Stathopulos, R. Schindl, G. Y. Li, C. Romanin, and M. Ikura. 2011. "Auto-inhibitory role of the EF-SAM domain of STIM proteins in store-operated calcium entry." *Proc Natl Acad Sci U S A* 108 (4):1337-42. doi: 10.1073/pnas.1015125108.

Zhou, Y., X. Wang, X. Wang, N. A. Loktionova, X. Cai, R. M. Nwokonko, E. Vrana, Y. Wang, B. S. Rothberg, and D. L. Gill. 2015. "STIM1 dimers undergo unimolecular coupling to activate Orai1 channels." *Nat Commun* 6:8395. doi: 10.1038/ncomms9395.

VIII. VITA

Name: Pascal Yazbeck

EDUCATION: PhD, Cellular and Molecular Pharmacology, University of Illinois at Chicago (Expected 2017)

M.S., Molecular Biology, Lebanese American University, Byblos, Lebanon 2008

B.S., Biomedical Sciences, Haigazian University, Beirut, Lebanon 2006

HONORS: International Vascular Biology Meeting, Boston MA, Travel award, 2016

University of Illinois at Chicago Graduate Council (GSC) Travel award, 2016

Experimental Biology 2016 San Diego, American Physiological Society Respiration Section Best poster award, April 2016

NIH National Institute of Allergy and Infectious Diseases, UTMB Health Center of Biodefense and Emerging Infectious Diseases, Galveston TX, Travel award, 2015

University of Illinois at Chicago Graduate Council (GSC) Travel award, 2015

University of Illinois at Chicago Graduate Council (GSC) Travel award, 2014

PUBLICATIONS: Yazbeck, P., Tauseef, M., Kruse, K., MD-Ruhul., Rayees, S., Feske, S., Komarova, Y., Mehta, D. (2016). STIM1 Phosphorylation at Y361 Recruits Orai1 to STIM1 Puncta and Induces Ca2+ Entry. *Scientific Reports*, 2017.

Rajput, C., Tauseef, M., Farazuddin, M., Yazbeck, P., MD-Ruhul, A., Vijay, A., Sharma, T., Mehta, D. (2015). MicroRNA-150 in endothelial cells suppresses angiopoetin-2 generation and signaling to resolve vascular injury. *ATVB*, 2016.

Chavez, A., Schmidt, T. T., Yazbeck, P., Rajput, C., Desai, B., Sukriti, S., Mehta, D. (2015). S1PR1 Tyr143 phosphorylation downregulates endothelial cell surface S1PR1 expression and responsiveness. *J Cell Sci, 128*(5), 878-887.

Sukriti, S., Tauseef, M., Yazbeck, P., & Mehta, D. (2014). Mechanisms regulating endothelial permeability. *Pulm Circ, 4*(4), 535-551.

Rajput, C., Kini, V., Smith, M., **Yazbeck, P**., Chavez, A., Schmidt, T., Zhang, W., Knezevic, N., Komarova, Y., Mehta, D. (2012). Neural Wiskott-Aldrich syndrome protein (N-WASP)-mediated p120-catenin interaction with Arp2-Actin complex stabilizes endothelial adherens junctions**.** *JBC,* Feb 8; 288(6):4241-50. (Paper chosen by the faculty of 1000).

ABSTRACTS: Yazbeck, P., Schmidt, T., Tauseef, M., Mehta, D. (2016). Transcriptional Regulation of S1PR1 through FAK and KLF2 is Required for Maintaining Endothelial Barrier Integrity. FASEB J. April, 2016 30:980.15

Yazbeck, P., Schmidt, T., Tauseef, M., Mehta, D. (2015). Endothelial Focal Adhesion Kinase Transcriptionally Regulates S1P1 to Maintain Lung Vascular Barrier Function FASEB J April 2015 29:625.4

PRESENTATION: Oral Presentation at NAVBO, Boston, MA, 2016

Oral/poster Presentation Experimental Biology Meeting, APS San Diego, 2016

Oral/poster Presentation Experimental Biology Meeting, APS Boston, 2015

Oral Presentation Microcirculation in Acute Infections, Galveston, TX, 2015